Automated Management of Virtualized Data Centers

by

Pradeep Padala

A dissertation submitted in partial fulfillment
of the requirements for the degree of
Doctor of Philosophy
(Computer Science and Engineering)
in The University of Michigan
2010

Dedicated to my lovely wife **Rachna Lal**,

who always offered constant support and unconditional love.

ACKNOWLEDGEMENTS

As I take a trip down memory lane, I see three pillars that helped me build this thesis: my advisor Kang Shin, my mentor Xiaoyun Zhu and my wife Rachna Lal. Without these three people, I wouldn't have been where I am today.

My first and foremost thanks are to my advisor, Prof. Shin, for his guidance and support during my research. I am always amazed at his unending passion to do great research, and his enthusiasm and energy were a source of constant inspiration to me. He was always there with his help and encouragement whenever I needed it. It is because of him that my doctoral years were so productive and happy.

I would like to express my heartfelt gratitude to Xiaoyun Zhu, my mentor at HP Labs (now at VMware). She has been more than a mentor, a teacher, a guide and a great friend. Xiaoyun has helped me a great deal in learning control theory, and in particular how to apply it to computer systems. She has the uncanny ability of seeing through theory clearly, and explaining it to systems people in a way they can easily understand.

I am indebted to Mustafa Uysal, Arif Merchant, Zhikui Wang and Sharad Singhal of HP Labs for their invaluable guidance and support during my internships at HP labs and later. Tathagata Das, Venkat Padmanabhan, and Ram Ramji of Microsoft Research have greatly helped in shaping the last piece of my thesis, LiteGreen.

I want to thank my committee members, Peter Chen, Dawn Tilbury and Thomas Wenisch for reviewing my proposal and dissertation and offering helpful comments to improve my work. Many members of our RTCL lab including Karen Hou, Jisoo Yang and Howard Tsai have given valuable comments over the course of my PhD, and I am grateful for their input.

My years at Ann Arbor were enriched and enlivened by my friends, Akash Bhattacharya, Ramashis Das, Arnab Nandi, Sujay Phadke and Saurabh Tyagi. Life would have been a lot less fun without them around. Their help and support has contributed to making my PhD fun.

I would like to thank my parents for their love and support. Their blessings have always been with me as I continued in my doctoral research.

There were ecstatic times, there were happy times, there were tough times, there were depressing times and then there were unbearable times. All through this, my wife Rachna has always been there for me, supporting, encouraging, and loving.

TABLE OF CONTENTS

LIST OF FIGURES

LIST OF TABLES

ABSTRACT

Automated Management of Virtualized Data Centers

by

Pradeep Padala

Chair: Kang Geun Shin

Virtualized data centers enable sharing of resources among hosted applications. However, it is difficult to manage these data centers because of ever-changing application requirements. This thesis presents a collection of tools called *AutoControl* and *LiteGreen*, that automatically adapt to dynamic changes to achieve various SLOs (service level objectives) while maintaining high resource utilization, high application performance and low power consumption.

AutoControl resource manager is based on novel control theory and optimization techniques. The central idea of this work is to apply control theory to solve resource allocation in virtualized data centers while achieving applicaiton goals. Applying control theory to computer systems, where first-principle models are not available, is a challenging task, and is made difficult by the dynamics seen in real systems including changing workloads, multi-tier dependencies, and resource bottleneck shifts.

To overcome the lack of first principle models, we build black-box models that not only capture the relationship between application performance and resource allocations, but also incorporate the dynamics of the system using an *online adaptive model.*

The next challenge is to design a controller that uses the online model to compute optimal allocations to achieve applicaiton goals. We are faced with two conflicting goals: *quick response* and *stability.* Our solution is an adaptive multi-input, multi-output (MIMO) controller that uses a simplified Linear Quadratic Regulator (LQR) formulation. The LQR formulation treats the control as an optimization problem and balances the tradeoff between quick response and stability to find the right set of resource allocations to meet application goals.

We also look at the idea of leveraging server consolidation to save desktop energy. Due to the lack of energy proportionality in desktop systems, a great amount of energy is wasted even when the system is idle. We design and implement a novel power manager called *LiteGreen* to save desktop energy by virtualizing the users desktop computing environment as a virtual machine (VM) and then migrating it between the user's physical desktop machine and a VM server, depending on whether the desktop computing environment is being actively used or is idle. A savings algorithm based on statistical inferences made from a collection of traces is used to consolidate desktops on a remote server to save energy.

AutoControl and *LiteGreen* are built using Xen and Hyper-V virtualization technologies and various experimental testbeds including a testbed on Emulab are built to evaluate different aspects of *AutoControl* and *LiteGreen*.

CHAPTER 1

Introduction

1.1 The Rise of Data Centers

There is a tremendous growth of data centers fueled by increasing demand for large-scale processing. The growth is fueled by many factors including:

- Explosion of data in the cloud. Social networking site Facebook has 120 million users with an average of 3% weekly growth since January 2007. E-mail services like Gmail allows us to store every e-mail we ever sent or received.
- Growth of computing in the cloud. Services like Amazon EC2 [1] offer computing power that can be dynamically allocated. Figure 1.1a shows the increase in network bandwidth in Amazon web services. Figure 1.1b shows the explosion in S3 [42] storage data.
- Increased demand for electronic transactions like on-line banking and trading.
- Growth of instant communication on the Internet. Twitter, a popular messaging site, has grown from 300,000 users to 800,000 users in a matter of one year. Twitter servers handle thousands of Tweets (instant messages) per second.

Today's data centers hosting these applications often are designed with a silo-oriented architecture in mind: each application has its own dedicated servers, storage and network infrastructure, and a software stack tailored for the application that controls these resources

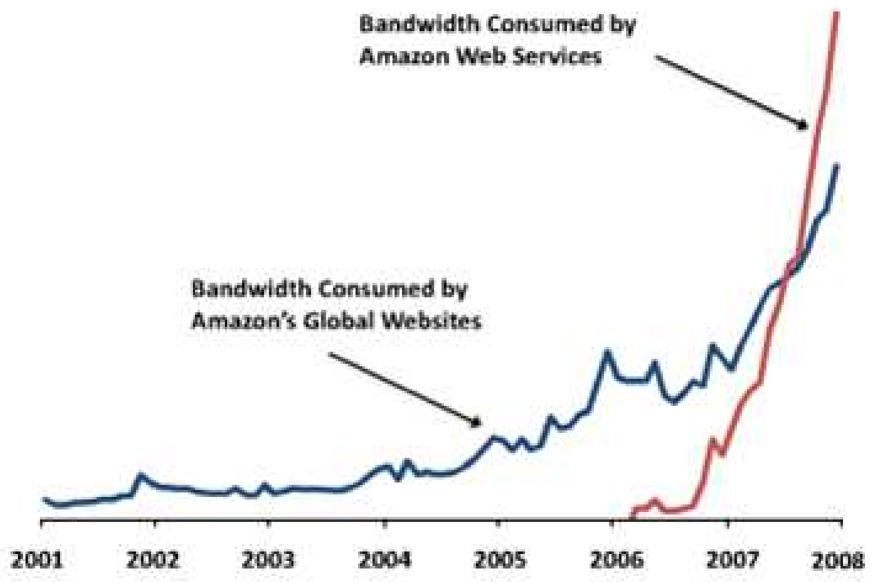

(a) Network statistics

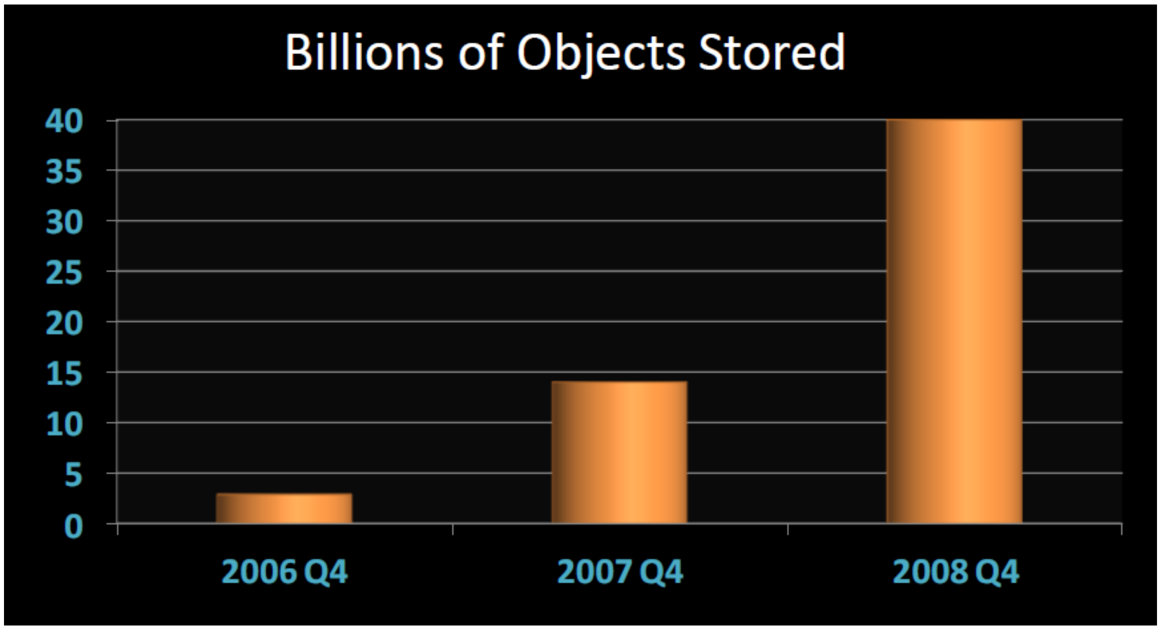

(b) Storage statistics

Figure 1.1: Growth of Amazon web services compared to traditional Amazon web site (source: Jeff Bezos at startup school 2008, Stanford and Alyssa Henry at FAST 2009)

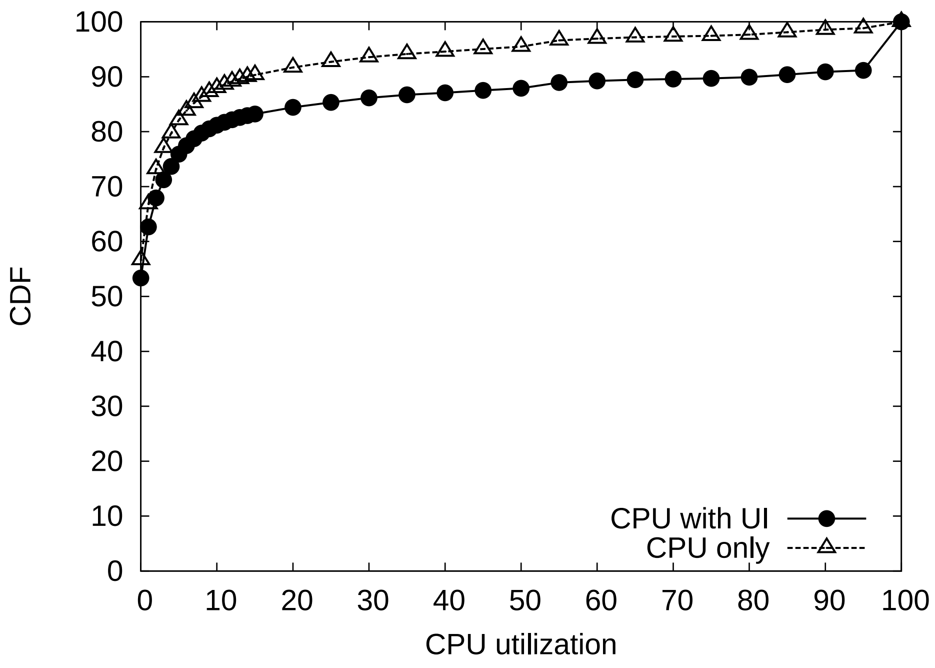

Figure 1.2: Distribution of CPU utilization in measurement analysis of PC usage data at MSR India

as a whole. Due to the stringent requirements placed on the applications and the time-varying demands that they experience, each application silo is vastly over-provisioned to meet the application service goals (e.g. number of transactions per second).

As a result, data centers are often under-utilized, while some nodes may sometimes become heavily-loaded, resulting in service-level violations due to poor application performance [26]. For example, Figures 1.3a and 1.3b show the CPU consumption of two nodes in an enterprise data center for a week. Each node has 6 CPUs, and we can see that both nodes are utilized under 10% most of the time. We also note that the maximum CPU usage is much higher than the average CPU usage. Similar problems are observed in other resources including disk, network and memory. So, if we were to provision the resources based on either the maximum or the average demand, the data center may either be grossly under-utilized or experience poor application-level QoS due to insufficient resources under peak loads.

Similar under-utilization is seen in desktop PCs in enterprises with vast majority of them in idle state but consuming power. Figure 1.2 plots the distribution of CPU usage and UI activity, binned into 1-minute buckets and aggregated across all of the PCs in a measurement study (more details in Chapter 6). To allow plotting both CPU usage and UI activity in the same graph, we adopt the convention of treating the presence of UI activity in a bucket as 100% CPU usage. The "CPU only" curve in the figure shows that CPU usage is low, remaining under 10% for 90% of the time. The "CPU + UI" curve shows that UI activity is present, on average, only in 10% of the 1-minute buckets, or about 2.4 hours in a day.

Vast over-provisioning also causes high power consumption in the data centers. The estimated amount of power consumption by data centers during 2006 in the US is 61 billion kilowatt-hours (kWh) [24], which is about 1.5% of total US consumption of electricity. The report [24] also noted that the energy usage of data centers in 2006 is estimated to be more than double the energy consumed in 2000. Similar reports have also estimated that the energy usage of desktops has skyrocketed. A recent study [74] estimates that PCs and their monitors consume about 100 TWh/year, constituting 3% of the annual electricity consumed in the U.S. Of this, 65 TWh/year is consumed by PCs in enterprises, which constitutes 5% of the commercial building electricity consumption.

Virtualization is causing a disruptive change in enterprise data centers and giving rise to a new paradigm: *shared virtualized infrastructure*. In this new paradigm, multiple enterprise applications share dynamically allocated resources. These applications are also consolidated to reduce infrastructure, operating, management, and power costs, while simultaneously increasing resource utilization. Revisiting the previous scenario of two application servers, Figure 1.3c shows the sum of the CPU consumptions from both nodes. It is evident that the combined application demand is well within the capacity of one node at any particular time. If we can dynamically allocate the server capacity to these two applications as their demands change, we can easily consolidate these two nodes into one server.

1.2 Research Challenges

Unfortunately, the complex nature of enterprise desktop and server applications pose further challenges for this new paradigm of shared data centers. Data center administrators

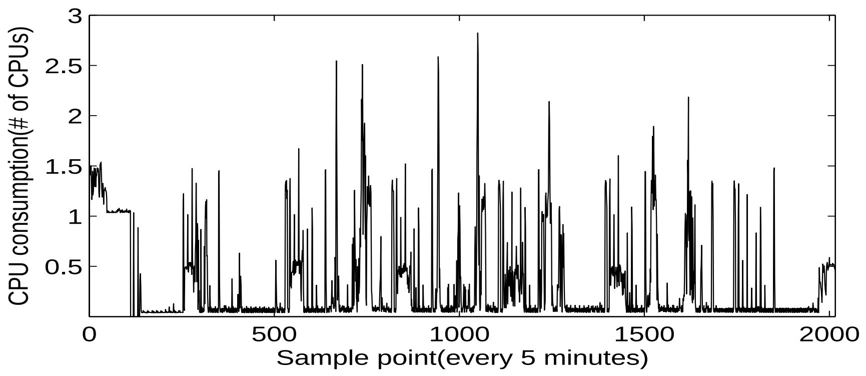

(a) CPU consumption of node 1

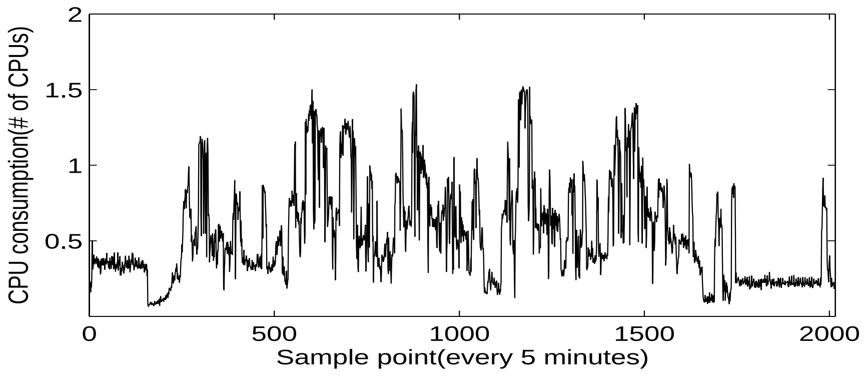

(b) CPU consumption of node 2

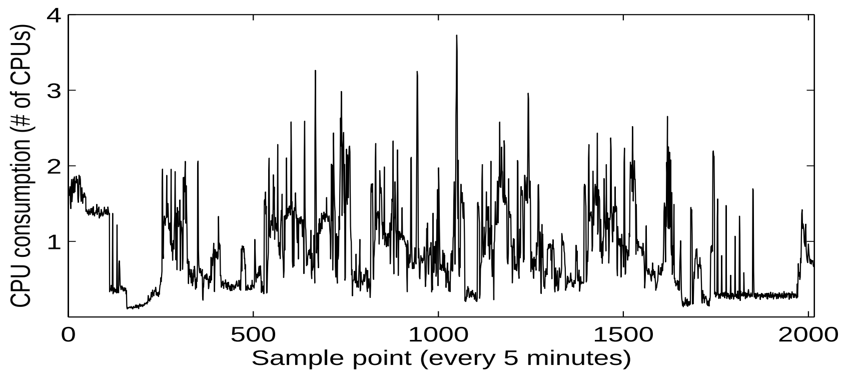

(c) Sum of CPU consumptions from both nodes

Figure 1.3: An example of data center server consumption

are faced with growing challenges to meet service level objectives (SLOs) in the presence of dynamic resource sharing and unpredictable interactions across many applications. These challenges include:

- *Complex SLOs*: It is non-trivial to convert individual application SLOs to corresponding resource shares in the shared virtualized platform. For example, determining the amount of CPU and the disk shares required to achieve a specified number of financial transactions per unit time is difficult.

- *Changing resource requirements over time*: The intensity and the mix of enterprise application workloads change over time. As a result, the demand for individual resource types changes over the lifetime of the application. For example, Figure 1.4 shows the CPU and disk utilization of an SAP application for a day. The utilization for both resources varies over time considerably, and the peaks of the two resource types occurred at different times of the day. This implies that static resource allocation can meet application SLOs only when the resources are allocated for peak demands, wasting a great deal of resources.

- *Distributed resource allocation*: Multi-tier applications spanning across multiple nodes require resource allocations across all tiers to be at appropriate levels to meet end-to-end application SLOs.

- *Resource dependencies*: Application-level performance often depends on the application's ability to simultaneously access multiple system-level resources.

- *Complex power consumption*: Consolidation of machines to reduce power consumption is complicated by the fact that desktops have complex power usage behavior. Many desktop applications have bursty resource demand, making a bad consolidation decision affect application performance.

Researchers have studied capacity planning for such an environment by using historical resource utilization traces to predict the application resource requirements in the future and to place compatible sets of applications onto the shared nodes [82]. Such an approach aims to ensure that each node has enough capacity to meet the aggregate demand of all the applications, while minimizing the number of active nodes. However, past demands are not always accurate predictors of future demands, especially for Web-based, interactive applications. Furthermore, in a virtualized infrastructure, the performance of a given application depends on other applications sharing resources, making it difficult to predict its behavior using pre-consolidation traces. Other researchers have considered use of live VM

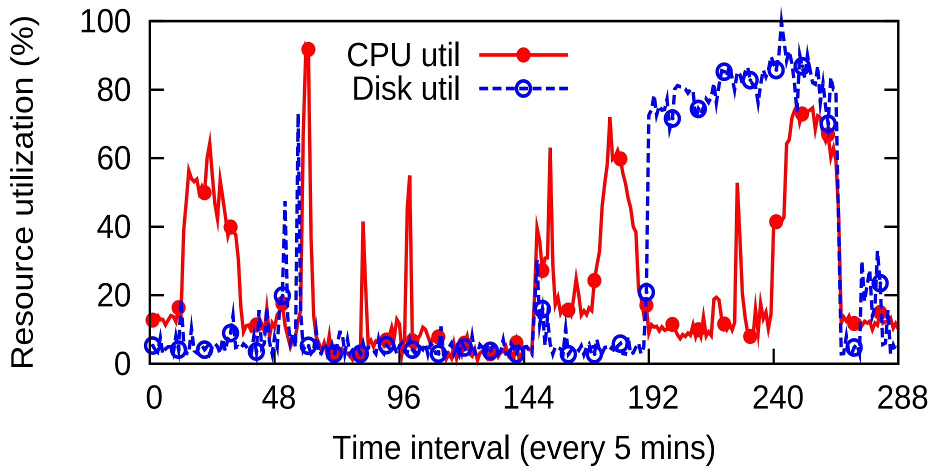

Figure 1.4: Resource usage in a production SAP application server for a one-day period.

migration to alleviate overload conditions that occur at runtime [39]. However, the CPU and network overheads of VM migration may further degrade application performance on the already-congested node, and hence, VM migration is mainly effective for sustained, rather than transient, overload.

To overcome the difficulties, in this thesis, we develop various tools for managing resources and energy consumption as follows:

- **AutoControl - resource manager**: AutoControl is a feedback-based resource allocation system that manages dynamic resource sharing within the virtualized nodes and that *complements* the capacity planning and workload migration schemes others have proposed to achieve application-level SLOs on shared virtualized infrastructure.

- **LiteGreen - power manager**: LiteGreen is an automated system that consolidates idle desktops onto a central server to reduce the energy consumption of desktops as a whole. LiteGreen uses virtual machine migration to move idle desktops into a central server. The desktop VM is moved back when the user comes back seamlessly and a remote desktop client is used to mask the effect of migration.

1.3 Research Goals

The main theme of this research is: **Automation**. The goal of this work is to develop *automated* mechanisms to meet application goals in a virtualized data center in changing workload conditions.

1.3.1 AutoControl

We set the following goals in designing *AutoControl*:

Performance assurance: If all applications can meet their performance targets, *AutoControl* should allocate resources properly to achieve them. If they cannot be met, *AutoControl* should provide service differentiation according to application priorities.

Automation: While performance targets and certain parameters within *AutoControl* may be set manually, all allocation decisions should be made *automatically* without human intervention.

Adaptation: The controller should adapt to variations in workloads or system conditions.

Scalability: The controller architecture should be distributed so that it can handle many applications and nodes, and also limit the number of variables each controller deals with.

1.3.2 LiteGreen

The following goals are set in designing *LiteGreen*:

Energy conservation: *LiteGreen* should try to conserve as much energy as possible, while maintaining acceptable desktop application performance.

Automation: The decisions for consolidation of desktop applications should be done automatically.

Adaptation: The controller should adapt to variations in desktop workloads.

Scalability: The *LiteGreen* should be scalable to many desktops.

1.4 Research Contributions

As discussed in the previous sections, there are many challenges in managing complex shared virtualized infrastructure. The *AutoControl* tools, we have developed, make the management of these virtualized data centers easy.

More specifically, we make the following contributions.

1.4.1 Utilization-based CPU Resource Controller

In our earlier attempts to apply control theory, we have developed a two-layered controller that accounts for the dependencies and interactions among multiple tiers in an application stack when making resource allocation decisions. The controller is designed to adaptively adjust to varying workloads so that high resource utilization and high application-level QoS (Quality of Service) can be achieved. Our design employs a *utilization controller* that controls the resource allocation for a single application tier and an *arbiter controller* that controls the resource allocations across multiple application tiers and multiple application stacks sharing the same infrastructure.

This contribution is unique in providing a valuable insight into applying control theory to a complex virtualized infrastructure. We have succeeded in applying control theory in this simplified case, but there is more to be achieved, before we can claim that we have built a completely automated management platform. This work is published in Eurosys 2007 and Chapter 3 in part, is a reprint of the published paper.

1.4.2 Multi-resource Controller

To address the deficiencies of CPU-only controller, we build a MIMO modeler and controller that can control multiple resources. More specifically, our contributions are two-fold.

1. *Dynamic black-box modeler*: We design an online model estimator to dynamically determine and capture the relationship between application-level performance and the allocation of individual resource shares. Our adaptive modeling approach captures the complex behavior of enterprise applications including time-varying resource demands,

resource demands from distributed application tiers, and shifting demands across multiple resource types.

2. *Multi-input, multi-output controller*: We design a two-layer, multi-input, multi-output (MIMO) controller to *automatically* allocate multiple types of resources to enterprise applications to achieve their SLOs. The first layer consists of a set of application controllers that automatically determine the amount of resources necessary to achieve individual application SLOs, using the estimated models and a feedback-based approach. The second layer is comprised of a set of node controllers that detect resource bottlenecks on the shared nodes and properly allocate multiple types of resources to individual applications. Under overload, the node controllers provide service differentiation according to the priorities of individual applications.

This work is published in Eurosys 2009, and Chapter 4 in part, is a reprint of the published paper.

1.4.3 Multi-port Storage Controller

We extend our multi-resource controller to solve a special case of controlling access to multiple ports in a large-scale storage system to meet competing application goals.

Applications running on the shared storage present very different storage loads and have different performance requirements. When the requirements of all applications cannot be met, the choice of which application requirements to meet and which ones to abandon may depend upon the priority of the individual applications. For example, meeting the I/O response time requirement of an interactive system may take precedence over the throughput requirement of a backup system. A data center operator needs the flexibility to set the performance metrics and priority levels for the applications, and to adjust them as necessary.

The proposed solutions to this problem in the literature include using proportional share I/O schedulers (e.g., SFQ [55]) and admission control (I/O throttling) using feedback controllers (e.g., Triage [60]). Proportional share schedulers alone cannot provide application performance differentiation for several reasons: First, the application performance depends on the proportional share settings and the workload characteristics in a complex, non-linear, time-dependent manner, and it is difficult for an administrator to determine in advance the share to assign to each application, and how/when to change it. Second, applications have several kinds of performance targets, such as response time and bandwidth requirements, not just throughput. Finally, in overload situations, when the system is unable to meet all of the application QoS requirements, prioritization is necessary to enable important applications to meet their performance requirements.

We combine an optimization-based feedback controller with an underlying I/O scheduler. Our controller accepts performance metrics and targets from multiple applications, monitors the performance of each application, and periodically adjusts the IO resources given to the applications at the disk array to make sure that each application meets its performance goal. The performance metrics for the applications can be different: the controller normalizes the application metrics so that the performance received by different applications can be compared and traded off. Our controller continually models the performance of each application relative to the resources it receives, and uses this model to determine the appropriate resource allocation for the application. If the resources available are inadequate to provide all the applications with their desired performance, a Linear Programming optimizer is used to compute a resource allocation that will degrade each application's performance in inverse proportion to its priority.

This work is published in International Workshop on Feedback Control Implementation and Design in Computing Systems and Networks (FEBID) 2009, and Chapter 4 in part, is a reprint of the published paper.

1.4.4 Idle Desktop Consolidation to Conserve Energy

While the previous work focused on consolidation of server workloads, we have also looked at consolidating idle desktops onto servers to save energy. It is well-known that desktops running in virtual machines can be consolidated onto servers, but it is unclear how to do this while maintaining good *user experience* and low *energy usage*. If we keep all desktops on the server and use thin clients to connect to them, energy usage is low, but performance may suffer because of resource contention. Users also lose the ability to control many aspects of their desktop environment (e.g., for playing games). On the other hand, leaving all desktops on all the time gives high performance, and great user experience, but loses on energy.

We present *LiteGreen*, a system to save desktop energy by employing a novel approach to avoiding user disruption as well as the complexity of application-specific customization. The basic idea of *LiteGreen* is to virtualize the user's desktop computing environment as a virtual machine (VM) and then migrate it between the user's physical desktop machine and a server hosting VMs, depending on whether the desktop computing environment is being actively used or is idle. When the desktop becomes idle, say when the user steps away for several minutes (e.g., for a coffee break), the desktop VM is migrated away to the VM server and the physical desktop machine is put to sleep. When the desktop becomes active again (e.g., when the user returns), the desktop VM is migrated back to the physical desktop machine. Thus, even when it has been migrated to the VM server, the user's desktop environment remains alive (i.e., it is "always on"), so ongoing network connections and other activity (e.g., background downloads) are *not* disturbed, regardless of the application involved.

The "always on" feature of LiteGreen allows energy savings whenever the opportunity arises, without having to worry about disrupting the user. Besides long idle periods (e.g., nights and weekends), energy can also be saved by putting the physical desktop computer to sleep even during short idle periods, such as when a user goes to a meeting or steps out for coffee.

More specifically, the main contributions of LiteGreen are as follows.

1. A novel system that leverages virtualization to consolidate idle desktops on a VM server, thereby saving energy while avoiding user disruption.

2. Automated mechanisms to drive the migration of the desktop computing environment between the physical desktop machines and the VM server.

3. A prototype implementation and the evaluation of LiteGreen through a small-scale deployment.

4. Trace-driven analysis based on an aggregate of over 65,000 hours of desktop resource

usage data gathered from 120 desktops, demonstrating total energy savings of 72-86%.

1.4.5 Performance Evaluation of Server Consolidation

We have seen that server consolidation is not a trivial task, and we require many technologies including capacity planning, virtual machine migration, slicing and automated resource allocation to achieve the best possible results. However, there is another aspect of server consolidation that is often glossed over: *virtualization technology.* The explosive growth of virtualization has produced many virtualization technologies including VMware ESX [11], Xen [30], OpenVZ [6], and many more.

In this thesis, we try to answer a key research question: *Which virtualization technology works best in server consolidation and why?.* We compare Xen (hypervisor-based technology) and OpenVZ (OS container-based technology), and conclude that OpenVZ performs better than Xen, but Xen provide more isolation.

1.5 Organization of the Thesis

The organization of the thesis closely follows the contributions mentioned above. We first provide the background and related work in Chapter 2. Our first experience with using control theory to build a CPU controller that allocates CPU resources to competing multi-tier applications is described in Chapter 3. Design, implementation and evaluation of a fully automated multi-resource controller is provided in Chapter 4. The special case of applying multi-resource controller to multi-port large-scale storage system is presented in Chapter 5. Consolidation of desktops for saving energy is described in Chapter 6. The virtualization technologies Xen and OpenVZ are evaluated in Chapter 7 to get insight into different aspects of the two technologies for server consolidation. The thesis is concluded with avenues for future work in Chapter 8.

CHAPTER 2

Background and Related Work

In this chapter, we provide a broad overview of the background required to understand the techniques described in the thesis. References to more detailed information are provided for interested readers.

2.1 Virtualization

Virtualization refers to many different concepts in computer science [100], and is often used to describe many types of abstractions. In this work, we are primarily concerned with *Platform Virtualization*, which separates an operating system from the underlying hardware resources. *Virtual Machine* (VM) refers to the abstracted machine that gives the illusion of a “real machine”.

The earliest experiments with virtualization date back to 1960s, when IBM built VM/370 [40, 68] and operating system that gives the illusion of multiple independent machines. VM/370 is built for System/370 mainframe computers built by IBM, and the virtualization features are used to maintain backward compatibility with the instruction set in System/360 mainframes (precursor to System/370 mainframes). Similar attempts were made to provide virtual machines on DEC PDP-10 [45].

The popularity of mainframes has declined in later years, with much lower priced high-end servers taking their roles. With the advent of multi-core computing and ever increasing power of servers, virtualization has seen resurgence. Research system Disco [33] is one of the first research efforts to bring the old virtual machine concepts to the front. In

Disco, Stanford university researchers have developed a virtual machine monitor (VMM) that allows multiple operating systems to run giving the illusion of multiple machines. The techniques described in Disco are commercialized later by VMware [83]. Countless commercial virtualization techniques followed VMware.

2.2 Virtualization Requirements

How to build virtual machines on a specific hardware architecture? - This is one of the questions that irked researchers in the 70s, and Goldberg and Popek [77] are the first ones to identify the hardware requirements to build a virtual machine. They define two important concepts: *virtual machine* and *virtual machine monitor (VMM).*

1. A virtual machine is taken to be an efficient, isolated duplicate of the real machine.

2. As a piece of software a VMM has three essential characteristics. First, the VMM provides an environment for programs which is essentially identical with the original machine; second, programs run in this environment show at worst only minor decreases in speed; and last, the VMM is in complete control of system resources.

Goldberg and Popek also define the requirements of an instruction set architecture (ISA) to be virtualizable.

> For any conventional third-generation computer, a VMM may be constructed if the set of sensitive instructions for that computer is a subset of the set of privileged instructions.

Before, we understand their requirements, we need define a few terms. Third generation computers refer to computers based on integrated circuits. Other terms are defined as follows:

- **Privileged instructions**: Those that trap if the processor is in user mode and do not trap if it is in system mode.

- **Control sensitive instructions**: Those that attempt to change the configuration of resources in the system.
- **Behavior sensitive instructions**: Those whose behavior or result depends on the configuration of resources (the content of the relocation register or the processor's mode).

This simply states that if sensitive instructions can be executed in user-mode without the VMM's knowledge, VMM may no longer have the full control of resources violating the third VMM property described above.

Intel's x86 architecture, the predominant ISA in current computers is famously non-virtualizable [62]. However, dynamic recompilation can be used to dynamically modify sensitive instructions to trap so that VMM can take appropriate action. These techniques have been used in many virtualization technologies including QEMU [31] and Virtual box [9].

Another approach called para-virtualization, pioneered by Xen [30] makes minimal modifications to operating systems hosted by the VMM, so that sensitive instructions can be handled appropriately.

The advent of virtualization enabled processors by Intel and AMD called VT-x and AMD-V respectively allow hardware-assisted virtualization [91] which does not require any modifications to operating systems.

2.2.1 Operating System Level Virtualization

VMMs described above provide a virtual machine that gives the illusion of a real machine. This allows running of multiple operating systems on the same physical hardware. In a single operating system, however, partition of resources can be done such that multiple partitions do not harm each other. In earlier UNIX systems, these partitions are implemented using `chroot` environment, and the multiple environments are called `jails`. Though jails had some isolation, it was easy for one jail to impact another jail.

More sophisticated mechanisms called *resource containers* [29] have tried to build more isolation. Many similar container architectures followed including [81, 6, 85] and many commercial implementations [10] are available as well.

The main benefits of operating system level virtualization is performance, while sacrificing some isolation. A more detailed comparison of hypervisor based virtualization and operating system level virtualization is in Chapter 7.

2.3 Virtualized Data Centers

Though virtualization was originally seen as a technique to provide backward compatibility and isolation among competing environments, it has given rise to *virtualized data centers*. We define a virtualized data center as a data center running the applications only in virtual machines.

2.3.1 Benefits of Virtualized Data Centers

Why do we want to run applications in a data center in virtual machines? - There are many benefits to running applications in virtual machines compared to running on physical machines including

1. **High Utilization**: As we saw in Chapter 1, sharing resources allows better utilization of overall data center resources.

2. **Performance Isolation**: The applications can be isolated by running them in different virtual machine. Different virtualization technologies differing levels of performance isolation, but most of them offer safety, correctness and fault-tolerance isolation. Though many virtualization technologies can be used for isolation, we choose hypervisor-based virtualization. The reasoning for choosing this method is described in Chapter 7.

   Though physical machine can offer isolation by running multiple applications in different physical machines, such scenario would waste great amount of resources.

3. **Low Management Costs**: Virtual machines allow easy provisioning of resources in a data center and virtual machine migration [39] allows easy movement of virtual machines to save energy and for other purposes.

4. **High Adaptability**: The resources to virtual machines can be dynamically changed allowing highly adaptive data centers. Major portion of this thesis is concerned with creating a dynamic resource control system that can make automatic decisions for high adaptability.

However, virtualization is not free, and causes overhead that may not be suitable for some applications.

2.4 Server Consolidation

The main benefit of virtualized data centers comes from server consolidation, in which multiple applications are consolidated onto a single physical machine. However, figuring out the right way to consolidate still remains an unsolved research problem.

2.4.1 Capacity Planning

Traditionally consolidation is done through capacity planning. Researchers have studied capacity planning for such an environment by using historical resource utilization traces to predict application resource requirements in the future and to place compatible sets of applications onto shared nodes [82]. This approach aims to ensure that each node has enough capacity to meet the aggregate demand of all the applications, while minimizing the number of active nodes. However, past demands are not always accurate predictors of future demands, especially for Web-based, interactive applications. Furthermore, in a shared virtualized infrastructure, the performance of a given application depends on other applications sharing resources, making it difficult to predict its behavior using pre-consolidation traces.

2.4.2 Virtual Machine Migration

Virtual machine migration involves migration of a running VM from one machine to another machine where it can continue execution. Migration is made practical with techniques that allow *live migration* [39], where the original VM continues to run while VM is being migrated, and has a very low downtime.

Live migration allows movement of resources based on VM resource usage and many strategies have been proposed for the allocation [101, 92].

2.4.3 Resource Allocation using Slicing

There are many ways to allocate resources in a single machine, in this work we primarily focus on proportional sharing. Proportional sharing is often touted as the mechanism to allocate resources in certain ratio (also called shares), as that allows operators to specify the ratios to achieve certain quality of service for individual applications.

Proportional share schedulers allow reserving CPU capacity for applications [56, 72, 94]. While these can enforce the desired CPU shares, our controller also dynamically adjusts these share values based on application-level QoS metrics. It is similar to the feedback controller in [87] that allocates CPU to threads based on an estimate of each thread's progress, but our controller operates at a much higher layer based on end-to-end application performance that spans multiple tiers in a given application.

In the past few years, there has been a great amount of research in improving scheduling in virtualization mechanisms. Virtualization technologies including VMware [83] and Xen [30], offer proportional share schedulers for CPU in the hypervisor layer that can be used to set the allocation for a particular VM. However, these schedulers only provide mechanisms for controlling resources. One also has to provide the right parameters to the schedulers in order to achieve desired application-level goals.

For example, Xen's CPU credit scheduler provides two knobs: `cap` and `share`. The `cap` allows one to set a hard limit on the amount of CPU used by a VM. The `share` knob is expected to be used for proportional sharing. However, in our practice we found out that using caps as the single knob for enforcing proportions works better than trying to use both knobs together.

Xen does not provide any native mechanisms for allocating storage resources to individual VMs. Prior work on controlling storage resources independent of CPU includes systems that provide performance guarantees in storage systems [36, 47, 55, 65]. However, one has to tune these tools to achieve application-level guarantees. Our work builds on top of others work, where the authors developed an adaptive controller [59] to achieve performance differentiation, and efficient adaptive proportional share scheduler [48] for storage systems.

Similar to storage, knobs for network resources are not yet fully developed in virtualization environments. Our initial efforts in adding network resource control have failed, because of inaccuracies in network actuators. Since Xen's native network control is not fully implemented, we tried to use Linux's existing traffic controller (`tc`) to allocate network resources to VMs. We found that the network bandwidth setting in (`tc`) is not enforced correctly when heavy network workloads are run. However, the theory we developed in this work is directly applicable to any number of resources.

The memory ballooning supported in VMware [93] provides a way of controlling the memory required by a VM. However, the ballooning algorithm does not know about application goals or multiple tiers, and only uses the memory pressure as seen by the operating system. We have done preliminary work [54] in controlling CPU and memory together with other researchers. In many consolidation scenarios, memory is the limiting factor in achieving high consolidation.

2.4.4 Slicing and AutoControl

In this thesis, we do not intend to replace capacity planning or migration mechanisms, but augment them by dynamic resource allocation that manages dynamic resource sharing within the virtualized nodes.

We assume that the initial placement of applications onto nodes has been handled by a separate capacity planning service. The same service can also perform admission control for new applications and determine if existing nodes have enough idle capacity to accommodate the projected demands of the applications [82]. We also assume that a workload migration system [101] may re-balance workloads among nodes at a time scale of minutes or longer. These problems are complementary to the problem solved by *AutoControl*. Our system deals with runtime management of applications sharing virtualized nodes, and dynamically adjusts resource allocations over short time scales (e.g., seconds) to meet the application SLOs. When any resource on a shared node becomes a bottleneck due to unpredicted spikes in some workloads, or because of complex interactions between co-hosted applications, *AutoControl* provides performance differentiation so that higher-priority applications experience lower performance degradation.

2.4.5 Migration for Dealing with Bottlenecks

Naturally, the question arises about whether we can use migration as the sole mechanism for re-balancing. *AutoControl* enables dynamic re-distribution of resources between competing applications to meet their targets, so long as sufficient resources are available. If a node is persistently overloaded, VM migration [39, 101] may be needed, but the overhead of migration can cause additional SLO violations. We performed experiments to quantify these violations. A detailed study showing this behavior is provided in Chapter 4.

2.4.6 Performance Evaluation of Server Consolidation

In this thesis, we evaluate the two virtualization technologies Xen and OpenVZ for server consolidation. Our work was motivated by the need for understanding server consolidation in different virtualization technologies.

A performance evaluation of Xen was provided in the first SOSP paper on Xen [30] that measured its performance using SPEC CPU2000, OSDB, dbench and SPECWeb benchmarks. The performance was compared to VMWare, Base Linux and User-mode Linux. The results have been re-produced by a separate group of researchers [38]. In this thesis, we extend this evaluation to include OpenVZ as another virtualization platform, and test both Xen and OpenVZ under different scenarios including multiple VMs and multi-tiered systems. We also take a deeper look into some of these scenarios using OProfile [7] to provide some insight into the possible causes of the performance overhead observed.

Menon *et al.* [67] conducted a similar performance evaluation of the Xen environment and found various overheads in the networking stack. The work provides an invaluable performance analysis tool Xenoprof that allows detailed analysis of a Xen system. The authors identified the specific kernel subsystems that were causing the overheads. We perform a similar analysis at a macro level and apply it to different configurations specifically in the context of server consolidation. We also investigate the differences between OpenVZ and Xen specifically related to performance overheads.

Menon *et al.* [66] use the information gathered in the above work and investigate causes of the network overhead in Xen. They propose three techniques for optimizing network virtualization in Xen. We believe that our work can help develop similar optimizations that help server consolidation in both OpenVZ and Xen.

Soltesz *et al.* [85] have developed Linux VServer, which is another implementation of container-based virtualization technology on Linux. They have done a comparison study between VServer and Xen in terms of performance and isolation capabilities. In this thesis, we conduct performance evaluation comparing OpenVZ and Xen when used for consolidating multi-tiered applications, and provide detailed analysis of possible overheads.

Gupta *et al.* [49] have studied the performance isolation provided by Xen. In their work, they develop a set of primitives to address the problem of proper accounting of work done in device drivers by a particular domain. Similar to our work, they use XenMon [50] to detect performance anomalies. Our work is orthogonal to theirs by providing insight into using Xen vs. OpenVZ and different consolidation techniques.

Server consolidation using virtual containers brings new challenges and, we comprehensively evaluate two representative virtualization technologies in a number of different server consolidation scenarios. See Chapter 7 for the full evaluation.

2.5 Resource Control before Virtualization

Dynamic resource allocation in distributed systems has been studied extensively, but the emphasis has been on allocating resources across multiple nodes rather than in time, because of lack of good isolation mechanisms like virtualization. It was formulated as an online optimization problem in [27] using periodic utilization measurements, and resource allocation was implemented via request distribution. Resource provisioning for large clusters hosting multiple services was modeled as a "bidding" process in order to save energy in [37]. The active server set of each service was dynamically resized adapting to the offered load. In [84], an integrated framework was proposed combining a cluster-level load balancer and a node-level class-aware scheduler to achieve both overall system efficiency and individual response time goals. However, these existing techniques are not directly applicable to allocating resources to applications running in VMs. They also fall short of providing a way of allocating resources to meet the end-to-end SLOs.

Our approach of achieving QoS in virtualized data centers differs from achieving QoS for OS processes. Earlier work focused on processes often had to deal with the lack of good isolation mechanisms, and more focus was spent on building the mechanisms like proportional share scheduling. Earlier work on OS processes also did not look at allocation of multiple resources to achieve end-to-end application QoS.

2.6 Admission Control

Traditional admission control to prevent computing systems from being overloaded has focused mostly on web servers. A "gatekeeper" proxy developed in [44] accepts requests based on both online measurements of service times and offline capacity estimation for web sites with dynamic content. Control theory was applied in [57] for the design of a self-tuning admission controller for 3-tier web sites. In [59], a self-tuning adaptive controller was developed for admission control in storage systems based on online estimation of the relationship between the admitted load and the achieved performance. These admission control schemes are complementary to the our approach, because the former shapes the resource demand into a server system, whereas the latter adjusts the supply of resources for handling the demand.

2.7 A Primer on Applying Control Theory to Computer Systems

Control theory is a rich body of theoretical work that is used to control dynamic systems. Though, this thesis is about building a system for automated management, a major part of this thesis uses control theory to solve important problems. Applying control theory to computer systems is still an evolving field. For a detailed study of applying control theory to computing systems, see [53]. In this section, we provide a brief primer on how to apply

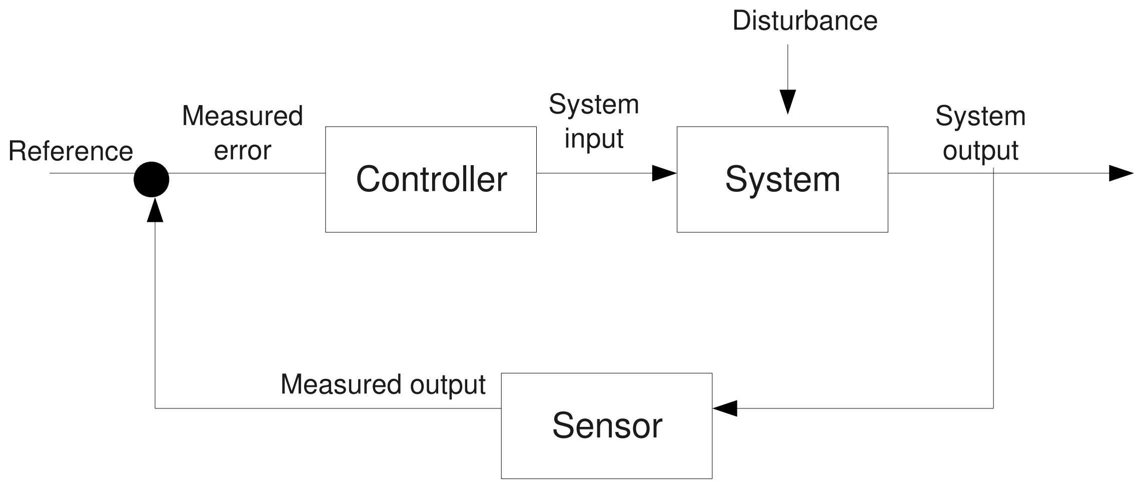

(a) Standard control feedback loop

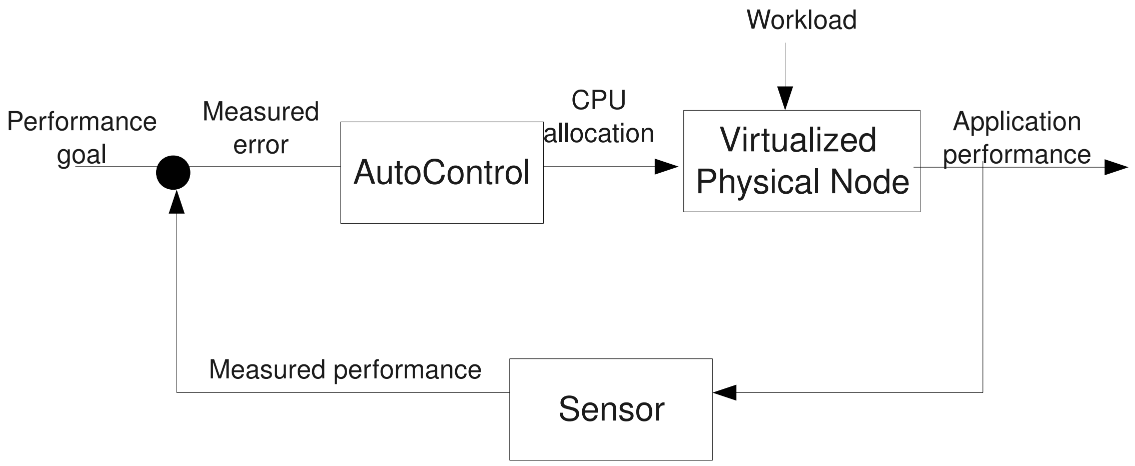

(b) Simplified AutoControl feedback loop

Figure 2.1: Feedback loops in AutoControl

control theory.

2.7.1 Feedback Control

In feedback control, the main objective of the *controller* is to achieve a certain goal (called *reference*) by manipulating some *input* to the *system*. The *input* to the system are dynamically adjusted based on the measurements from the system called *output*. Both *input* and *output* can both be vectors as well. There are often external influence on the system that are not modeled, which are called *disturbances*. Figure 2.1a shows a standard feedback loop.

When applied to virtualized data centers, the system is a single physical node or multiple physical nodes running virtual machines. The input to the system is the resource allocation for the VMs. The output is the performance of application and the reference is the SLO for the performance metric. We consider workload as the disturbance in this case. Figure 2.1b shows the various elements in the *AutoControl* feedback loop. For simplicity, only CPU resource is shown, and a single physical node is used as the system.

2.7.2 Modeling

The traditional way to designing controller in classical control theory is to first build and analyze a model of the system, and then to develop a controller based on the model.

For traditional control systems, such models are often based on first principles. For computer systems, although there is queueing theory that allows for analysis of aggregate statistical measures of quantities such as utilization and latency, it may not be fine-grained enough for run-time control over short time scales, and its assumption about the arrival process or service time distribution may not be met by certain applications and systems. Therefore, most prior work on applying control theory to computer systems employs an empirical and "*black box*" approach to system modeling by varying the inputs in the operating region and observing the corresponding outputs. We adopted this approach in our work.

2.7.3 Offline and Online Black Box Modeling

To build a black box model describing a computer system, we run the system in various operating conditions, when we dynamically vary the inputs to the system and observe the outputs. For example, a web server can be stressed by dynamically adjusting its resource allocation, and observing the throughput and response time, where the number of serving threads is being changed in each experiment. This is the approach used in build a CPU controller in Chapter 3. After observing the system in many operating conditions, a model can be developed based on the collected measurements often using regression techniques.

However, this offline modeling approach suffers from the problem of not being able to adapt to changing workloads and conditions. It is impossible to completely model a system prior to the production deployment, so an online adaptive approach is needed. In chapters 4 and 5, we build a dynamic system based on sophisticated adaptive modeling techniques.

2.7.4 Designing a Controller

In traditional control theory, the controller is often built by making use of standard proportional (P), integral(I), derivative(D), PI, PID or other non-linear controllers [53]. There is a rich body of literature describing these controllers, and one can often use them directly in certain systems.

However, for computer systems, often the models are not derived from first principles, so black-box models with adaptive controllers are required. Adaptive control [28] again contains a large body of research that allows changing of the control law based on dynamic conditions. We refer the reader to [28] for a detailed study.

In this work, we have used an adaptive integral controller and adaptive multiple-input, multiple-output optimal controllers, details of which are described in subsequent chapters.

2.7.5 Testing Controllers

In traditional control theory, controllers are theoretically analyzed for various properties including stability, optimality and robustness. The analysis often depends on model construction and how the models are evaluated.

In this work, since we use black box models and adaptive control, it is often difficult to directly apply theoretical analysis to test the controllers. We use a methodical systems approach, where the controller is evaluated in various operating conditions. Along with the classical control theory metrics, we also evaluate our system for scalability and performance.

2.8 Control Theory Based Related Work

In recent years, control theory has been applied to computer systems for resource management and performance control [52, 58]. Examples of its application include web server performance guarantees [22], dynamic adjustment of the cache size for multiple request classes [64], CPU and memory utilization control in web servers [43], adjustment of resource demands of virtual machines based on resource availability [103], and dynamic CPU allocations for multi-tier applications [63, 76]. These concerned themselves with controlling only a single resource (usually CPU), used mostly single-input single-output (SISO) controllers (except in [43]), and required changes in the applications. In contrast, our MIMO controller operates on multiple resources (CPU and storage) and uses the sensors and actuators at the virtualization layer and external QoS sensors without requiring any modifications to applications.

In [43], the authors apply MIMO control to adjust two configuration parameters within Apache to regulate CPU and memory utilization of the Web server. They used fixed linear models, which are obtained by offline system identification for modeling the system. Our earlier attempts at fixed models for controlling CPU and disk resources have failed, and therefore, we used an online adaptive model in this thesis. Our work also extends MIMO control to controlling multiple resources and virtualization, which has more complex interactions than controlling a single web server.

In [95], the authors build a cluster-level power controller that can distribute power based on the application performance needs. The authors develop a MIMO controller for achieveing the power distribution, which is similar to our approach.

CHAPTER 3

Utilization-based CPU Resource Controller

3.1 Introduction

In our first attempt to apply control theory to resource allocation in virtualized systems, we have built an integral controller that allocates CPU resource based on QoS differentiation metric. We address the problem of dynamically controlling resource allocations to individual components of complex, multi-tier enterprise applications in a shared hosting environment. We rely on control theory as the basis for modeling and designing such a feedback-driven resource control system. We develop a two-layered controller architecture that accounts for the dependencies and interactions among multiple tiers in an application stack when making resource allocation decisions. The controller is designed to adaptively adjust to varying workloads so that high resource utilization and high application-level QoS can be achieved. Our design employs a *utilization controller* that controls the resource allocation for a single application tier and an *arbiter controller* that controls the resource allocations across multiple application tiers and multiple application stacks sharing the same infrastructure.

To test our controllers, we have built a testbed for a virtual data center using Xen virtual machines (VMs)[30]. We encapsulate each tier of an application stack in a virtual machine and attempt to control the resource allocation at the VM level. We experimented with two multi-tier applications in our testbed: a two-tier implementation of RUBiS [25], an online auction application, and a two-tier Java implementation of TPC-W [34], an online ecommerce application. We ran experiments to test our controller under a variety of

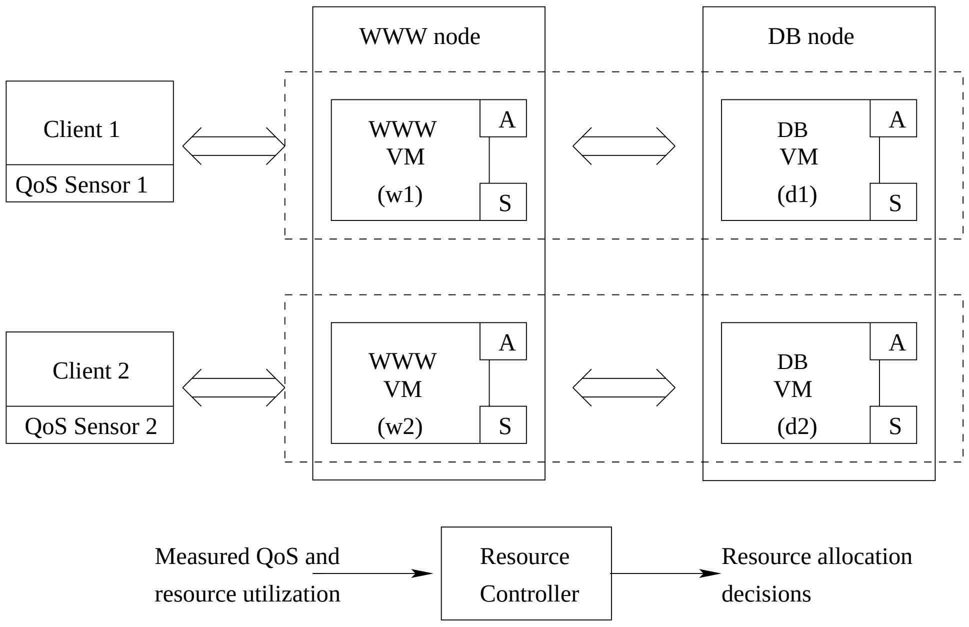

Figure 3.1: A testbed of two virtualized servers hosting two multi-tier applications

workload conditions that put the system in different scenarios, where each node hosting multiple virtual machines is either saturated or unsaturated.

Our experimental results indicate that the feedback control approach to resource allocation and our two-layered controller design are effective for managing virtualized resources in a data center such that the hosted applications achieve good application-level QoS while maintaining high resource utilization. Also, we were able to provide a certain degree of QoS differentiation between co-hosted applications when there is a bottleneck in the shared infrastructure, which is hard to do under standard OS-level scheduling.

3.2 Problem Overview

In this work, we consider an architecture for a virtual data center where multiple multi-tier applications share a common pool of server resources, and each tier for each application is hosted in a virtual machine. This type of shared services environment has become of interest to many enterprises due to its potential of reducing both infrastructure and operational cost in a data center.

Figure 3.1 shows a testbed we built as an example of such an environment. This setup forms a small but powerful system, which allows for testing our controller in various scenarios. To avoid confusion in terminology, we use “WWW VM” and “DB VM” to refer to the two virtual machines that are used to host the web server and DB server software, respectively. We use “WWW node” and “DB node” to refer to the two physical machines that are used to host the web tier and the DB tier, respectively.

The high level goal of the resource controller is to guarantee application-level QoS as much as possible while increasing resource utilization in a utility computing environment. More specifically, our controller design has the following three main objectives:

- **Guaranteed application-level QoS**: When system resources are shared by multiple multi-tier applications, it is desirable to maintain performance isolation between them and to ensure that each application can achieve its QoS goals. In this work, this is realized by dynamically allocating virtualized resources to each virtual machine hosting an application component and always providing a safety margin below 100% utilization if possible, which generally leads to high throughput and low response time in the application.

- **High resource utilization**: It is also desirable to increase overall utilization of the shared resources so that more applications can be hosted. One way to achieve this is to maintain a high enough utilization in individual virtual machines such that there is more capacity for hosting other applications. There is a fundamental trade-off between this goal and the previous goal. It is up to the data center operators to choose an appropriate utilization level to balance these two objectives.

- **QoS differentiation during resource contention**: Whenever a bottleneck is detected in the shared resources, the controller needs to provide a certain level of QoS differentiation that gives higher priority to more critical applications. For example, one can aim to maintain a certain ratio of response times when the system is overloaded based on service level agreements of the respective applications.

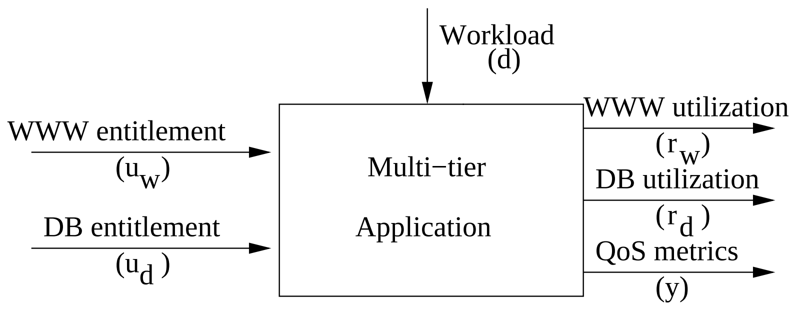

Figure 3.2: An input-output model for a multi-tier application

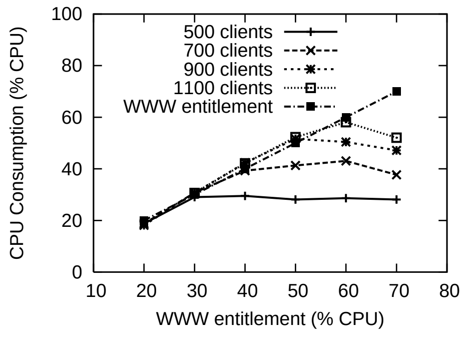

(a) WWW CPU consumption

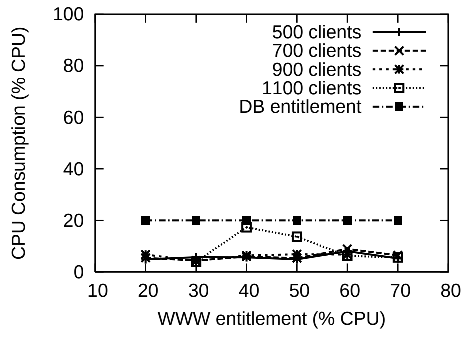

(b) DB CPU consumption

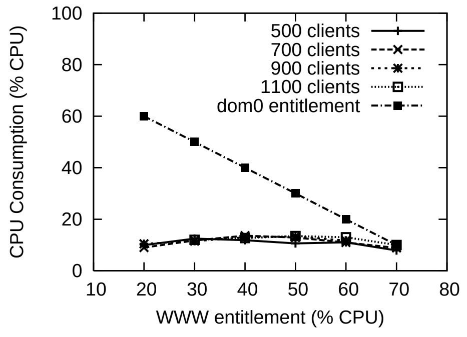

(c) dom0 CPU consumption

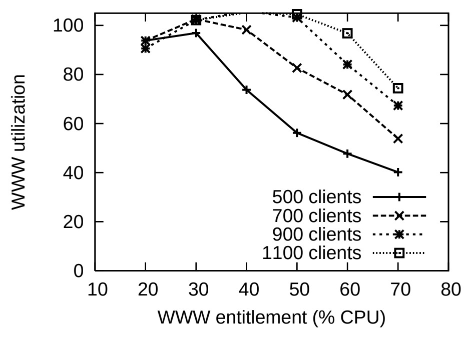

(d) WWW VM utilization

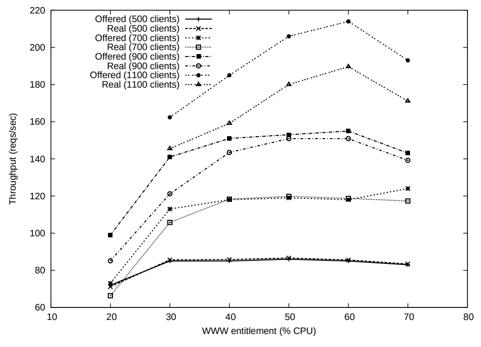

(e) Throughput

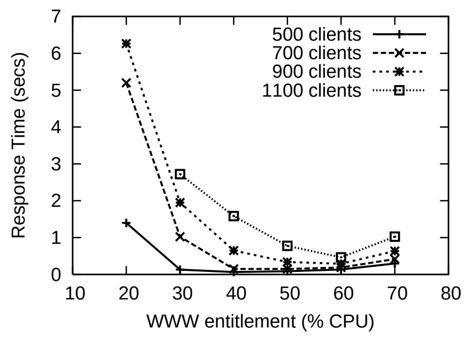

(f) Response time

Figure 3.3: Input-output relationship in a two-tier RUBiS application for [500, 700, 900, 1100] clients

3.3 System Modeling

In control theory, an object to be controlled is typically represented as an input-output system, where the inputs are the control knobs and the outputs are the metrics being controlled. Control theory mandates that a system model that characterizes the relationship between the inputs and the outputs be specified and analyzed before a controller is designed. For traditional control systems, such models are often based on first principles. For computer systems, although there is queueing theory that allows for analysis of aggregate statistical measures of quantities such as utilization and latency, it may not be fine-grained enough for run-time control over short time scales, and its assumption about the arrival process may not be met by certain applications and systems. Therefore, most prior work on applying control theory to computer systems employs an empirical and "*black box*" approach to system modeling by varying the inputs in the operating region and observing the corresponding outputs. We adopted this approach in our work.

A feedback control loop requires an actuator to implement the changes indicated by the control knobs and a sensor to measure the value of the output variables. We use the CPU scheduler of the virtual machine monitor (or hypervisor) that controls the virtual machines as our actuator. The hypervisor we used provides an SEDF (Simple Earliest Deadline First) scheduler that implements weighted fair sharing of the CPU capacity between multiple virtual machines. The scheduler allocates each virtual machine a certain share of the CPU cycles in a given fixed-length time interval. Since these shares can be changed at run time, the scheduler serves as an actuator (A) in our control loop to effect allocation decisions made by the controller. The SEDF scheduler can operate in two modes: capped and non-capped. In the capped (or non-work-conserving) mode, a virtual machine cannot use more than its share of the total CPU time in any interval, even if there are idle CPU cycles available. In contrast, in the non-capped (or work-conserving) mode, a virtual machine can use extra CPU time beyond its share if other virtual machines do not need it. We use the capped mode in our implementation as it provides better performance isolation between the VMs sharing the same physical server.

The hypervisor also provides a sensor (S) to measure how many of the allocated CPU cycles are actually consumed by each virtual machine in a given period of time. This gives the resource controller information on utilization levels of individual virtual machines. In addition, we modified the RUBiS client and the TPC-W client to generate various application-level QoS metrics, including average response time and throughput in a given period.

Before describing our modeling approach, we first define some terminology. We use "entitlement" (u) to refer to the CPU share (in percentage of total CPU capacity) allocated to a virtual machine. We use "consumption" (v) to refer to the percentage of total CPU capacity actually used by the virtual machine. The term "VM utilization" (r) is used to refer to the ratio between consumption and entitlement, i.e., $r = v/u$. For example, if a virtual machine is allocated 40% of the total CPU and only uses 20% of the total CPU on average, then its CPU entitlement is 40%, the CPU consumption is 20%, and the VM utilization is 20%/40% = 50%. Note that all of these terms are defined for a given time interval.

Figure 3.2 illustrates an input-output representation of the system we are controlling, a multi-tier application hosted in multiple virtual machines. The inputs to the system are the resource entitlements for the WWW VM (u_w) and the DB VM (u_d). The outputs include the utilizations of the WWW VM (r_w) and the DB VM (r_d), as well as the application-level QoS metrics (y) such as response time and throughput. The incoming workload (d) to the hosted application is viewed as a "disturbance" to the controlled system because it is not directly under control while having an impact on the system outputs. Typically as the workload varies, the input-output relationship changes accordingly, which increases the difficulty in modeling as well as controller design.

In the remainder of this section, we first describe our experimental testbed. Then we describe a set of system modeling experiments we performed to determine a model for the dynamic behavior of our multi-tier application under various configurations. Our modeling experiments consists of two parts. First, we model the dynamic behavior of a single instance of our multi-tier application, and then we develop a model for the dynamic behavior of two multi-tier applications sharing the same infrastructure.

3.3.1 Experimental Testbed

Our experimental testbed consists of five HP Proliant servers, two of which are used to host two applications. Each application consists of two tiers, a web server tier and a database server tier. Apache and MySQL are used as the web server and database server, respectively, hosted inside individual virtual machines. Although the grouping of application tiers on each physical server can be arbitrary in principle, we specifically chose the design where one machine hosts two web servers and the other hosts two DB servers. This is a natural choice for many consolidated data centers for potential savings in software licensing costs.

We chose Xen as the virtualization technology and we use Xen-enabled 2.6 SMP Linux kernel in a stock Fedora 4 distribution. Each of the server nodes has two processors, 4 GB of RAM, one Gigabit Ethernet interface, and two local SCSI disks. These hardware resources are shared between the virtual machines (or domains in Xen terminology) that host the application components and the management virtual machine (which we will refer as `dom0` as in the Xen terminology). In a few testing scenarios, we restrict the virtual machines hosting the applications to share a designated CPU and direct the `dom0` to use the other CPU to isolate it from interference.

Two other nodes are used to generate client requests to the two applications, along with sensors that measure the client-perceived quality of service such as response time and throughput. The last node runs a feedback-driven resource controller that takes as inputs the measured resource utilization of each virtual machine and the application-level QoS metrics, and determines the appropriate resource allocation to all the virtual machines on a periodic basis. This setup forms a small but powerful system, which allows for testing our controller in various scenarios.

We have used two workload generators for our experiments: RUBiS [25], an online auction site benchmark, and a Java implementation of the TPC-W benchmark [34]. The RUBiS clients are configured to submit workloads of different mixes as well as workloads of time-varying intensity. We have used a workload mix called the *browsing mix* that consists primarily of static HTML page requests that are served by the web server. For more details on the workload generation using RUBiS see [25]. The TPC-W implementation also provides various workload mixes. We have used the *shopping mix*, which primarily stresses the DB server.

The use of two different workloads allows us to change overall workload characteristics by varying the intensities of the individual workloads. In particular, by increasing the relative intensity of the TPC-W workload we can increase the load on the database tier (relative to the load on the web tier), and vice versa. We are now ready to describe our system modeling experiments in this testbed.

3.3.2 Modeling Single Multi-tier Application

In this subsection, we would first like to understand how the outputs in Figure 3.2 change as we vary the inputs, i.e., how the changes in the WWW/DB entitlements impact the utilization of virtual machines and the QoS metrics.

For this experiment, a single testbed node was used to host a two-tier implementation of RUBiS. A single RUBiS client with the browsing mix was used with a certain number of threads simulating many concurrent users connecting to the multi-tier application. In our experiment, we pinned the WWW VM, the DB VM, as well as `dom0` to one processor. We varied the CPU entitlement for the WWW VM from 20% to 70%, in 10% increments. Since the DB consumption for the browsing mix is usually low, we did not vary the CPU entitlement for the DB VM and kept it at a constant of 20%. The remaining CPU capacity was given to `dom0`. For example, when $u_w = 50\%$, we have $u_d = 20\%$, and $u_{\texttt{dom0}} = 30\%$. At each setting, the application was loaded for 300 seconds while the average utilization of the three virtual machines and the average throughput and response time experienced by all the users were measured. The experiment was repeated at different workload intensities, as we varied the number of threads in the RUBiS client from 500 to 1100, in 200 increments.

Figures 3.3a, 3.3b, 3.3c show the CPU consumption by the WWW VM (v_w), the DB VM (v_d), and `dom0` ($v_{\texttt{dom0}}$), respectively, as a function of the WWW entitlement (u_w). In each figure, the four different curves correspond to a workload intensity of 500, 700, 900, 1100 concurrent clients, respectively, while the straight line shows the CPU entitlement for the respective virtual machine, serving as a cap on how much CPU each virtual machine can consume. As we can see from Figure 3.3a, with 500 concurrent clients, the WWW CPU consumption goes up initially as we increase u_w, and becomes flat after u_w exceeds 30%. Figure 3.3d shows the corresponding utilization for the WWW VM, $r_w = v_w/u_w$, as a function of u_w. Note that the utilization exceeds 1 by at most 5% sometimes, which is within the range of actuation error and measurement noise for CPU consumption. We can see that the relationship between the virtual machine utilization and its entitlement can be approximated by the following equation:

$$r_w = \begin{cases} 100\%, & \text{if} \quad u_w <= V; \\ \frac{V}{u_w}, & \text{if} \quad u_w > V, \end{cases} \tag{3.1}$$

where V is the maximum CPU demand for a given workload intensity. For example, for 500 concurrent clients, $V = 30\%$ approximately. This relationship is similar to what we observed for a single-tier web application as described in [96]. With a workload of 700 concurrent clients and above, the relationship remains similar, except when u_w reaches 70%, the WWW consumption starts to drop. This is because when $u_w = 70\%$, `dom0` is only entitled to 10% of the total CPU capacity (see Figure 3.3c), which is not enough to handle workloads with higher intensity due to higher I/O overhead. When `dom0` becomes a bottleneck, the web server CPU consumption decreases accordingly. We do not see correlation between the DB CPU consumption and the DB entitlement or the workload intensity from Figure 3.3b, other than the fact that the consumption is always below 20%.

Figure 3.3e shows the average offered load and achieved throughput (in requests/second) as a function of the WWW entitlement for different workload intensities. We observe that the offered load is not a constant even for a fixed workload intensity. This is because RUBiS is designed as a closed-loop client where each thread waits for a request to be completed before moving on to the next request. As a result, a varying amount of load is offered depending on how responsive the application is. For all workload intensities that were tested, an entitlement of 20% is too small for the web server, and thus the application responds slowly causing the offered load to drop below its maximum. As the WWW entitlement increases, the offered load increases as well because the multi-tier system is getting more work done and responding more quickly. The offered load finally reaches a constant when the

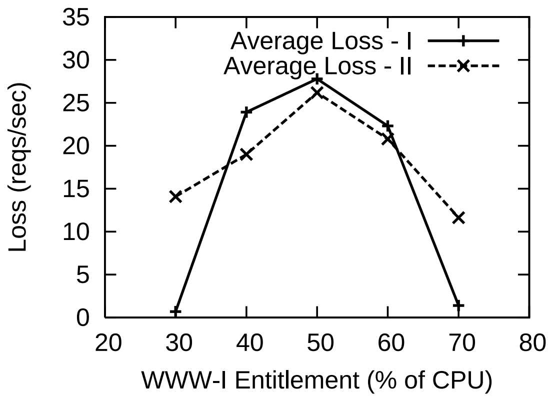

(a) Loss

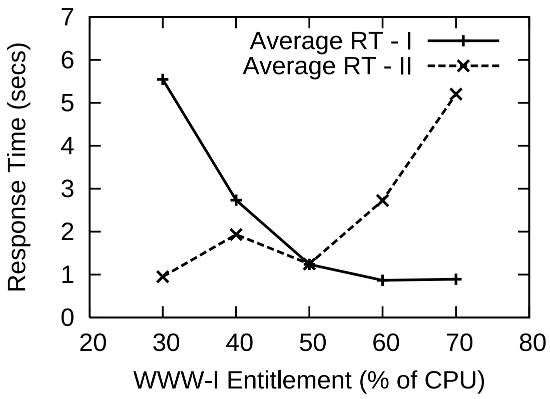

(b) Response time

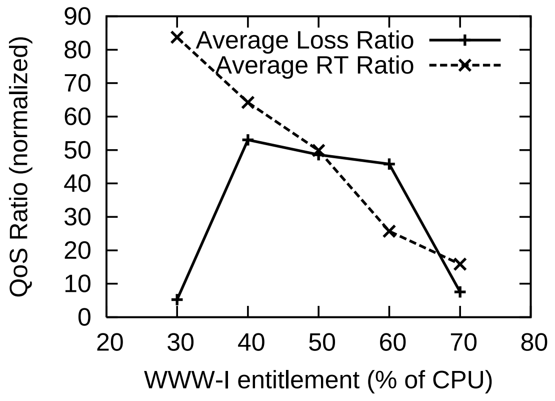

(c) Loss ratio and RT ratio

Figure 3.4: Loss ratio and response time ratio for two RUBiS applications in the WS-DU scenario

web server is getting more than its need. Similarly, as the WWW entitlement is increased, the throughput increases initially and then reaches a constant load. For a larger number of clients (700 and above), we see a similar drop at $u_w = 70\%$ in both the offered load and the throughput because `dom0` starts to become a bottleneck as discussed earlier. We also see a significant loss (requests not completed) with a larger number of clients.

Figure 3.3f shows the average response time as a function of the WWW entitlement, validating our observation on the throughput-entitlement relationship. As u_w increases, response time decreases initially reaching a minimum and then rises again at 70% entitlement because of `dom0` not getting enough CPU. We also note that the response time is roughly inversely proportional to the throughput because of the closed-loop nature of the RUBiS client.

	DB node unsat.	DB node sat.
WWW node unsat.	WU-DU	WU-DS
WWW node sat.	WS-DU	WS-DS

Table 3.1: Four scenarios for two multi-tier applications

3.3.3 Modeling Co-hosted Multi-tier Applications

Now we move on to consider a model for two multi-tier applications sharing the same infrastructure, as illustrated in Figure 3.1. The two applications may be driven with different workload mixes and intensities that can change over time, resulting in different and likely time-varying resource demands for the individual virtual machines hosting different application components. At any given time, either the WWW node or the DB node may become saturated, meaning the total CPU demand from both virtual machines exceeds the capacity of the node, or they may be saturated at the same time. If we use W to represent the WWW node, D to represent the DB node, S to represent saturated, and U to represent unsaturated, then the four cases in Table 3.1 capture all the scenarios that may occur in the shared hosting environment.

The input-output model in Figure 3.2 needs to be augmented to capture the inputs and outputs for both multi-tier applications. In particular, it will have four inputs (u_{w1}, u_{d1}, u_{w2}, u_{d2}) to represent the CPU entitlement for all the four virtual machines. It will also have four outputs (r_{w1}, r_{d1}, r_{w2}, r_{d2}) to represent the utilization of the four virtual machines, and two more outputs (y_1, y_2) to represent the end-to-end QoS metrics for the two applications. We also need a relative metric to enable differentiated service to the two applications when at least one of the nodes is saturated and both applications are contending for resources. Here we define a QoS differentiation metric as follows:

$$y_{ratio} = \frac{y_1}{y_1 + y_2}. \tag{3.2}$$

Note that we use a normalized ratio as opposed to a direct ratio to avoid numerical ill-conditioning. The QoS metric y can be average response time, throughput, or loss as measured in the number of connections that are reset due to timeouts, etc. in a given time interval.

In the following subsections, we explain the relationship between the inputs (entitlement) and the outputs (VM utilization and QoS) in all the four scenarios. We used two RUBiS instances in WU-DU, WS-DU cases and two TPC-W instances in WU-DS case, because the TPC-W clients stress the database more than the RUBiS clients.

3.3.3.1 WU-DU case

When neither the WWW node nor the DB node is saturated, the two applications can have access to the shared resource as much as they need to. Therefore they can be viewed as two independent applications as if they each had their own dedicated nodes. In this case, the model we showed in Section 3.3.2 is applicable to each application and no QoS differentiation metric is necessary. As a result, we can have a controller that controls the resource entitlements for the two applications independently.

3.3.3.2 WS-DU case

This is the scenario where the WWW node is saturated but the DB node is unsaturated. In this case, the CPU capacity of the WWW node cannot satisfy the needs of the two WWW VMs simultaneously. Arbitration is required to decide how much CPU capacity each WWW VM is entitled to based on a given QoS differentiation metric. We can either use a loss ratio or a response time ratio as defined in equation (3.2) as the differentiation metric.

Figures 3.4a and 3.4b show the average loss (number of connections reset per second) and average response time (seconds) for two RUBiS applications as a function of the WWW entitlement (percentage) for application 1 (u_{w1}). Note that $u_{w2} = 1 - u_{w1}$. Figure 3.4c shows the normalized loss ratio and response time ratio between the two applications as a function of u_{w1}.

As we can see from Figure 3.4a, as the first WWW entitlement increases, the loss experienced by clients of both applications first increases and then decreases, resulting in a non-monotonic relationship between the loss ratio and u_{w1} as evident from Figure 3.4c. This is again due to the closed-loop nature of the RUBiS client where the offered load is reduced as either of the application components becomes a bottleneck.

Figure 3.4b shows a different behavior for response time, where the response time for

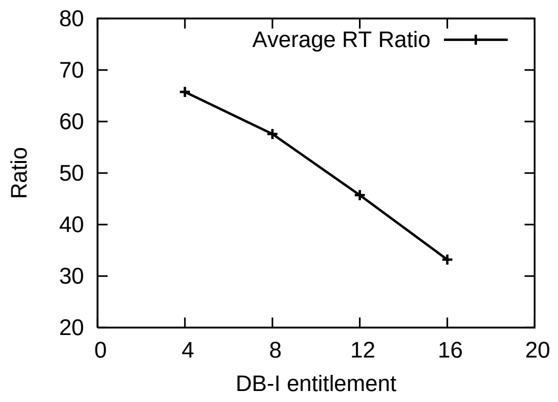

Figure 3.5: Response time ratio for two TPC-W applications in the WU-DS scenario

application 1 goes up and the response time for application 2 goes down, when u_{w1} is increased and u_{w2} is reduced, showing a monotonic relationship between the response time and the WWW entitlement, when the WWW VM is a bottleneck and the DB VM is not. As a result, the response ratio also shows a monotonic relationship with u_{w1} as indicated in Figure 3.4c. Furthermore, the relationship is close to linear. Simple linear regression shows the following relationship,

$$\Delta y_{ratio} = -1.65 \Delta u_{w1}. \tag{3.3}$$

This means a simple linear controller can be designed to find the right value of u_{w1} (and u_{w2} accordingly) to achieve a given target for the response time ratio.

3.3.3.3 WU-DS case

In this scenario, the WWW node is unsaturated but the DB node is saturated. We use TPC-W as the hosted application since it has a higher DB load than what RUBiS has. We use a total capacity of 40% on the DB node to force it to be saturated. (The reason why we cannot make the DB node 100% utilized is due to anomalies in the Xen SEDF scheduler.) This means, $u_{d2} = 40\% - u_{d1}$.

The relationship between the response time ratio and u_{d1} is similar to the WS-DU case, as shown in Figure 3.5. Again the relationship can be approximated using the following linear equation:

$$\Delta y_{ratio} = -2.75 \Delta u_{d1}. \tag{3.4}$$

Again, a simple linear controller can be designed to manage the response time ratio between the two applications.

3.3.3.4 WS-DS case

We were unable to create this scenario in our testbed due to anomalies in the Xen SEDF scheduler. The problem is pronounced with the capping option in scheduling (which provides us with an actuator). Whenever capping is enabled, we always ran into very low CPU consumption on WWW VMs which resulted in low consumption in the DB VMs as well. After various experiments, we concluded that the problem lies in how the Xen scheduler handles capping in the context of I/O-intensive applications.

3.4 Controller Design

In order to achieve the controller objectives outlined in Section 3.4, we designed a two-layered architecture for the controller, as illustrated in Figure 3.6.

The first layer consists of four independent controllers, each of which can be viewed as an “agent” for each of the four virtual machines, $w1$, $w2$, $d1$, $d2$. The role of these agents is to compute the required CPU entitlement ($ureq$) for each virtual machine such that, 1) the hosted application component gets enough resource so that it does not become a bottleneck in the multi-tier application; 2) the virtual machine maintains a relatively high resource utilization. In our design, the way to achieve these goals is to maintain a specified level of utilization in each virtual machine. Therefore, the first layer controllers are referred to as *utilization controllers* (UCs). We describe how the utilization controllers work in Section 3.4.1.

The second layer controller works on behalf of the shared nodes and serves as an “arbiter” that determines whether the requested CPU entitlements ($ureq$) for all of the virtual machines can be satisfied, and if not, decides the final CPU entitlement (u) for each VM

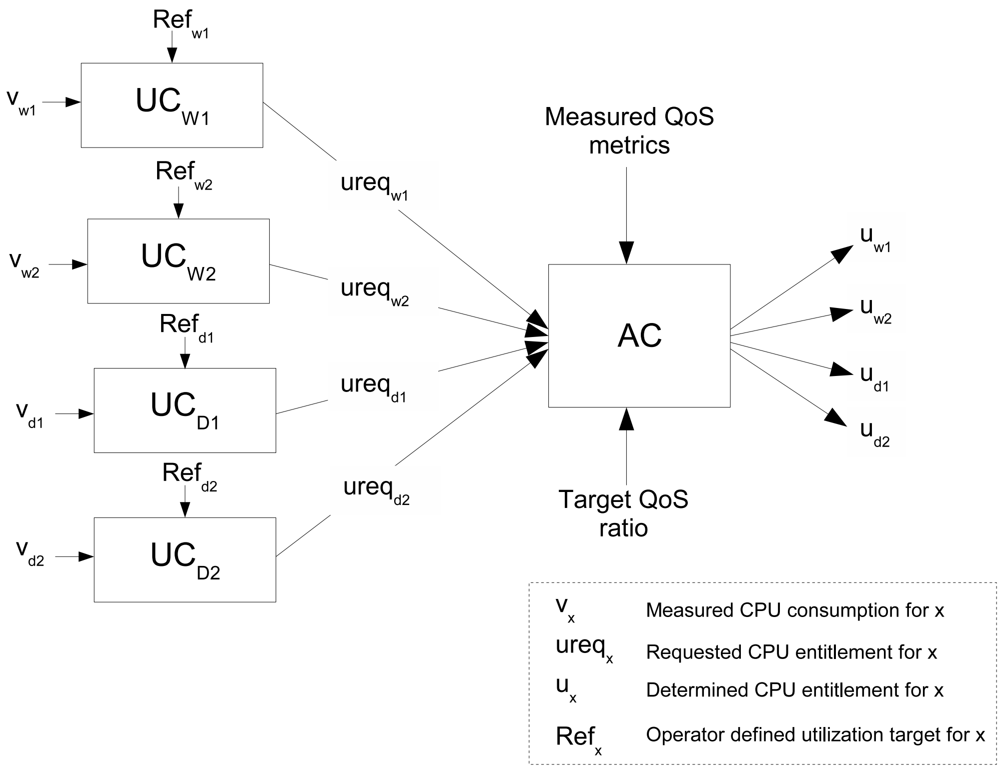

Figure 3.6: A two-layered controller architecture

based on a specified QoS differentiation metric, such as the response time ratio discussed earlier. It is hence referred to as the *arbiter controller* (AC) and will be described in Section 3.4.2.

3.4.1 Utilization Controller

Resource utilization is commonly used by data center operators as a proxy for application performance because of the monotonic relationship between the two and the fact that utilization is easily measurable at the OS level. Take response time as an example. Simple queuing theory indicates that, when CPU is the bottleneck resource, the response time increases sharply as the CPU utilization gets close to 100%. Therefore, most operators prefer to maintain their server utilization below 100% with a certain safety margin to ensure good application performance. At the same time, utilization should be high enough in order to maintain high resource efficiency in the data center. In our design, we choose 80% as the desired utilization level for the individual VMs. This is determined by examining Figures

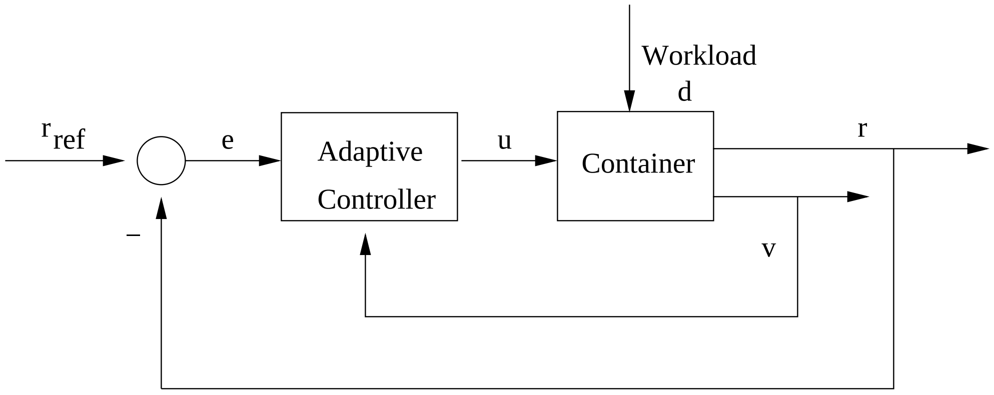

Figure 3.7: Adaptive utilization controller

3.3d, 3.3e and 3.3f together, which show that both the response time and the throughput are at an acceptable level when the utilization of the bottleneck tier, the WWW VM, stays below this target.

We have developed an adaptive integral controller in [96] for dynamic sizing of a virtual machine based on its consumption such that the relative utilization of the VM can be maintained in spite of the changing demand. The block diagram for the controller is shown in Figure 3.7. At the beginning of the control interval k, the controller takes as inputs the desired utilization (r_{ref}) and the measured consumption during the previous interval ($v(k-1)$). The controller computes the utilization of the VM (r) as $r(k-1) = v(k-1)/u(k-1)$ and the tracking error (e) as $e(k-1) = r_{ref} - r(k-1)$, and decides the resource entitlement (u) for the VM for the next interval.

This controller is applied in our work as the utilization controllers in the first layer of our controller architecture. For each VM, the UC calculates the required CPU entitlement ($ureq$) using the following control law:

$$ureq(k) = ureq(k-1) - K(k)e(k-1). \tag{3.5}$$

The integral gain parameter $K(k)$ determines how aggressive the controller is in correcting the observed error. The value of $K(k)$ adapts automatically to the varying workload by calculating $K(k) = \lambda * v(k-1)/r_{ref}$, where λ is a tunable constant. Compared to a standard integral controller that has a fixed K value, our adaptive integral controller with a self-tuning gain makes a better tradeoff between stability and efficiency of the closed-loop system. In addition, it has been proven that this controller is globally stable if $\lambda < 1/r_{ref}$ [96].

3.4.2 Arbiter Controller

The four utilization controllers submit the requested CPU entitlements, $ureq_{w1}$, $ureq_{w2}$, $ureq_{d1}$, and $ureq_{d2}$, to the arbiter controller as shown in Figure 3.6. There are four possible scenarios the arbiter controller needs to deal with, as shown in Table 3.1 in the previous section. Next, we describe the controller logic for each of the scenarios.

- **WU-DU case** ($ureq_{w1} + ureq_{w2} \leq 1$ & $ureq_{d1} + ureq_{d2} \leq 1$): In this case, all of the requested CPU entitlements can be satisfied. Therefore, the final CPU entitlements are, $u_i = ureq_i, i \in \{w1, w2, d1, d2\}$.

- **WS-DU case** ($ureq_{w1} + ureq_{w2} > 1$ & $ureq_{d1} + ureq_{d2} \leq 1$): In this case, the DB node has enough CPU capacity to satisfy both DB VMs, but the WWW node does not have sufficient capacity. Therefore, the arbiter controller grants the DB VMs their requested entitlements, i.e., $u_{d1} = ureq_{d1}$, $u_{d2} = ureq_{d2}$. At the same time, another control algorithm is needed to compute the appropriate values for u_{w1} (and $u_{w2} = 1 - u_{w1}$) such that the QoS ratio y_{ratio} is maintained at a specified level. Here we use a simple integral controller to perform this task. A regular integral controller implements a control law similar to the one in Eq. (3.5), except with a constant gain value K, which determines the aggressiveness of the controller in its corrective actions. We use a fixed gain instead of a variable one in this case because the relationship between y_{ratio} and u_{w1} is linear, as indicated by the empirical model in Eq. (3.3). As a result, we can show that this controller is stable if $K < 1/1.65 = 0.61$. We chose $K = 0.1$ in our implementation to provide some stability margin in face of model uncertainty and measurement noise.

- **WU-DS case** ($ureq_{w1} + ureq_{w2} \leq 1$ & $ureq_{d1} + ureq_{d2} > 1$): This case is similar to the WS-DU case, except that now it is the DB node that does not have enough capacity to satisfy both DB VMs. Therefore, we let $u_{w1} = ureq_{w1}$, $u_{w2} = ureq_{w2}$, and a similar integral controller is implemented to compute u_{d1} (and $u_{d2} = 1 - u_{d1}$) to maintain the same QoS ratio. A similar analysis shows that we need to have an integral gain $K < 1/2.75 = 0.36$ for stability. Similarly, we chose $K = 0.1$ for better robustness of the controller.

- **WS-DS case** ($ureq_{w1} + ureq_{w2} > 1$ & $ureq_{d1} + ureq_{d2} > 1$): This occurs when both the WWW and DB nodes are saturated. In principle, the arbiter controller needs to compute both u_{w1} and u_{d1} in order to maintain the desired QoS ratio. However, we could not produce this scenario in our experiments as mentioned earlier and therefore, will not discuss it further.

The QoS ratio is the key metric that drives the arbiter controller. We have discussed the properties of both the loss ratio and the response time (RT) ratio in Section 4. In the next section, we will show experimental results using both metrics, and validate that the RT ratio is a more sensible metric for QoS differentiation between two applications.

3.5 Evaluation Results

This section presents experimental results that validate the effectiveness of our controller design in a variety of scenarios.

3.5.1 Utilization Controller Validation

We first need to validate the behavior of the utilization controllers to move forward with more complex experiments. The goal is to validate that when the two nodes are not saturated, 1) the utilization controllers achieve a set target utilization for the individual virtual machines; 2) both applications have QoS metrics that are satisfactory.

In this experiment, two RUBiS clients with 300 threads each were used to submit requests under a browsing mix. In the middle of the run, 300 more threads were added to the first client for a duration of 300 seconds. Initially, the two WWW VMs were each given a 50% CPU entitlement, and the two DB VMs were each given a 20% entitlement. Then the four utilization controllers adjusted the entitlement for each VM every 10 seconds, using a

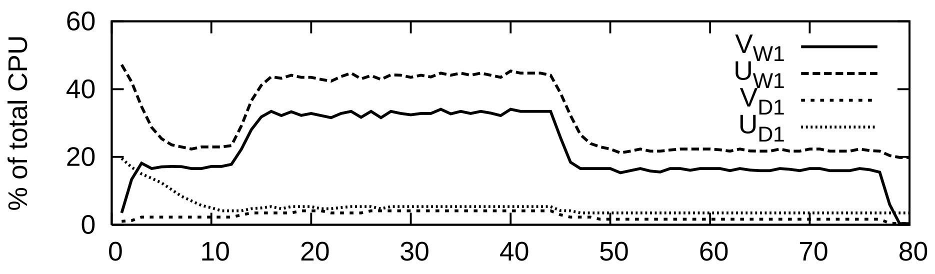

(a) CPU entitlement (u) and consumption (v)

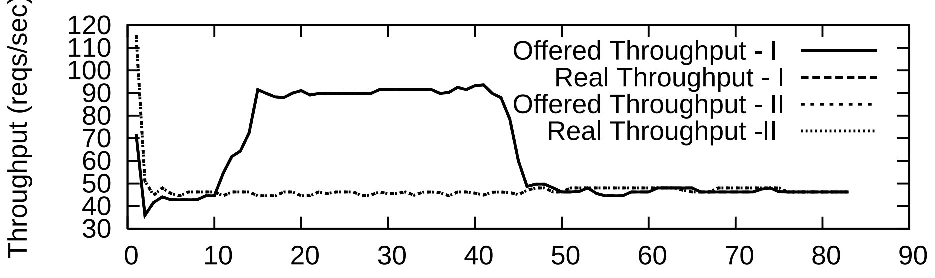

(b) Throughput

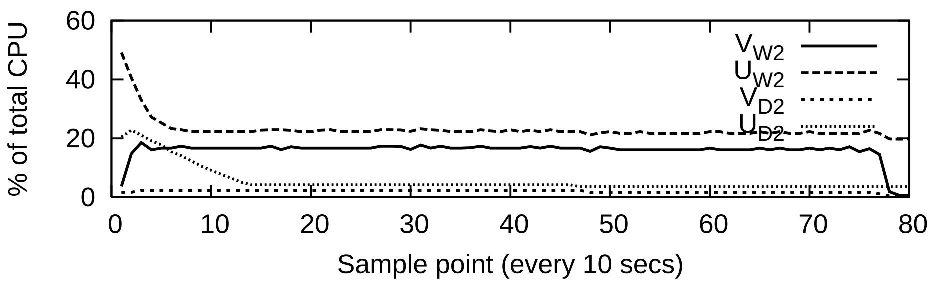

(c) CPU entitlement (u) and consumption (v)

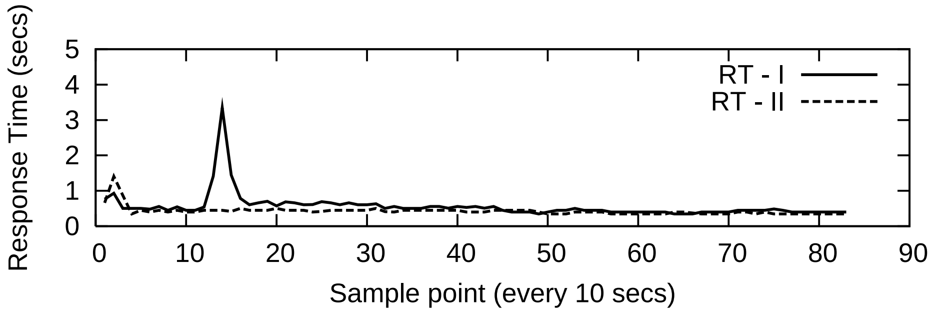

(d) Response time

Figure 3.8: Utilization controller results in the WU-DU case

target utilization of 80%.

Figures 3.8a and 3.8c show the measured CPU consumption (v) of all the VMs, and how the entitlement (u) for each VM was adjusted by the utilization controller such that a roughly 20% buffer was always maintained above the consumption. It is clear that the utilization controller can automatically allocate higher CPU capacity to the first WWW VM when its user demand was increased.

Figures 3.8b and 3.8d show the resulting throughput (requests/second) and response time (seconds) for the two applications. Both applications were shown to achieve their maximum throughput and a low response time in spite of changes in resource demands throughout the run, except during the transient period.

3.5.2 Arbiter Controller - WS-DU Scenario

In this scenario, the WWW node is saturated, but the DB node is not saturated. Based on the two-layered controller design, the two utilization controllers for the two DB VMs are used to compute CPU entitlements on the DB node (u_{d1} and u_{d2}), while the arbiter controller is used to determine entitlements for the two WWW VMs, where $u_{w1} + u_{w2} = 1$. We performed a set of experiments to understand the behavior of the arbiter controller with different QoS ratio metrics. Again we used two RUBiS clients under a browsing mix.

3.5.2.1 Experiment with Loss Ratio

First, we drive the arbiter controller using a target for the ratio of loss seen by both clients. Loss is defined as the number of connections that are dropped after five retries. Intuitively it looks like a good metric capturing the level of performance loss when at least one component of the multi-tier application is overloaded.

In this experiment, we used 1000 threads on each client so that the total required CPU entitlement, $ureq_{w1} + ureq_{w2} > 1$, causing the WWW node to become saturated. As a result, both applications may experience some performance degradation. We set the target loss ratio to be 1:1, or the target for the normalized ratio, $y_{ratio} = \frac{y_1}{y_1+y_2}$, at 50%, where the loss (y_i) is normalized with respect to the offered load for application i. The two WWW VMs were given a CPU entitlement of 70% and 30% initially. The desirable behavior of the arbiter controller is that it should eventually (after transients) distribute the WWW node's CPU capacity equally between the two WWW VMs because the resource demands from the two hosted applications are identical.

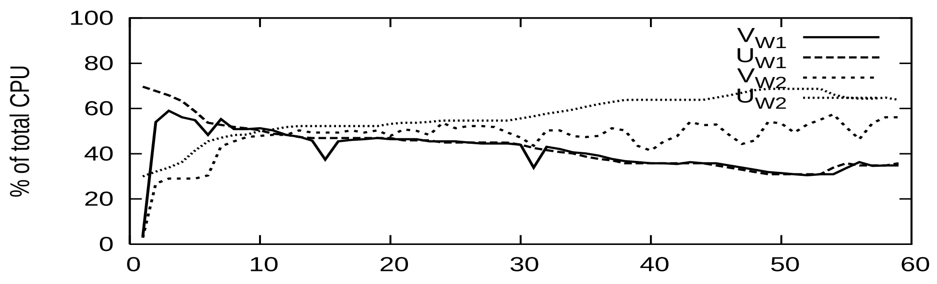

(a) CPU entitlement (u) and consumption (v)

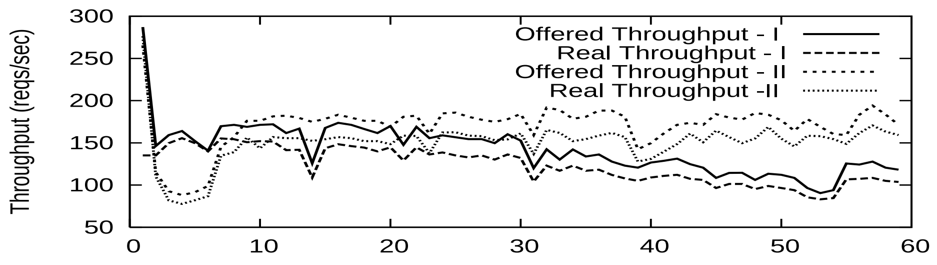

(b) Throughput

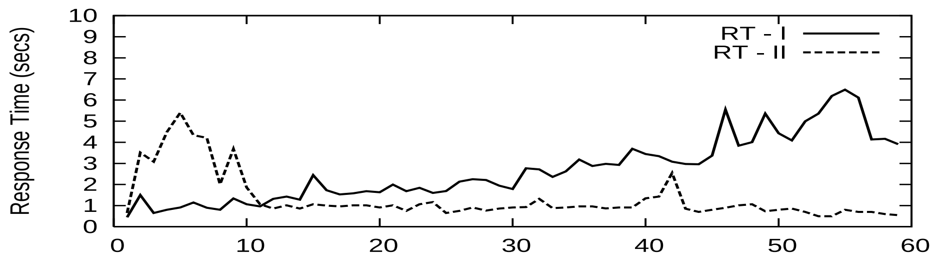

(c) Response time

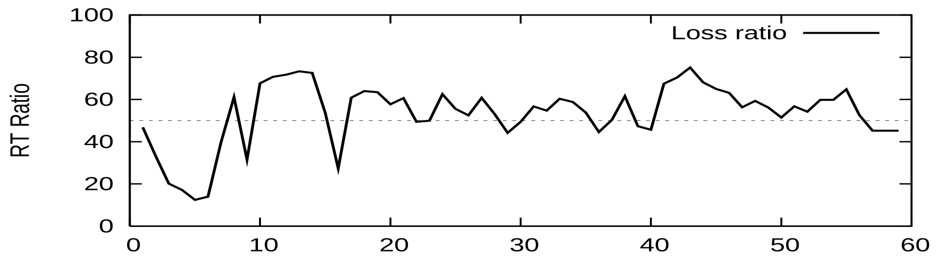

(d) Normalized loss ratio

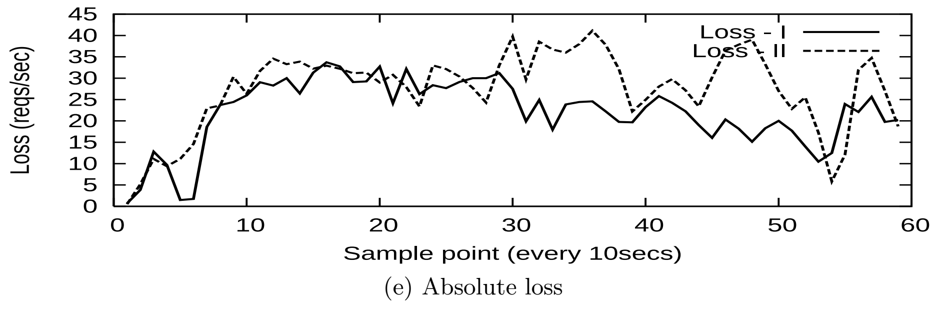

(e) Absolute loss

Figure 3.9: Loss ratio experiment results

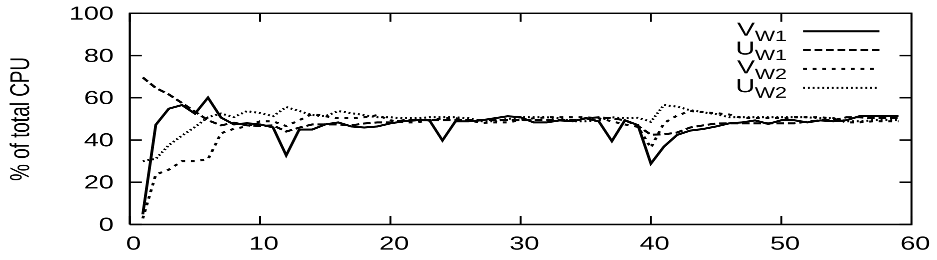

(a) CPU entitlement (u) and consumption (v)

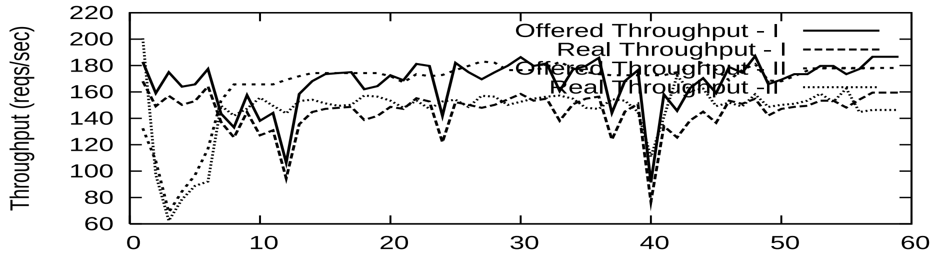

(b) Throughput

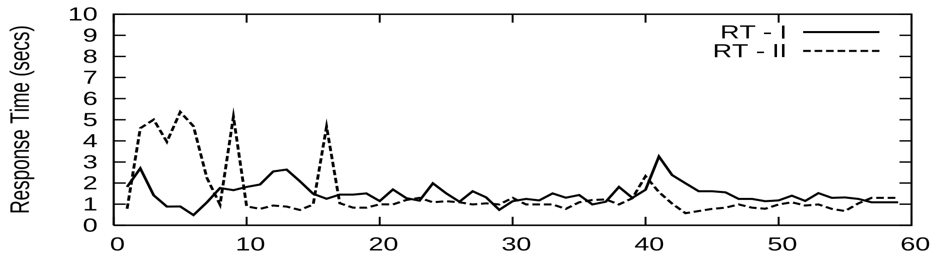

(c) Response time

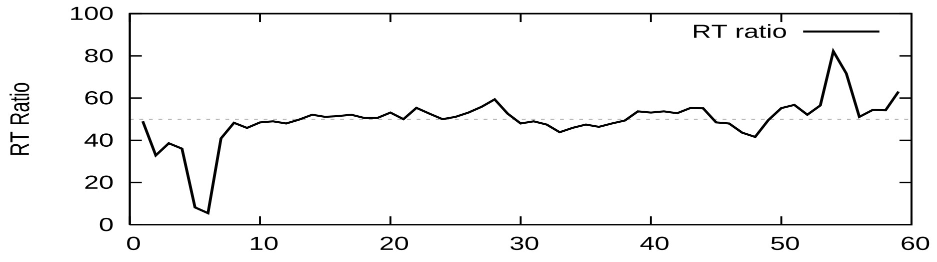

(d) Normalized RT ratio

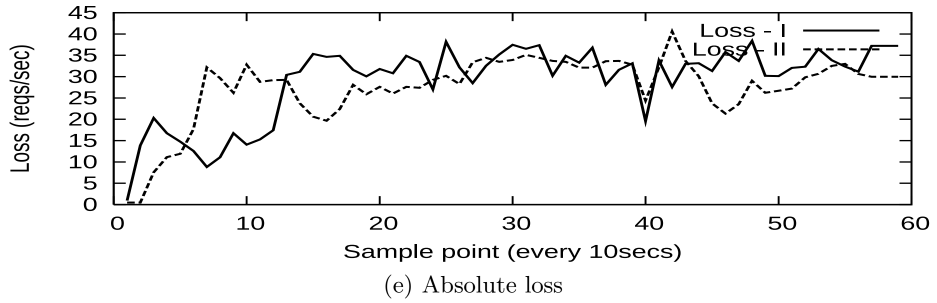

(e) Absolute loss

Figure 3.10: RT ratio experiment results

Figure 3.9a shows the measured CPU consumption (v_{w1} and v_{w2}) and the CPU entitlement (u_{w1} and u_{w2}) determined by the arbiter controller for the two WWW VMs. Figures 3.9b and 3.9c show the resulting throughput and response time for the two applications. Figures 3.9d and 3.9e show the the normalized loss ratio (y_{ratio}) and absolute loss (requests/second) seen by the two clients. As we can see, although the normalized loss ratio was maintained around 50%, as time progressed, the second WWW VM was actually receiving higher and higher CPU entitlement over time. As a result, application 2 was able to deliver much better throughput and response time compared to application 1.

This behavior is highly undesirable. It can be explained by revisiting Figure 3.4c in Section 3.3. Because the relationship between the loss ratio and the entitlement is not monotonic, any given target loss ratio can either be unachievable (if too high or too low), or may have more than one equilibrium. This means that a loss ratio of 1:1 can be achieved not only when $u_{w1} = u_{w2}$, but also when $u_{w1} \neq u_{w2}$. This again is due to the closed-loop nature of the RUBiS client. A slight disturbance in the CPU entitlement can cause one client to submit less load thus getting less throughput. However, the normalized loss seen by this client may still be equal to that of the other client, resulting in the loss ratio maintained at 1:1, and the controller cannot see the erratic behavior. This problem can be fixed by using the response time ratio as the QoS differentiation metric.

3.5.2.2 Experiments with RT Ratio

Figures 3.10a, 3.10b, 3.10c, 3.10d, 3.10e show the results using the RT ratio as the driving metric for the arbiter controller. The remaining test conditions were kept the same, and an RT ratio of 1:1 was used. Here, we see very desirable behavior where the arbiter controller grants equal entitlements to the CPU capacity between the two WWW VMs. Consequently, the two multi-tier applications achieve fairly comparable performance in terms of throughput and response time. Comparison between this result and the result from the previous experiment shows that the RT ratio is a fairer metric than the loss ratio to be used for QoS differentiation among co-hosted applications. One natural question around this subject is, why not use a throughput ratio instead? The answer is two-fold. First, for a closed-loop client, response time is on average inversely proportional to throughput when the server is overloaded. Therefore, an RT ratio implicitly determines a throughput ratio. Second, the absolute throughput is upper-bounded by the offered load. Therefore, it is not sensible to enforce an arbitrary throughput ratio between two applications if they have drastically different offered loads.

We repeated the experiment using RT ratio under different workload conditions, including workloads with different intensities and time-varying workloads, to make sure that the controller is behaving properly. Time-varying workloads can be realized by starting and stopping different numbers of threads in either of the clients over time. Figures 3.11a, 3.11b, 3.11c, 3.11d, and 3.11e show the the behavior of the controller in an experiment where both clients started with 500 threads each, and client 2 jumped to 1000 threads at the 20th control interval and dropped back to 500 threads later. The target for the normalized RT ratio is set to 70%. When both workloads were at 500 threads (before sample 20 and after sample 95), only the utilization controllers were used because neither node was saturated. Note that in Figure 3.11d, the RT ratio is shown at exactly 70% for the initial period. This is not from measurement. Rather it is an indication of the fact that the arbiter controller was not used and the target RT ratio was not enforced during these two periods. The arbiter controller was only triggered when the demand from client 2 was suddenly increased and the WWW node became saturated. During this period of time, the arbiter controller was able to maintain the normalized RT ratio at the target. Since the target gives priority to application 2, it was able to achieve lower response time and higher throughput than application 1.

For comparison, we ran the experiment under similar time-varying workload without using a controller. The results are shown in Figures 3.12a, 3.12b, 3.12c, 3.12d, and 3.12e. In this case, no resource entitlements are enforced. This is done by using the non-capped mode of the SEDF scheduler in Xen, which allows both VMs to use as much CPU as needed until the node is saturated. As we can see, the two WWW VMs consumed roughly equal amount of CPU capacity on the WWW node when both clients had 500 threads. The situation on the DB node was similar. As a result, both applications achieved comparable throughput and response time during this period of time, and the normalized RT ratio is kept around 50% on average. However, when client 2 jumped to 1000 threads at the

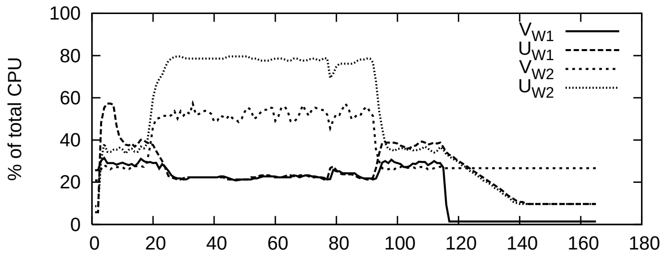

(a) CPU entitlement (u) and consumption (v)

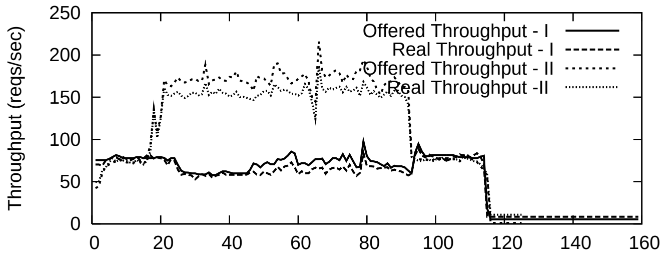

(b) Throughput

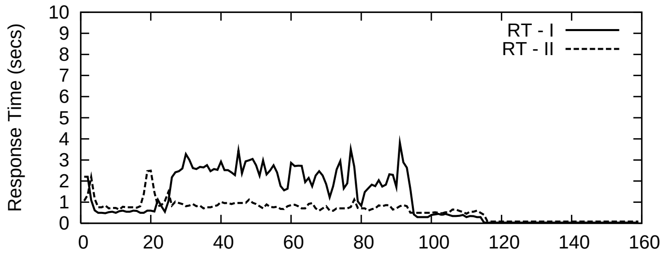

(c) Response time

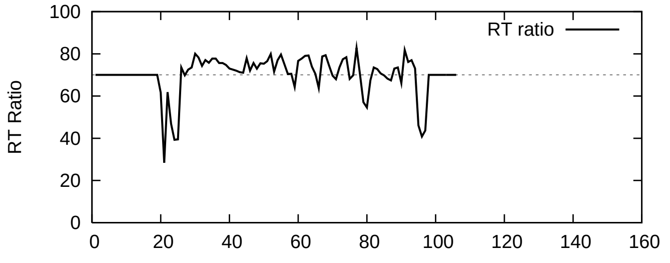

(d) Normalized RT ratio

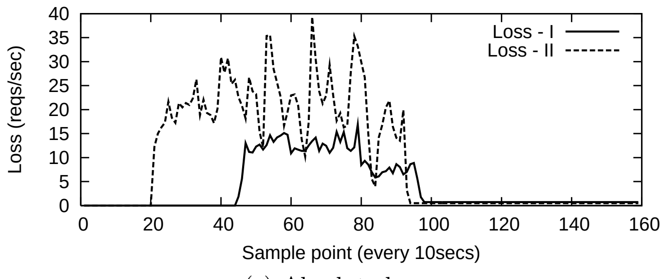

(e) Absolute loss

Figure 3.11: RT ratio experiments - time-varying workload, with controller

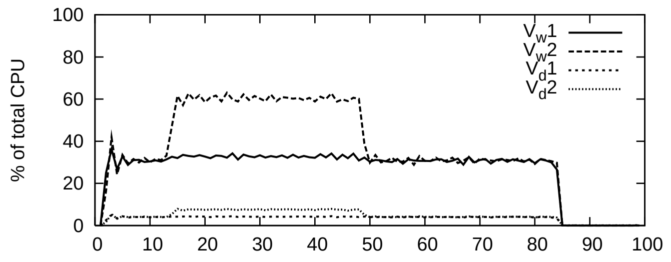

(a) CPU entitlement (u) and consumption (v)

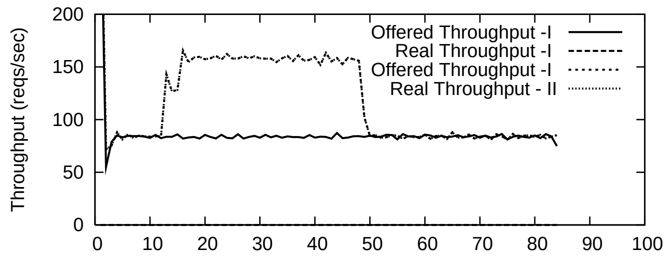

(b) Throughput

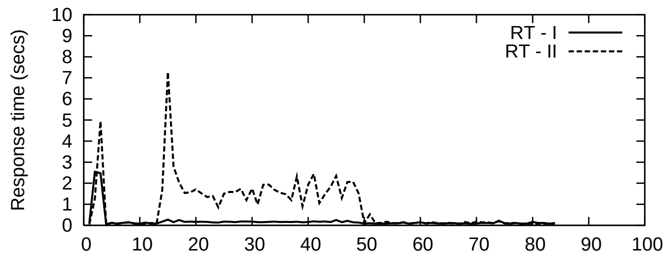

(c) Response time

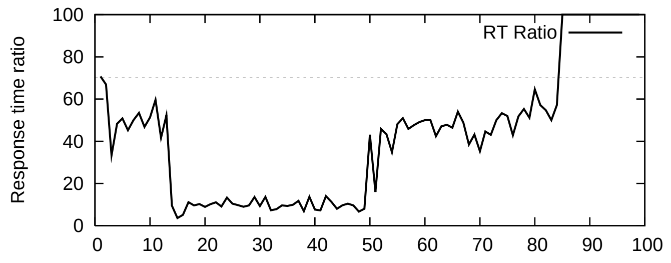

(d) Normalized RT ratio

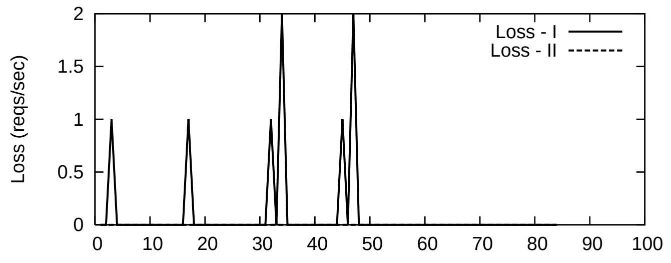

(e) Absolute loss

Figure 3.12: RT ratio experiments - time-varying workload, without controller

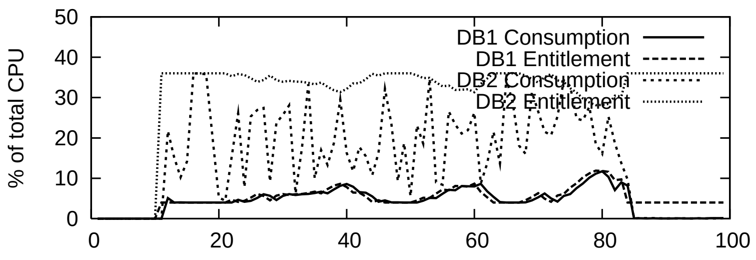

(a) CPU entitlement and consumption

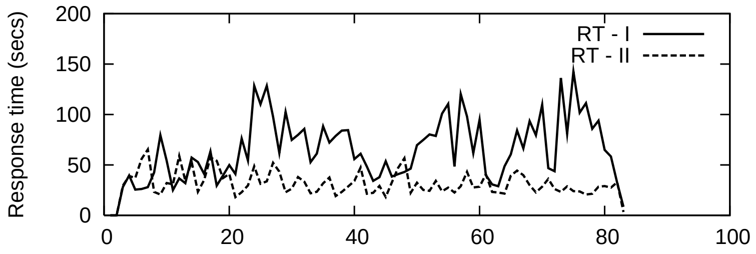

(b) Response time

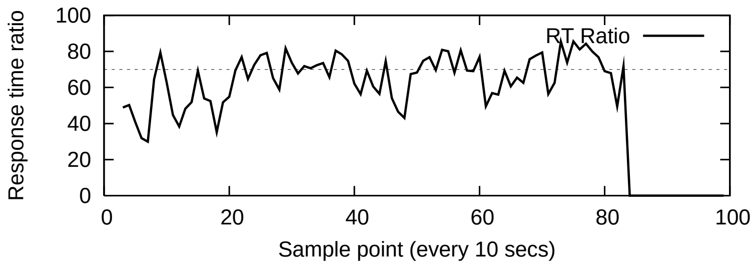

(c) Normalized RT ratio

Figure 3.13: Database heavy load - with controller

15th interval, the resource demand for application 2 suddenly increased. This led to an increase in CPU consumption in both WWW VM 2 and DB VM 2, and an increase in both the throughput and response time for this application. Consequently, the normalized RT ratio becomes approximately 10%, as shown in Figure 3.12d. The exact value will be different for different combinations of workload intensities. Because we do not have control over how CPU capacity is scheduled inside the kernel, we cannot enforce a specific level of differentiation between the two applications.

3.5.3 Arbiter Controller - WU-DS Scenario

This is the case where the WWW node is un-saturated but the DB node is saturated. Similarly, the arbiter controller is needed to determine the CPU entitlements for the two

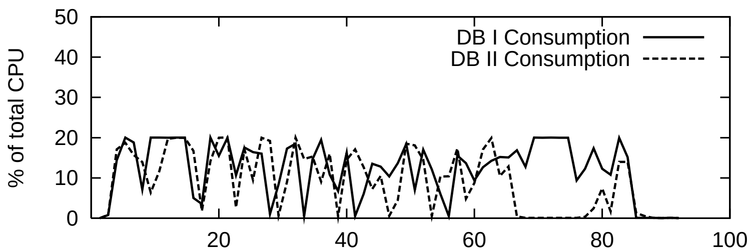

(a) CPU consumption for two DB VMs

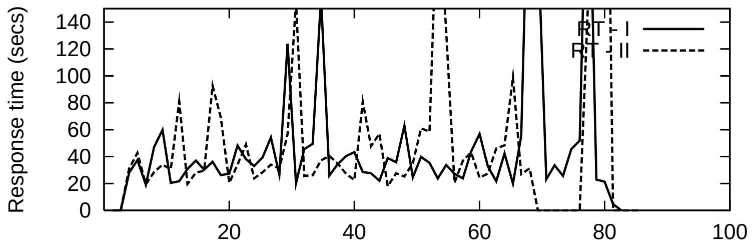

(b) Response time

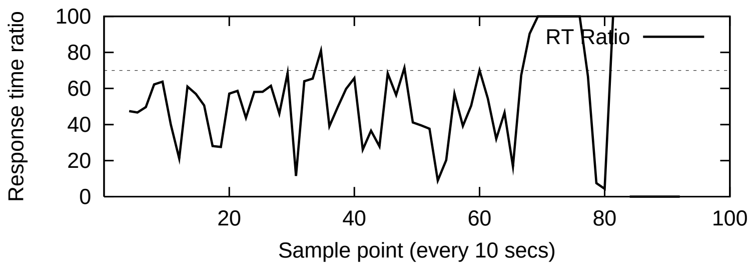

(c) Normalized RT ratio

Figure 3.14: Database heavy load - without controller

DB VMs. We tested our controller by using two instances of the TPC-W benchmark as the two applications. A shopping mix was used to generate the client requests in order to place more stress on the DB tier. Since the total DB load does not go up to 100%, we capped the sum of u_{d1} and u_{d2} at 40% in order to create the WU-DS scenario for testing our controller. Again, a target RT ratio of 70% was used.

We tested the controller against different workload combinations. An example is shown in Figures 3.13a, 3.13b, and 3.13c where two TPC-W clients each with 300 threads were used. The arbiter controller was able to maintain the normalized RT ratio around the target, but with more oscillation than was present in the WS-DU case. This can be explained by inspecting the measured CPU consumption and response time over time. Both metrics show a great deal of variation, indicating the greater burstiness of a DB-intensive workload compared to a web-intensive workload. It is also shown in the larger scaling factor in Eq. (3.4) compared to Eq. (3.3), indicating a higher sensitivity of the response time with respect to a small change in the entitlement. In spite of the noise in the various metrics, application 2 did receive better QoS from the system in general, as driven by the RT ratio for service differentiation.

Again, for comparison, we ran the experiment under the same workload condition without using a controller. The results are shown in Figures 3.14a, 3.14b, and 3.14c. As we can see, the CPU capacity of the DB node was shared roughly equally between the two DB VMs resulting in comparable average response time for the two applications. Figure 3.14c shows the resulting RT ratio oscillating around an average value of 50%. This result re-confirms that, without a feedback-driven resource controller, we cannot provide QoS differentiation between the two applications at a specified level when the system is overloaded.

3.6 Summary

In this work, we built a testbed for a data center hosting multiple multi-tier applications using virtualization. We have developed a two-layered controller using classical control theory. The controller algorithms were designed based on input-output models inferred from empirical data using a black-box approach. The controller was tested in various scenarios including stressing the web and the database tier separately. The experimental results confirmed that our controller design achieves high utilization of the data center while meeting application-level QoS goals. Moreover, it is able to provide a specified level of QoS differentiation between applications under overload conditions, which cannot be obtained under standard OS-level scheduling that is not QoS-driven.

We still see space for improvement in controller performance, in terms of better stability and responsiveness, especially for DB intensive workloads. In this work, only fixed models were used to capture the input-output relationship in the steady state, which simplifies both the modeling process and the controller design. In the next chapter, we explore the use of a dynamic model to capture more transient behavior of the system and use it as the basis for better controller design. We also want to explore the effect of VM migration on our controller.

We would like to extend our work to control sharing of memory, disk I/O, and network resources. These resources pose unique challenges as sharing I/O resources usually involves sharing of related buffers in the kernel as well. Currently, the virtualization technologies do a poor job of providing control of sharing and isolation of I/O resources. With the advent of I/O virtualization technologies from CPU vendors, this may change and we would like to apply our algorithms to take full advantage of the new hardware capabilities.

In the next chapter, we describe a multi resource controller that uses an adpative online model and can control multiple resources.

CHAPTER 4

Multi-resource Controller

4.1 Introduction

In this chapter, we address the problem of managing the allocation of computational resources in a shared, virtualized infrastructure to achieve application-level SLOs. Our solution to this problem is *AutoControl*, an automated resource control and adaptation system.

Our main contributions are twofold: First, we design an online model estimator to dynamically determine and capture the relationship between application level performance and the allocation of individual resource shares. Our adaptive modeling approach captures the complex behavior of enterprise applications including varying resource demands over time, resource demands from distributed application components, and shifting demands across multiple resources types. Second, we design a two-layered, multi-input, multi-output (MIMO) controller to *automatically* allocate multiple types of resources to multiple enterprise applications to achieve their SLOs. The first layer consists of a set of application controllers that automatically determines the amount of resources necessary to achieve individual application SLOs, using the estimated models and a feedback approach. The second layer is comprised of a set of node controllers that detect resource bottlenecks on the shared nodes and properly allocate resources of multiple types to individual applications. In overload cases, the node controllers can provide service differentiation by prioritizing allocation among different applications.

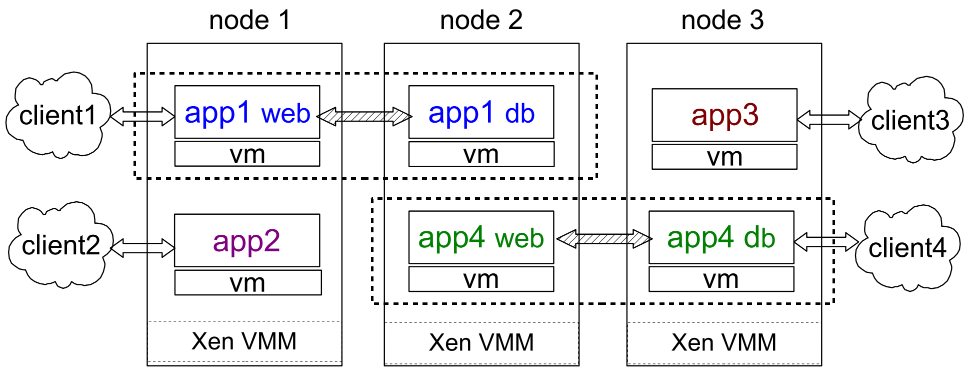

Figure 4.1: **Physical organization**: Each node hosts multiple applications running on VMs. Applications can span multiple nodes

We have built a testbed using Xen [30], and evaluated our controller in various scenarios. Our experimental results indicate that *AutoControl* can detect and adapt to bottlenecks happening in both CPU and disk across multiple nodes. We show that the controller can handle multiple multi-tier applications running RUBiS and TPC-W benchmarks along with workloads driven by production traces. We also show that priorities can be enforced among different applications during resource contention.

4.2 Problem Overview

In this section, we present an overview of our system architecture and the assumptions and goals that drive our design. We assume that applications are hosted within containers or virtual machines (VM) [30] to enable resource sharing within a virtualized server node. A multi-tier application may run on multiple VMs that span nodes. Figure 4.1 shows an example with three nodes hosting four applications.

In *AutoControl*, operators can specify the requirements for an application in a tuple $(priority, metric, target)$, where *priority* represents the priority of the application, *metric* specifies the performance metric (e.g., transaction throughput, 90th percentile of response time), and *target* specifies the performance target. Currently, our implementation supports only a single metric specification within *AutoControl* at a time, although the architecture can be generalized to support different metrics for different applications.

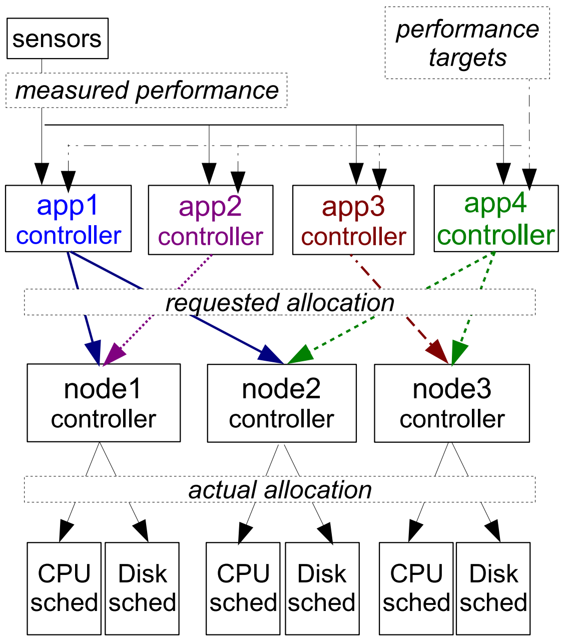

Figure 4.2: **Logical controller organization**: Each application has one application controller. Each node has one node controller that arbitrates the requests from multiple application controllers

AutoControl can use any resources that affect the application metrics of interest and that can be allocated between the applications; in this paper, we use CPU and disk I/O as the resources, and application throughput or average response time as the performance metric. *AutoControl* consists of a set of application controllers (AppControllers) and a set of node controllers (NodeControllers). There is one AppController for each hosted application, and one NodeController for each virtualized node. Figure 4.2 shows the logical controller architecture for the system shown in Figure 4.1. For each application, its AppController periodically polls an application performance sensor for the measured performance. We refer to this period as the *control interval*. The AppController compares this measurement with the application performance target, and based on the discrepancy, automatically determines the resource allocations needed for the next control interval, and sends these requests to the NodeControllers for the nodes that host the application.

For each node, based on the collective requests from all relevant AppControllers, the corresponding NodeController determines whether it has enough resource of each type to satisfy all demands, and computes the actual resource allocation using the methods described in Section 4.3. The computed allocation values are fed into the resource schedulers in the virtualization layer for actuation, which allocate the corresponding portions of the node resources to the VMs in real time. Figure 4.2 shows CPU and disk schedulers as examples.

The *AutoControl* architecture allows the placement of AppControllers and NodeControllers in a distributed fashion. NodeControllers can be hosted in the physical node they are controlling. AppControllers can be hosted in a node where one of the application tiers is located. We do not mandate this placement, however, and the data center operator can choose to host a set of controllers in a node dedicated for control operations.

We assume that all nodes in the data center are connected with a high speed network, so that sensor and actuation delays within *AutoControl* are small compared to the control interval. We also require accurate system sensors and actuators, and assume that the underlying system schedulers provide a rich enough interface to dynamically adjust resource shares for VMs.

We set the following goals in designing *AutoControl*:

Performance assurance: If all applications can meet their performance targets, *AutoControl* should allocate resources properly to achieve them. If they cannot be met, *AutoControl* should provide service differentiation according to application priorities.

Automation: While performance targets and certain parameters within *AutoControl* may be set manually, all allocation decisions should be made *automatically* without human intervention.

Adaptation: The controller should adapt to variations in workloads or system conditions.

Scalability: The controller architecture should scale to a large environment with many applications and nodes by not requiring a single centralized controller.

4.3 Controller Design

This section details the design of both AppController and NodeController in the two-layered architecture of *AutoControl*. For easy reference, Table 4.1 summarizes the mathe-

Table 4.1: Notation

A	set of all hosted applications
T_a	set of all the tiers in application $a \in A$, e.g., $T_a = \{web, db\}$
R	set of all resource types controlled, e.g., $R = \{cpu, disk\}$
k	index for control interval
$x(k)$	value of variable x in control interval k
$ur_{a,r,t}$	requested allocation of resource type r to tier t of application a, $0 \leq u_{a,r,t}(k) \leq 1$ ($ur_{a,r}$ for single-tier applications)
$u_{a,r,t}$	actual allocation of resource type r to tier t of application a, $0 \leq u_{a,r,t}(k) \leq 1$ ($u_{a,r}$ for single-tier applications)
y_a	measured performance of application a
yr_a	performance target for application a
yn_a	normalized performance for application a, where $yn_a = y_a/yr_a$
w_a	priority weight for application a
q	stability factor in the AppController

matical symbols that will be used for key parameters and variables in these controllers.

4.3.1 Design of AppController

As introduced in Section 4.2, every hosted application has an AppController associated with it. In order for each AppController to decide how much resource is needed for the application to meet its performance target, it first needs to determine the quantitative and dynamic relationship between the application's resource allocation and its performance. Such a relationship is captured in the notion of "transfer function" in traditional control theory for modeling of physical systems. However, most computing systems, such as the one considered in this paper, cannot be represented by a single, linear transfer function (or model) because their behavior is often nonlinear and workload-dependent. We assume, however, that the behavior of the system can be approximately characterized *locally* by a linear model. We periodically re-estimate the model online based on real-time measurements of the relevant variables and metrics, allowing the model to adapt to different operating regimes and workload conditions.

Every AppController has two modules as illustrated in Figure 4.3: (1) a *model estimator* that automatically learns in real time a model for the relationship between an application's resource allocation and its performance, and (2) an *optimizer* that predicts the resource allocation required for the application to meet its performance target based on the estimated

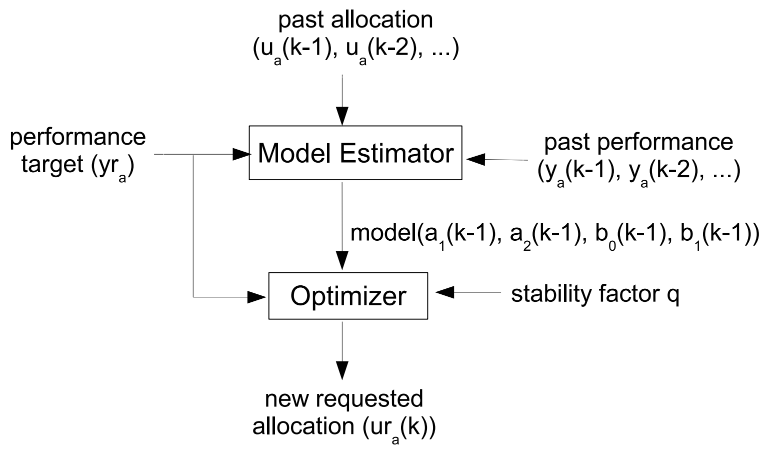
past allocation
(u_a(k-1), u_a(k-2), ...)
performance target (yr_a)
Model Estimator
past performance
(y_a(k-1), y_a(k-2), ...)
model(a_1(k-1), a_2(k-1), b_0(k-1), b_1(k-1))
Optimizer
stability factor q
new requested allocation (ur_a(k))

Figure 4.3: AppController's internal structure

model. For each application $a \in A$, let $y_a(k)$ be the value of its performance metric provided by an application performance sensor at the end of control interval k, and let yr_a be the desired value for its performance. Furthermore, we define $yn_a(k) = y_a(k)/yr_a$ to be the normalized performance value for interval k. We then define the resource-allocation variable $\mathbf{u}_a$ to be a vector that contains all the elements in the set $\{u_{a,r,t} : r \in R, t \in T_a\}$. For example, for a two-tier application whose performance depends on two critical resources, e.g., $T_a = \{web, db\}$ and $R = \{cpu, disk\}$, $\mathbf{u}_a$ is a 4-dimensional vector. $\mathbf{u}_a(k)$ represents the resource-allocation values for application a during interval k (we represent all vectors in boldface).

4.3.1.1 Model Estimator

For every control interval, the model estimator re-computes a linear model that approximates the nonlinear and time-varying relationship between the resource allocation to application a ($\mathbf{u}_a$) and its normalized performance (yn_a) around the current operating point. More specifically, the following auto-regressive-moving-average (ARMA) model is used to represent this relationship:

$$\begin{aligned} yn_a(k) = \;& a_1(k)\; yn_a(k-1) + a_2(k)\; yn_a(k-2) \\ & + \mathbf{b_0}^T(k)\mathbf{u}_a(k) + \mathbf{b_1}^T(k)\mathbf{u}_a(k-1), \end{aligned} \tag{4.1}$$

where the model parameters $a_1(k)$ and $a_2(k)$ capture the correlation between the application's past and present performance, and $\mathbf{b_0}(k)$ and $\mathbf{b_1}(k)$ are vectors of coefficients capturing the correlation between the current performance and the recent resource allocations. Both $\mathbf{u}_a(k)$ and $\mathbf{u}_a(k-1)$ are column vectors, and $\mathbf{b_0}^T(k)$ and $\mathbf{b_1}^T(k)$ are row vectors. We chose a linear model because it is easy to estimate online and simplifies the corresponding controller design problem. In our experiments, we have found that the second-order ARMA model in Eq. (4.1) (i.e., one that takes into account the past two control intervals) can predict the application performance with adequate accuracy. (Some evidence of this will be presented later in Section 4.6.) Note that the model developed may not be unique because of the adaptive nature, but is sufficient to allocate resources to meet application goals.

The reason why we model the normalized performance rather than the absolute performance is that the latter can have an arbitrary magnitude. The normalized performance yn_a has values that are comparable to those of the resource allocations in u_a, which are less than 1. This improves the numerical stability of the algorithm.

Note that the model represented in Eq. (4.1) is *adaptive* itself, because all the model parameters a_1, a_2, $\mathbf{b_0}$ and $\mathbf{b_1}$ are functions of time interval k. These parameters can be re-estimated online using the recursive least squares (RLS) method [28]. At the end of every control interval $k-1$, the model estimator collects the newly-measured performance value $y_a(k-1)$, normalizes it by the performance target yr_a, and uses it to update the values for the model parameters. The approach assumes that drastic variations in workloads that cause significant model parameter changes occur infrequently relative to the control interval, thus allowing the the model estimator to converge locally around an operating point and track changes in the operating point. The recursive nature of RLS makes the time taken for this computation negligible for control intervals longer than 10 seconds.

4.3.1.2 Optimizer

The main goal of the optimizer is to determine the resource allocation required ($\mathbf{ur_a}$) in order for the application to meet its target performance. An additional goal is to accomplish this in a stable manner, without causing large oscillations in the resource allocation. We achieve these goals by finding the value of $\mathbf{ur_a}$ that minimizes the following cost function:

$$J_a = (yn_a(k) - 1)^2 + q\|\mathbf{ur_a}(k) - \mathbf{u_a}(k-1)\|^2. \tag{4.2}$$

To explain the intuition behind this function, we define $J_p = (yn_a(k) - 1)^2$, and $J_c = \|\mathbf{ur_a}(k) - \mathbf{u_a}(k-1)\|^2$. It is easy to see that J_p is 0 when $y_a(k) = yr_a$, i.e., when application a is meeting its performance target. Otherwise, J_p serves as a penalty for the deviation of the application's measured performance from its target. Therefore, we refer to J_p as the *performance cost*.

The second function J_c, referred to as the *control cost*, is included to improve controller stability. The value of J_c is higher when the controller makes a larger change in the resource allocation in a single interval. Because $J_a = J_p + q \cdot J_c$, our controller aims to minimize a linear combination of both the performance cost and the control cost. Using the approximate linear relationship between the normalized performance and the resource allocation, as described by Eq. (4.1), we can derive the resource allocation required to minimize the cost function J_a, in terms of the recent resource allocation u_a and the corresponding normalized performance values yn_a:

$$\begin{aligned} \mathbf{ur_a^*}(k) = (\mathbf{b_0}\mathbf{b_0}^T + qI)^{-1}((1 - a_1\ yn_a(k-1) \\ -a_2\ yn_a(k-2) - \mathbf{b_1}^T\mathbf{u_a}(k-1))\mathbf{b_0} + q\mathbf{u_a}(k-1)). \end{aligned} \tag{4.3}$$

This is a special case of the optimal control law derived in [63]. Note that the dependency of the model parameters a_1, a_2, $\mathbf{b_0}$ and $\mathbf{b_1}$ on the control interval k has been dropped from the equation to improve its readability.

To understand the intuition behind this control law and the effect of the scaling factor q, we define $\Delta yn_a(k) = 1 - a_1\ yn_a(k-1) - a_2\ yn_a(k-2) - \mathbf{b_1}^T\mathbf{u_a}(k-1)$. This indicates the discrepancy between the model-predicted value for $yn_a(k)$ and its target (which is 1) that needs to be compensated by the next allocation ($\mathbf{u_a}(k)$). For a small q value, $\mathbf{ur_a^*}(k)$ is dominated by the effect of $\Delta yn_a(k)$, and the controller reacts aggressively to tracking errors in performance. As the value of q increases, $\mathbf{ur_a^*}(k)$ is increasingly dominated by the previous allocation ($\mathbf{u_a}(k-1)$), and the controller responds slowly to the tracking error with less oscillation in the resulting resource allocation. In the extreme of an infinitely large q value, we have $\mathbf{ur}^*_\mathbf{a}(k) = \mathbf{u_a}(k-1)$, meaning the allocation remains constant. As a result, the scaling factor q provides us an intuitive way to control the trade-off between the controller's stability and its ability to respond to changes in the workloads and performance, hence is referred to as the *stability factor*.

4.3.2 Design of NodeController

For each of the virtualized nodes, a NodeController determines the allocation of resources to the applications, based on the resources requested by the AppControllers and the resources available at the node. This is required because the AppControllers act independently of one another and may, in aggregate, request more resources than the node has available. The NodeController divides the resources between the applications as follows. For resources where the total resources requested are less than the available resources, the NodeController divides each resource in proportion to the requests from the AppControllers. For resources that are contested, that is, where the sum of the resource requests is greater than the available resource, the NodeController picks an allocation that locally minimizes the discrepancy between the resulting normalized application performance and its target value. More precisely, the cost function used is the weighted sum of the squared errors for the normalized application performance, where each application's weight represents its priority relative to other applications.

To illustrate this resource allocation method, let us take node1 in Figures 4.1 and 4.2 as an example (denoted as "n1"). This node is being used to host the web tier of application 1 and application 2. Suppose CPU and disk are the two critical and controllable resources being shared by the two applications. Then, the resource request from application 1 consists of two elements, $ur_{1,cpu,web}$ and $ur_{1,disk,web}$, one for each resource. Similarly, the resource request from application 2 consists of $ur_{2,cpu}$ and $ur_{2,disk}$. Because resource allocation is defined as a percentage of the total shared capacity of a resource, the resource requests from both applications need to satisfy the following capacity constraints:

$$ur_{1,cpu,web} + ur_{2,cpu} \leq 1 \tag{4.4}$$

$$ur_{1,disk,web} + ur_{2,disk} \leq 1 \tag{4.5}$$

When constraint (4.4) is violated, we say the virtualized node suffers *CPU contention.* Similarly, *disk contention* refers to the condition of the node when constraint (4.5) is violated. Next, we describe the four possible scenarios for the virtualized node n1, and the NodeController algorithm for dealing with each scenario.

4.3.2.1 Scenario I: Single resource contention

In this scenario, node n1 has enough capacity to meet the requests for one resource from the AppControllers, but not enough for the other resource; that is, one of constraints (4.4) and (4.5) is violated while the other is satisfied. The NodeController divides the resource that is enough in proportion to the requests. For the other resource $r \in R = \{cpu, disk\}$, the applications will receive less allocation than requested; let us denote the deficiencies as $\Delta u_{1,r,web} = ur_{1,r,web} - u_{1,r,web}$ and $\Delta u_{2,r} = ur_{2,r} - u_{2,r}$. The resulting discrepancy between the achieved and target normalized performance of application 1 can then be estimated as $\partial yn_1/\partial u_{1,r,web}\Delta u_{1,r,web}$, and similarly for application 2. The penalty function for not meeting the performance targets is defined as:

$$J_{n1} \quad = w_1(\tfrac{\partial yn_1}{\partial u_{1,r,web}}\Delta u_{1,r,web})^2 + w_2(\tfrac{\partial yn_2}{\partial u_{2,r}}\Delta u_{2,r})^2$$

The actual allocation is found by solving the following problem.

$$\begin{aligned} \text{Minimize } \ J_{n1} &\quad \text{subject to} \\ \Delta u_{1,r,web} + \Delta u_{2,r} &\geq ur_{1,r,web} + ur_{2,r} - 1, && (4.6) \\ \Delta u_{1,r,web} &\geq 0, && (4.7) \\ \Delta u_{2,r} &\geq 0. && (4.8) \end{aligned}$$

Constraint (4.6) is simply the capacity constraint (4.4), applied to actual allocations. Constraints (4.7) and (4.8) ensure that no application is throttled to increase the performance of another application beyond its target. In the objective function J_{n1}, the discrepancies for the applications are weighted by their priority weights, so that higher priority applications experience less performance degradation.

From Eq. (4.1), we know that $\frac{\partial yn_1}{\partial u_{1,r,web}} = b_{0,1,r,web}$, and $\frac{\partial yn_2}{\partial u_{2,r}} = b_{0,2,r}$. Both coefficients can be obtained from the model estimators in the AppControllers for both applications. This optimization problem is convex and a closed-form solution exists for the case of two applications sharing the node. For more than two applications, we use an off-the-shelf quadratic programming solver to compute the solution.

4.3.2.2 Scenario II: CPU and Disk Contention

This is the scenario where both CPU and disk are under contention. In this case, the actual allocations of CPU and disk for both applications will be below the respective requested amounts. The penalty function for not meeting the performance targets becomes:

$$\begin{aligned} J_{n1} &= w_1 (\textstyle\sum_{r\in R} \frac{\partial yn_1}{\partial u_{1,r,web}} \Delta u_{1,r,web})^2 \\ &+ w_2 (\textstyle\sum_{r\in R} \frac{\partial yn_2}{\partial u_{2,r}} \Delta u_{2,r})^2. \end{aligned}$$

The NodeController determines the actual allocations by minimizing J_{n1}, and by satisfying the constraints (4.6), (4.7), and (4.8) for both resources. This requires solving a convex optimization problem with the number of variables being the number of resource types multiplied by the number of VMs on the node. We have observed that the time taken for the online optimization is negligible (average of 40ms in our implementation).

4.4 Implementation and Performance Considerations

We have implemented the model estimator and the controllers in Java, and written Python wrappers for sensors and actuators provided by the system. The controllers communicate with the clients and the Python wrappers using XML-RPC. The optimization

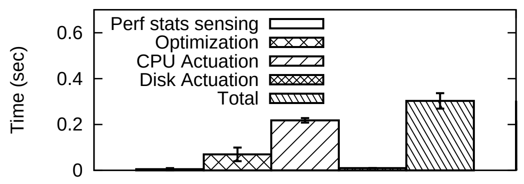

Figure 4.4: Average performance overhead

Component	SLOC
RLS Modeler	262
AppController	280
NodeController	327
Matlab Optimization code	35
Python wrappers	251

Figure 4.5: SLOC of major code components

code is written in Matlab and the Java program communicates with Matlab using pipes. A more efficient implementation can be developed using JNI (Java Native call Interface). The total number of lines of code in *AutoControl* is about 3000. Our code is written to be extensible and new controllers can be plugged into the framework easily.

The controllers are designed to be scalable by limiting the number of control variables each controller has to deal with. More specifically, the number of variables for each AppController is the number of tiers multiplied by the number of controlled resources, and the number of variables for each NodeController is the number of VMs on that node multiplied by the number of controlled resources. The performance of each decision in *AutoControl* is mainly affected by three factors: (1) time taken to collect statistics from clients, (2) Matlab optimization time, (3) actuation time. Figure 4.4 shows the average time taken on our testbed for each of these factors. The total time is less than 1.5% of the control interval.

4.5 Experimental Testbed

To evaluate *AutoControl*, we have built a testbed consisting of three virtualized nodes, each running multiple VMs hosting multiple applications. Clients running on other nodes generate workloads for these applications.

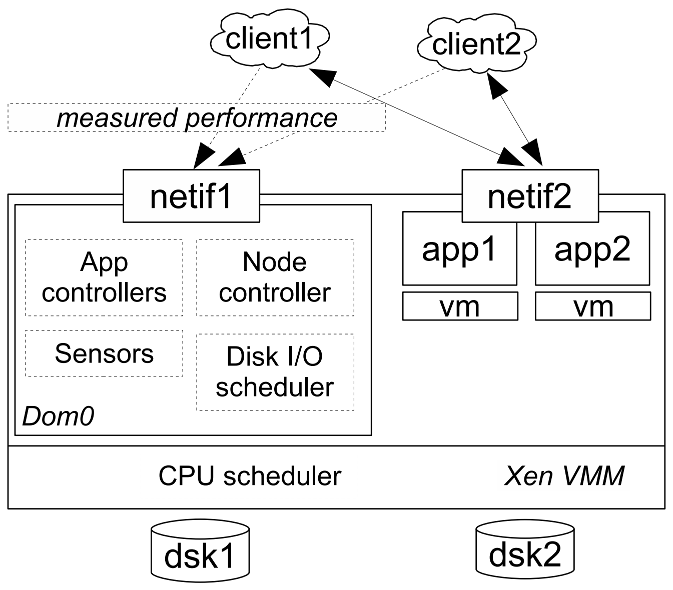

Figure 4.6: A virtualized node in the testbed

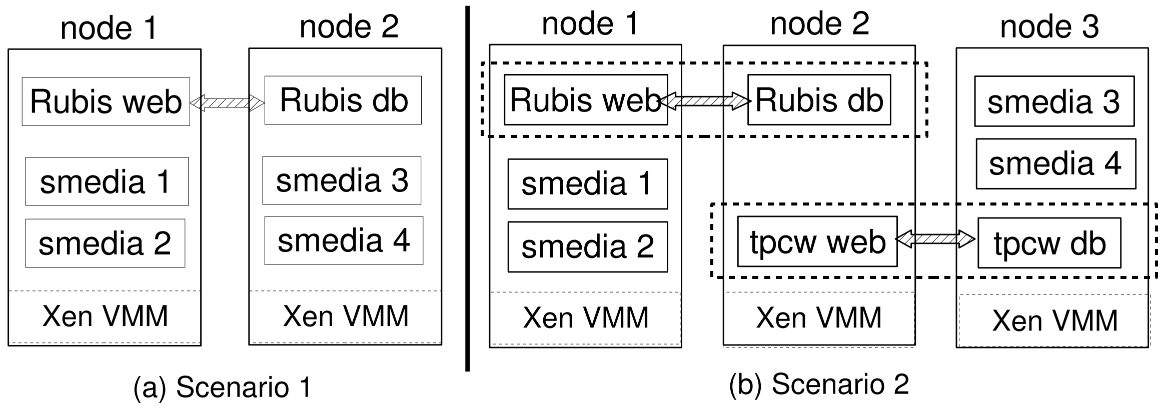

Figure 4.7: Experimental setup

All the experiments were conducted on HP C-class blades, each equipped with two dual-core 2.2 GHz 64-bit processors with 4GB memory, two Gigabit Ethernet cards and two 146 GB hard disks. The blades were installed with OpenSuse 10.3 and we used the default Xen (2.6.22.5-31-xen SMP) available in OpenSuse to run the VMs. The VM images were built using the same distribution, and no changes were made to the kernel.

One network interface and one disk were dedicated to Dom0, which ran the monitoring framework and our controllers. The VMs were allocated the second network interface and disk. The clients connected to the VMs using the network interface dedicated to the VMs.

The controller used its own network interface to poll application performance statistics from the clients. In order to demonstrate CPU bottlenecks more easily, we allocated one CPU to the VMs, and used the remaining CPUs for Dom0. Our controller is fully extensible to VMs sharing multiple processors as long as the CPU scheduler allows arbitrary slicing of CPU allocation. Figure 4.6 shows all the components in our experiments.

Our experiments were designed to answer the following questions:

1. Can the controller detect resource bottlenecks across time and application tiers?
2. Can the controller adjust resource allocations to overcome these bottlenecks?
3. Can the controller handle different application workloads?
4. Can the controller enforce performance targets for metrics including average throughput and response time?
5. Can the controller prioritize among applications when resources are scarce?

We used three different applications in our experiments: RUBiS [25], an online auction site benchmark, a Java implementation of the TPC-W benchmark [34], and a custom-built secure media server.

RUBiS and TPC-W use a multi-tier setup consisting of web and database tiers. They both provide workloads of different mixes and time-varying intensity. For RUBiS, we used a workload mix called the browsing mix that simulates a user browsing through an auction site. For TPC-W, we used the shopping mix, which simulates a user browsing through a shopping site. The browsing mix stresses the web tier, while the shopping mix exerts more demand on the database tier.

The custom-built secure media (smedia) server is a representation of a media server that can serve encrypted media streams. The smedia server runs a certain number of concurrent threads, each serving a client that continuously requests media files from the server. A media client can request an encrypted or unencrypted stream. Upon receiving the request, the server reads the particular media file from the disk (or from memory if it is cached), optionally encrypts it, and sends it to the client. A closed-loop client model is used where a new file is only requested after the previous request is complete. Reading a file from the disk consumes disk I/O resource, and encryption requires CPU resource. For a given number of threads, by changing the fraction of the client requests for encrypted media, we can vary the amount of CPU or disk I/O resource used. This flexibility allowed us to study our controller's behavior for CPU and disk I/O bottlenecks.

4.5.1 Simulating Production Traces

To test our controller under real workloads, we created workloads that simulate production traces. These traces were obtained from an SAP application server running in a production environment. We simulated the production traces using RUBiS and TPC-W by carefully selecting the number of concurrent threads at a particular time. For example, to create 40% average CPU utilization over a 5 minute period, we used 500 threads simulating 500 concurrent users. Note that we only simulated the CPU utilization of the production trace. We did not attempt to recreate the disk utilization, because the traces did not contain the needed metadata.

We also used traces generated from a media workload generator called MediSyn [88]. MediSyn generates traces that are based on analytical models drawn from real-world traces collected at an HP Labs production media server. It captures important properties of streaming media workloads, including file duration, popularity, encoding bit rate, and streaming session time. We re-created the access pattern of the trace by closely following the start times, end times, and bitrates of the sessions. Note that this is a re-creation of the stochastics rather than replaying an original trace. We did not attempt to re-create the disk access pattern, because of the lack of metadata.

4.5.2 Sensors

Our sensors periodically collect two types of statistics: real-time resource utilizations and performance of applications. CPU utilization statistics are collected using Xen's xm command. Disk utilization statistics are collected using the `iostat` command, which is part of the `sysstat` package. In our testbed, we measured both the application throughput and the server-side response time directly from the application, where throughput is defined as the total number of client requests serviced, and for each client request, response time is defined as the amount of time taken to service the request. In a real data center, application-level performance may be obtained from application logs or from tools like HP Openview.

4.5.3 Actuators

Our actuators included Xen's credit-based CPU scheduler and a custom-built proportional disk I/O scheduler. The credit scheduler provided by Xen allows each domain (or VM) to be assigned a *cap*. We used the cap to specify a CPU share for each VM. This non-work-conserving mode of CPU scheduling provided better performance isolation among applications running in different VMs. The proportional share scheduler for disk I/O was designed to maximize the efficiency of the disk access [48]. The scheduler is logically interposed between the virtual machines and the physical disks: we implemented it as a driver in the Dom0. The controller interacts with the disk I/O scheduler by assigning a *share* to each VM in every control interval.

The controller interacts with the CPU scheduler by specifying a non-zero *cap* for each VM in each control interval. Although the scheduler itself works in the non-work-conserving mode, there is minimum waste of CPU cycles because the controller always allocates 100% of the shared capacity to all the guest VMs, and because the controller automatically shifts idle capacity from one VM to another by dynamically adapting the individual caps in response to the changing needs of the individual applications.

4.6 Evaluation Results

We evaluated *AutoControl* in a number of experimental scenarios to answer the questions posed in Section 4.5. In all of the experiments, a control interval of 20 seconds was used[1]. In this section, we present the performance results from these experiments that demonstrate the effectiveness of the *AutoControl* design.

[1]A higher interval may cause the controller to miss some dynamic changes, while a smaller interval may cause oscillations.

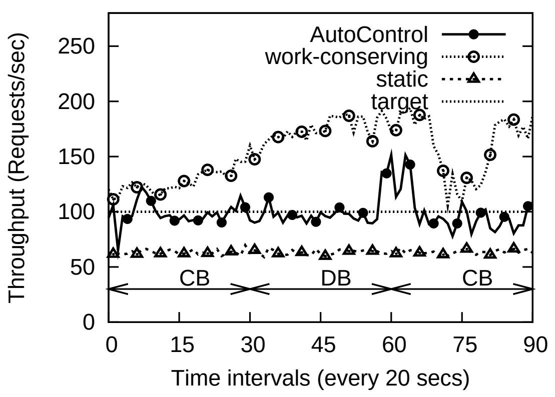

(a) RUBiS throughput

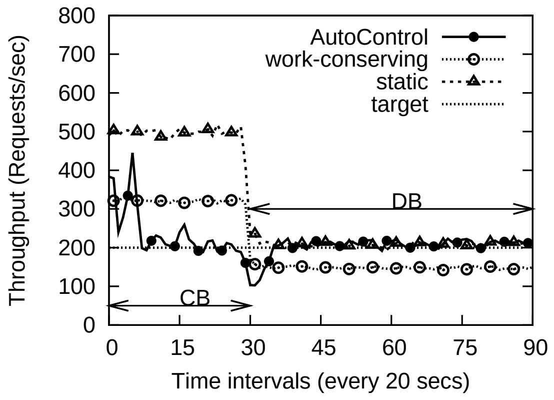

(b) Smedia1 throughput

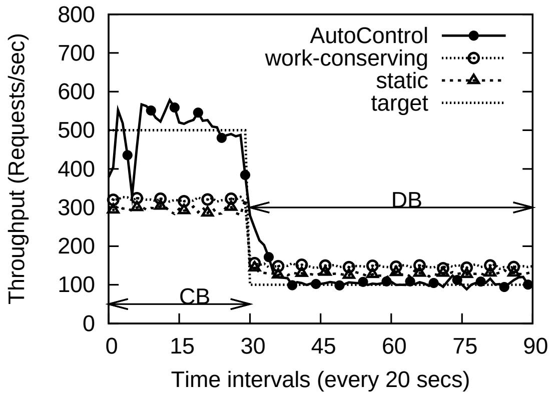

(c) Smedia2 throughput

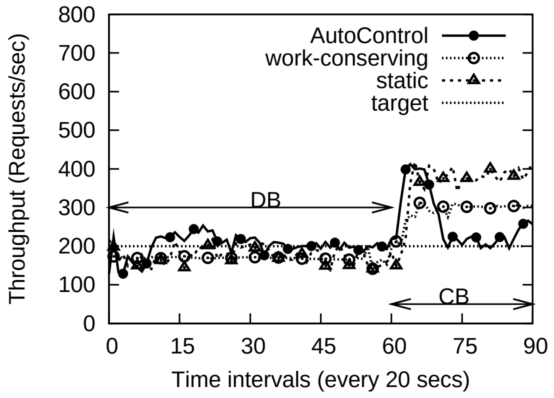

(d) Smedia3 throughput

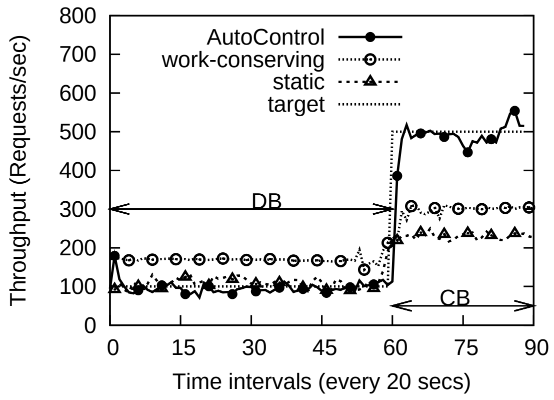

(e) Smedia4 throughput

Figure 4.8: Application throughput with bottlenecks in CPU or disk I/O and across multiple nodes

4.6.1 Scenario 1: Detecting and Mitigating Resource Bottlenecks in Multiple Resources and across Multiple Application Tiers

This scenario was designed to validate the following claims about *AutoControl*:

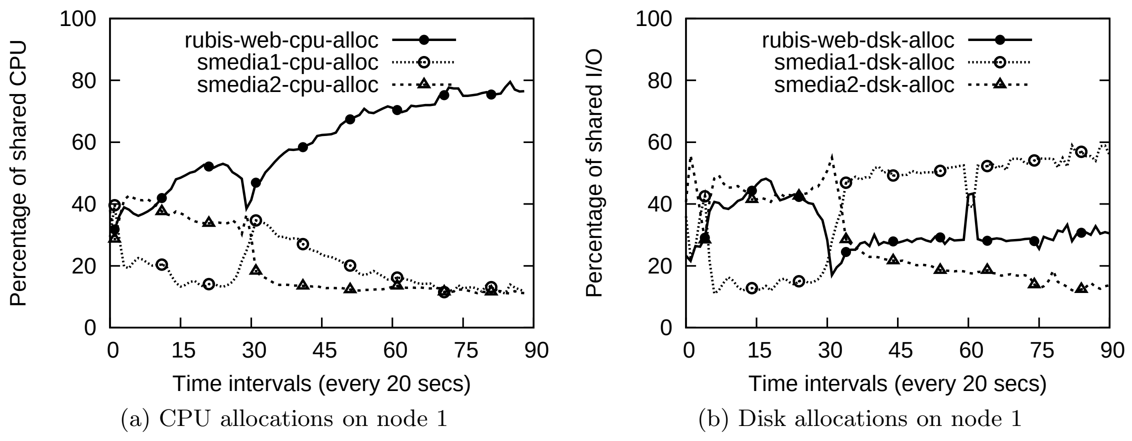

(a) CPU allocations on node 1 (b) Disk allocations on node 1

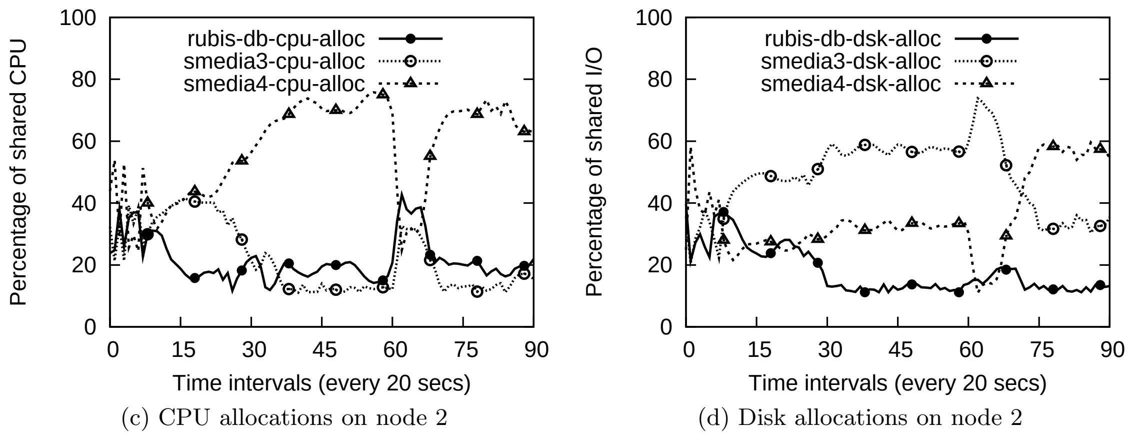

(c) CPU allocations on node 2 (d) Disk allocations on node 2

Figure 4.9: Resource allocations to different applications or application tiers on different nodes

- **Claim 1:** It can automatically detect resource bottlenecks and allocate the proper amount of resources to each application such that all the applications can meet their performance targets if possible. This occurs for different types of bottlenecks and for bottlenecks across multiple tiers of an application.

- **Claim 2:** It can automatically detect the shift of a bottleneck from one type of resource to another, and still allocate resources appropriately to achieve application-level goals.

We use the experimental setup shown in Figure 4.7(a), where two physical nodes host one RUBiS application spanning two nodes, and four smedia applications. For RUBiS, we used the default browsing mix workload with 600 threads emulating 600 concurrent clients

Table 4.2: Percentage of encrypted streams in each smedia application in different time intervals

Intervals	smedia1	smedia2	smedia3	smedia4
1-29	50%	50%	2%	2%
30-59	2%	2%	2%	2%
60-89	2%	2%	50%	50%

connecting to the RUBiS server, and used 100 requests/sec as the throughput target. Each of the smedia applications was driven with 40 threads emulating 40 concurrent clients downloading media streams at 350KB/sec. We ran calibration experiments to measure the total throughput achievable for each smedia application alone. We observe that, with 50% of clients requesting encrypted streams, the application is CPU-bound and the maximum throughput is just above 7000 KB/sec. If, however, only 2% of clients are requesting encrypted streams, the application becomes disk-bound and the maximum throughput is around 3000 KB/sec. The difference in throughput comes from the fact that we use different sized requests to create CPU-bound and disk-bound applications.

We then ran an experiment for 90 control intervals and varied the percentage of encrypted streams to create a shift of the resource bottleneck in each of the virtualized nodes. Table 4.2 illustrates these transitions. For the first 29 intervals, smedia1 and smedia2 on node 1 were CPU-bound, whereas smedia3 and smedia4 on node 2 were disk-bound. We considered a scenario where smedia1 and smedia3 always had a throughput target of 2000 KB/sec each. We then set the throughput targets for smedia2 and smedia4 at 5000 and 1000 KB/sec, respectively. At interval 30, smedia1 and smedia2 on node 1 were switched to disk-bound, and so the throughput target for smedia2 was changed to 1000 KB/sec. At interval 60, smedia3 and smedia4 on node 2 were switched to CPU-bound, and so the throughput target for smedia4 was adjusted to 5000 KB/sec. The targets were chosen such that both nodes were running near their capacity limits for either CPU or disk I/O.

Figure 4.8 shows the throughput of all the five applications as functions of the control interval. For the first 29 intervals, the RUBiS web tier, smedia1 and smedia2 contended for CPU on node 1, and the RUBiS db tier, smedia3 and smedia4 contended for disk I/O on node 2. *AutoControl* was able to achieve the targets for all the applications in spite of the fact that (i) the resource bottleneck occurs either in the CPU or in the disk; (ii) both tiers of the RUBiS application distributed across two physical nodes experienced resource contention.

To help understand how the targets were achieved, Figures 4.9a and 4.9b show the CPU and disk I/O allocations to the RUBiS web tier, smedia1 and smedia2 on node 1. For the first 29 intervals, these three VMs were contending for CPU. The controller gave different portions of both CPU and disk resources to the three VMs such that all of their targets could be met. In the same time period (first 29 intervals), on node 2, the RUBiS database tier, smedia3 and smedia4 were contending for the disk I/O. Figures 4.9c and 4.9d show the CPU and disk I/O allocations for all the three VMs on this node. The controller not only allocated the right proportion of disk I/O to smedia3 and smedia4 for them to achieve their throughput targets, it also allocated the right amount of CPU to the RUBiS database tier so that the two-tier application could meet its target.

At interval 30, the workloads for the smedia applications on node 1 were switched to be disk-heavy. As a result, smedia1 and smedia2 were contending for disk I/O, since RUBiS web tier uses minimal disk resource. The controller recognized this change in resource bottleneck automatically and ensured that both smedia1 and smedia2 could meet their new throughput targets by allocating the right amount of disk resources to both smedia applications (see Figure 4.9b).

At interval 60, the workloads for the smedia applications on node 2 were switched to be CPU-heavy. Because the RUBiS db tier also requires a non-negligible amount of CPU (around 20%), smedia3 and smedia4 started contending for CPU with the RUBiS db tier on node 2. Again, the controller was able to automatically translate the application-level goals into appropriate resource allocations to the three VMs (see Figure 4.9c).

For comparison, we repeated the same experiment using two other resource allocation methods that are commonly used on consolidated infrastructure, a work-conserving mode and a static mode. In the work-conserving mode, the applications run in the default Xen settings, where a cap of zero is specified for the shared CPU on a node, indicating that the applications can use any amount of CPU resources. In this mode, our proportional share disk scheduler was unloaded to allow unhindered disk access. In the static mode,

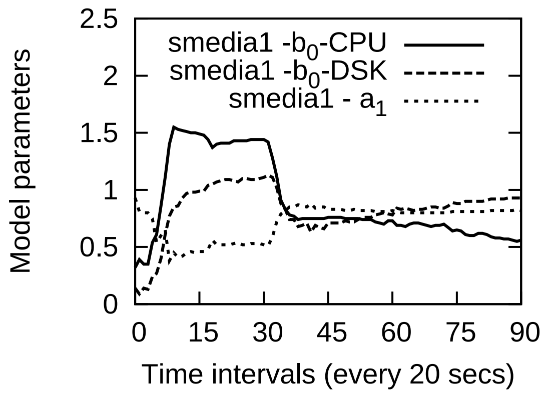

(a) Model parameter values for smedia1

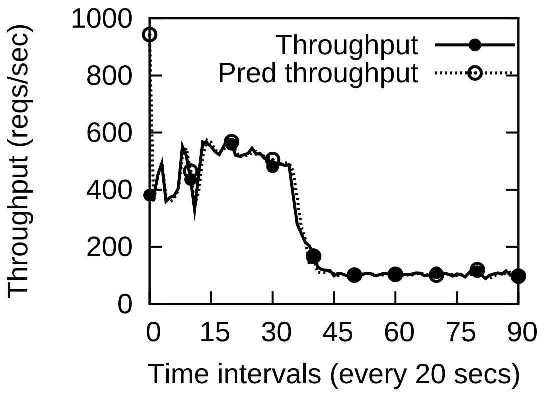

(b) Measured and model-predicted throughput for smedia2

Figure 4.10: Internal workings of the *AppController* - model estimator performance

the three applications sharing a node were allocated CPU and disk resources in the fixed ratio 20:50:30. The resulting application performance from both approaches is shown in Figure 4.8 along with the performance from *AutoControl*. As can be seen, neither approach was able to offer the degree of performance assurance provided by *AutoControl*.

For the work-conserving mode, RUBiS was able to achieve a throughput much higher than its target at the cost of performance degradation in the other applications sharing the same infrastructure. The remaining throughput on either node was equally shared by smedia1 and smedia2 on node 1, and smedia3 and smedia4 on node 2. This mode did not provide service differentiation between the applications according to their respective performance targets.

For the static mode, RUBiS was never able to reach its performance target given the fixed allocation, and the smedia applications exceeded their targets at some times and missed the targets at other times. Given the changes in workload behavior for the smedia applications, there is no fixed allocation ratio for both CPU and disk I/O that will guarantee the performance targets for all the applications. We chose to allocate both CPU and disk resources in the ratio 20:50:30, as a human operator might.

To understand further the internal workings of *AutoControl*, we now demonstrate a key element of our design - the model estimator in the *AppController* that automatically determines the dynamic relationship between an application's performance and its resource

Table 4.3: Predictive accuracy of linear models (in percentage)

	rubis	smedia1	smedia2	smedia3	smedia4
R^2	79.8	91.6	92.2	93.3	97.0
MAPE	4.2	5.0	6.9	4.5	8.5

allocation. Our online estimator continuously adapts the model parameters as dynamic changes occur in the system. Figure 4.10a(a) shows the model parameters ($b_{0,cpu}$, $b_{0,disk}$, and a_1) for smedia1 as functions of the control interval. As we can see, the values of $b_{0,cpu}$, representing the correlation between application performance and CPU allocation, dominated the $b_{0,disk}$, and a_1 parameters for the first 29 intervals. The disk allocation also mattered, but was not as critical. This is consistent with our observation that node 1 had a CPU bottleneck during that period. After the 30th interval, when disk became a bottleneck on node 1, while CPU became less loaded, the model coefficient $b_{0,disk}$ exceeded $b_{0,cpu}$ and became dominant after a period of adaptation.

To assess the overall prediction accuracy of the linear models, we computed two measures, the coefficient of determination (R^2) and the mean absolute percentage error (MAPE), for each application. R^2 and MAPE can be calculated as $R^2 = 1 - \frac{\sum_{k=1}(\hat{yn}_a(k) - yn_a(k))^2}{\sum_k (yn_a(k) - yn_{a,avg})^2}$, and MAPE $= \frac{1}{K}\sum_{k=1}^{K} |\frac{\hat{yn}_a(k) - yn_a(k)}{yn_a(k)}|$, where K is the total number of samples, $\hat{yn}_a(k)$ and $yn_a(k)$ are the model-predicted value and the measured value for the normalized performance of application a, and $yn_{a,avg}$ is the sample mean of yn_a. Table 4.3 shows the values of these two measures for all the five applications. As an example, we also show in Figure 4.10b(b) the measured and the model-predicted throughput for smedia2. From both the table and the figure, we can see that our model is able to predict the normalized application performance accurately, with R^2 above 80% and MAPE below 10%. This validates our belief that low-order linear models, when adapted online, can be good enough local approximations of the system dynamics even though the latter is nonlinear and time-varying.

4.6.2 Scenario 2: Enforcing Application Priorities

In this scenario, we use the experimental setup shown in Figure 4.7(b) to substantiate the following two claims:

- **Claim 3:** *AutoControl* can support different multi-tier applications.
- **Claim 4:** During resource contention, if two applications sharing the same resource have different priority weights, the application with a higher priority weight will see a lower normalized tracking error ($|yn_a - 1|$) in its performance.

In this setup, we have two multi-tier applications, RUBiS and TPC-W, and four smedia applications spanning three nodes. We ran the same workloads used in Scenario 1 for RUBiS, smedia1 and smedia2. TPC-W was driven with the shopping mix workload with 200 concurrent threads. Each of the smedia applications on node 3 was driven with a workload of 40 concurrent users, where 50% of clients requested encrypted streams (making it CPU-bound). We assume that the TPC-W application is of higher priority than the two smedia applications sharing the same node. Therefore, TPC-W is assigned a priority weight of $w = 2$ while the other applications have $w = 1$ in order to provide service differentiation.

Unlike the setup used in Scenario 1, there was no resource contention on node 2. For the first 29 intervals, all the six applications were able to meet their goals. Figure 4.11 shows the throughput target and the achieved throughput for TPC-W and smedia3. (The other four applications are not shown to save space.) At interval 30, 800 more threads were added to the TPC-W client, simulating increased user activity. The throughput target for TPC-W was adjusted from 20 to 50 requests/sec to reflect this change. This increases the CPU load on the database tier creating a CPU bottleneck on node 3. *AutoControl* responds to this change automatically and correctly re-distributes the resources. Note that not all three applications (TPC-W, smedia3, and smedia4) on node 3 can reach their targets. But the higher priority weight for TPC-W allowed it to still meet its throughput target while degrading performance for the other two applications.

The result from using the work-conserving mode for the same scenario is also shown in Figure 4.11. In this mode, smedia3 and smedia4 took up more CPU resource, causing TPC-W to fall below its target.

We also use this example to illustrate how a tradeoff between controller stability and responsiveness can be handled by adjusting the stability factor q. Figure 4.12 shows the achieved throughput for TPC-W and smedia3 under the same workload condition, for q

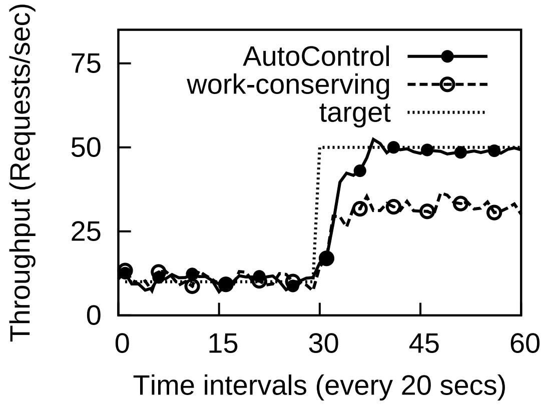

(a) TPC-W throughput

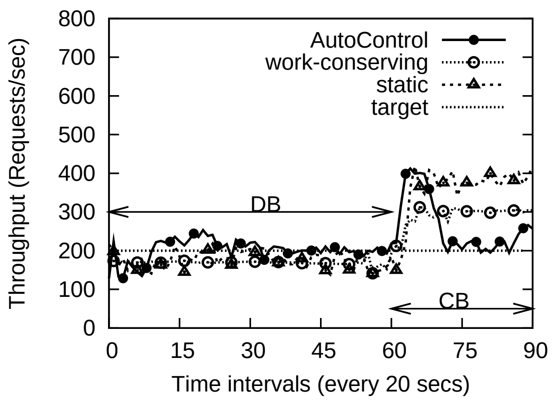

(b) Smedia3 throughput

Figure 4.11: Performance comparison between *AutoControl* and work-conserving mode, with different priority weights for TPC-W ($w = 2$) and smedia3 ($w = 1$).

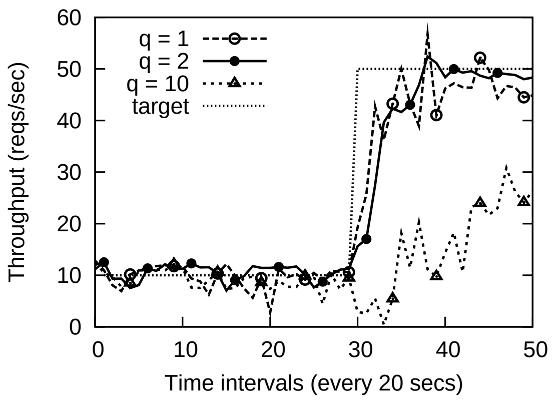

(a) TPC-W throughput

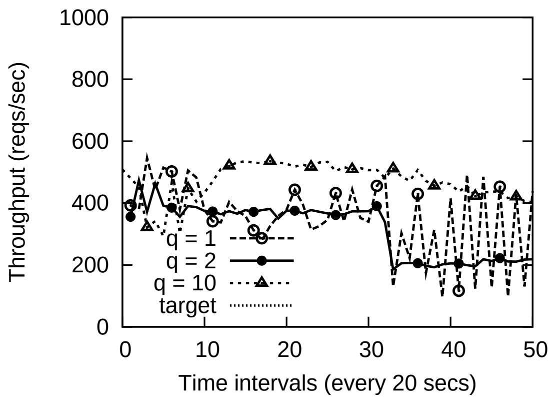

(b) Smedia3 throughput

Figure 4.12: Performance results for TPC-W and smedia3 with stability factor $q = 1, 2, 10$

values of 1, 2, and 10. The result for $q = 2$ is the same as in Figure 4.11. For $q = 1$, the controller reacts to the workload change more quickly and aggressively, resulting in large oscillations in performance. For $q = 10$, the controller becomes much more sluggish and does not adjust resource allocations fast enough to track the performance targets.

4.6.3 Scenario 3: Production-trace-driven Workloads

The last scenario is designed to substantiate the following two claims for *AutoControl*:

- **Claim 5:** It can be used to control application response time.
- **Claim 6:** It can manage workloads that are driven by real production traces.

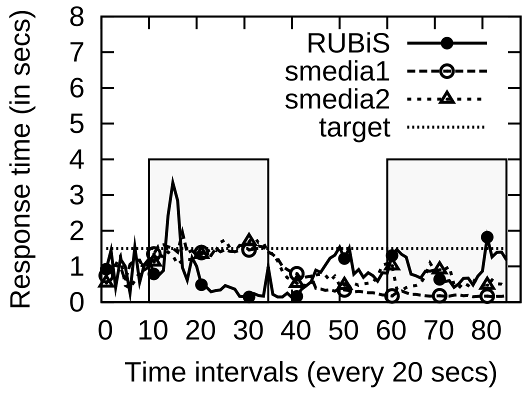

(a) *AutoControl*

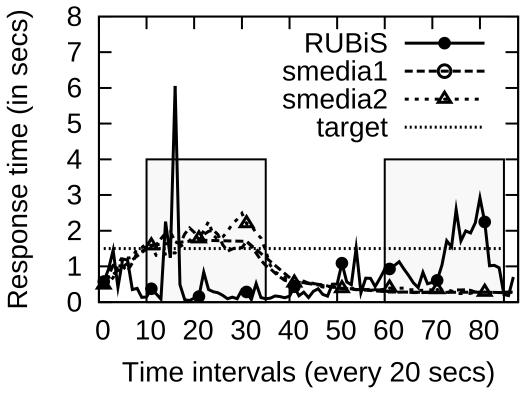

(b) Work-conserving mode

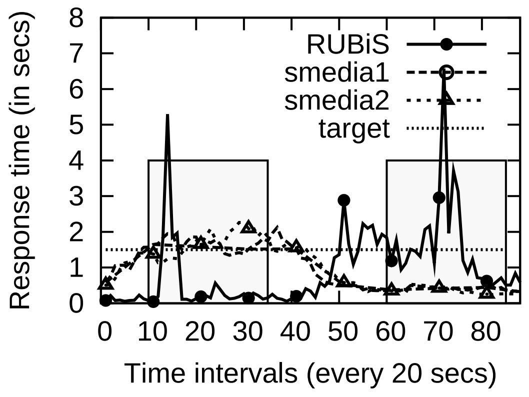

(c) Static allocation mode

Figure 4.13: Performance comparison of *AutoControl*, work-conserving mode and static allocation mode, while running RUBiS, smedia1 and smedia2 with production-trace-driven workloads.

In this scenario, we use the same setup as in Scenario 1, shown in Figure 4.7(a). We simulated the production workloads using the trace-driven approach as described in Section 4.5. Each of the RUBiS, smedia1 and smedia2 applications was driven by a production trace, while both smedia3 and smedia4 run a workload with 40 threads with a 2% chance of requesting an encrypted stream (making it disk-bound).

In this experiment, we use response time as the performance metric for two reasons.

1. Response time behaves quite nonlinearly with respect to the resource allocation and can be used to evaluate how *AutoControl* copes with nonlinearity in the system.

2. It is possible to specify the same response time target for all applications even if they are different, whereas specifying throughput targets are harder since they may depend

on the offered load.

For brevity, we only show the results for the three applications running on node 1. Figures 4.13a, 4.13b and 4.13c show the measured average response time of RUBiS, smedia1 and smedia2 as functions of the control interval, using *AutoControl*, work-conserving mode, and static allocation mode, respectively. We use a response time target of 1.5 second for all the three applications, and set the CPU allocation at a fixed 33% for each application in the static mode. The dark-shaded regions show the time intervals when a CPU bottleneck occurred.

In the first region, for the work-conserving mode, both smedia1 and smedia2 had high CPU demands, causing not only response time target violations for themselves, but also a large spike of 6 second in the response time for RUBiS at the 15th interval. In comparison, *AutoControl* allocated to both smedia1 and smedia2 higher shares of the CPU without overly penalizing RUBiS. As a result, all the three applications were able to meet the response time target most of the time, except for the small spike in RUBiS.

In the second shaded region, the RUBiS application became more CPU intensive. Because there is no performance assurance in the work-conserving mode, the response time of RUBiS surged and resulted in a period of target violations, while both smedia1 and smedia2 had response times well below the target. In contrast, *AutoControl* allocated more CPU capacity to RUBiS when needed by carefully reducing the resource allocation to smedia2. The result was that there were almost no target violations for any of the three applications.

The performance result from the static allocation mode was similar to that from the work-conserving mode, except that the RUBiS response time was even worse in the second region.

Despite the fact that response time is a nonlinear function of resource allocation, and that the real traces used here were much more dynamic than the static workloads with step changes tested in Scenario 1 and 2, *AutoControl* was still able to balance the resources and minimize the response time violations for all three applications.

4.6.4 Scalability Experiments

In this section, we evaluate the scalability of *AutoControl* using a larger testbed built on Emulab [99], using 16 server nodes, each running 4 smedia applications in 4 individual virtual machines. An additional 16 client nodes running 64 clients were used to generate the workloads for the 64 smedia servers. Initially, each application used a light workload keeping all the nodes underloaded. After 240 seconds, we increased the load for half of the applications (in 32 VMs) and updated their performance targets accordingly. These applications were chosen randomly and hence were not spread uniformly across all the nodes. The numbers of nodes that had 0, 1, 2, and 3 applications with increased load were 1, 4, 5, and 6, respectively.

Figure 4.14a and 4.14b show the SLO violations of the 64 applications over time, using the work-conserving mode and *AutoControl*, respectively. The x-axis shows the time in seconds and the y-axis shows the application index. The gray shades in the legend represent different levels of SLO violations (the darker the worse), whereas the white color indicates no SLO violations.

The nodes that had no or only one application with a heavy load remained underloaded and there were almost no SLO violations. When there were two applications with increased load on a single node, the node was slightly overloaded and the work-conserving mode resulted in SLO violations in the applications sharing the node, whereas *AutoControl* was able to re-distribute the resources and significantly reduce the SLO violations. However, if a node had three applications with increased load, even *AutoControl* was not able to avoid SLO violations for certain applications because no re-distribution policy could satisfy the resource demands of all the applications.

4.7 Discussion

This section describes some of the design issues in *AutoControl*, alternative methods and future research work.

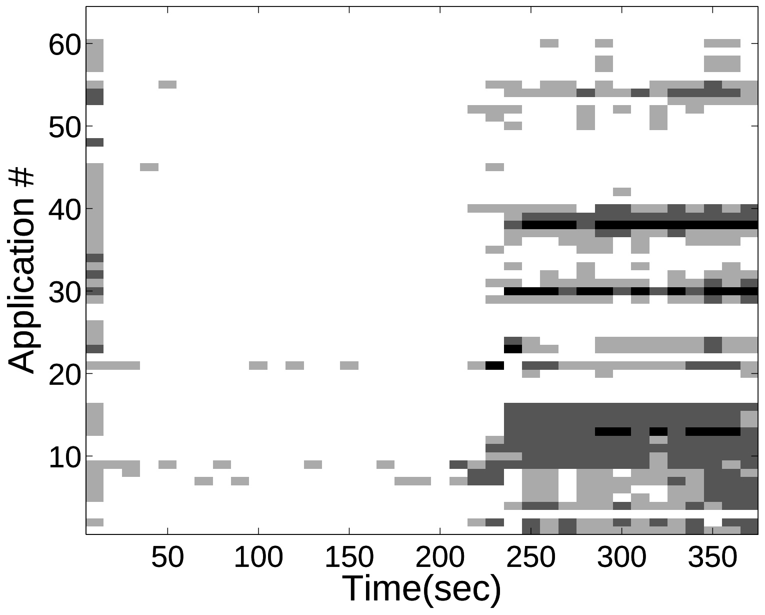

(a) Work-conserving mode

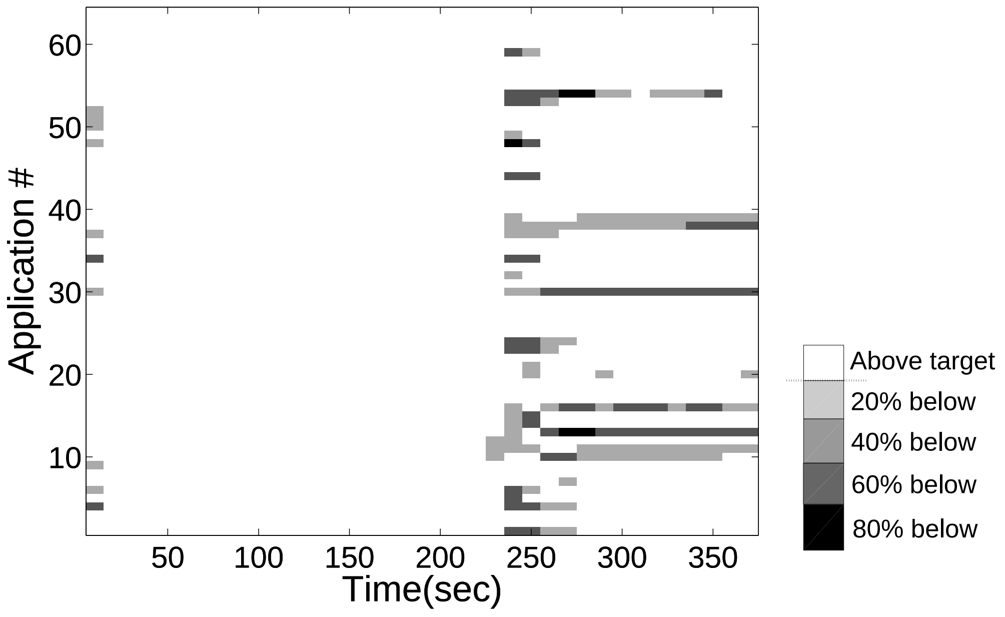

(b) *AutoControl*

Figure 4.14: SLO violations in 64 applications using work-conserving mode and *AutoControl*

4.7.1 Migration for dealing with bottlenecks

AutoControl enables dynamic re-distribution of resources between competing applications to meet their targets, so long as sufficient resources are available. If a node is persistently overloaded, VM migration [39, 102] may be needed, but the overhead of migration can cause additional SLO violations. We performed experiments to quantify these viola-

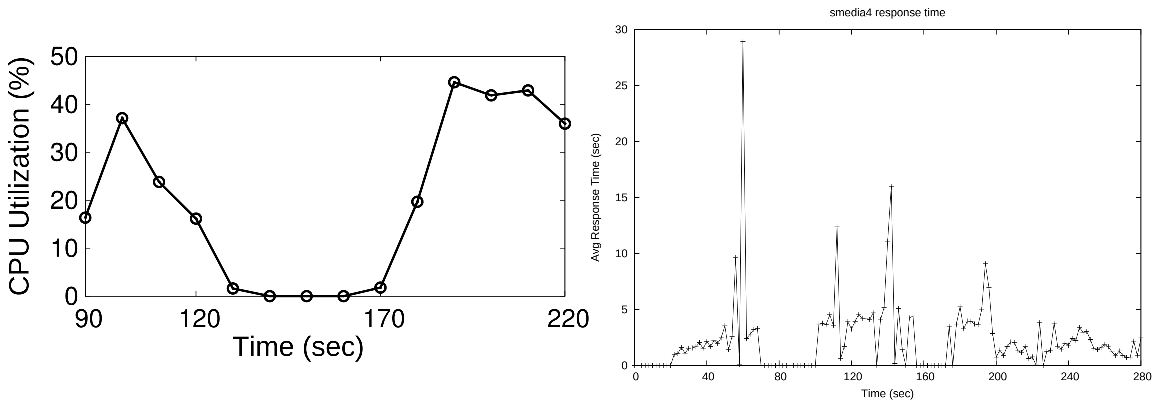

(a) Measurement of CPU utilization on a loaded VM during migration (b) Response Time of a loaded VM during migration

Figure 4.15: Behavior of Smedia Application During Migration

tions. Migrating a lightly-loaded smedia server hosted in a 512MB VM takes an average of 6.3 seconds. However, during the migration, we observed as much as 79% degradation of smedia throughput and CPU utilization as high as 94% on the source node. Since migration usually takes place when a node is heavily loaded, we also measured the overhead of migration under various overload conditions. We have used two or more smedia VMs with varying degrees of overload, and found the migration times vary between 13 to 50 seconds. Figure 4.15a shows the CPU utilization of one such migrating VM. There were four heavily-loaded smedia VMs on the source node and one lightly-loaded VM on the destination node in this setup. During the migration period (t=120-170), the VM showed CPU starvation, and we observed a significant decrease in smedia performance which can be seen in Figure 4.15b. We plan to extend *AutoControl* to include VM migration as an additional mechanism, and expect that a combination of VM migration and *AutoControl* will provide better overall performance than using one or the other.

4.8 Summary

In this chapter, we presented *AutoControl*, a feedback control system to dynamically allocate resources to applications running on shared virtualized infrastructure. It consists of an online model estimator that captures the dynamic relationship between application-level performance and resource allocations and a MIMO resource controller that determines appropriate allocations of multiple resources to achieve application-level SLOs.

We evaluated *AutoControl* using two testbeds consisting of varying numbers of Xen virtual machines and various single- and multi- tier applications and benchmarks. Our experimental results confirmed that *AutoControl* can detect dynamically-changing CPU and disk bottlenecks across multiple nodes and can adjust resource allocations accordingly to achieve end-to-end application-level SLOs. In addition, *AutoControl* can cope with dynamically-shifting resource bottlenecks and provide a level of service differentiation according to the priorities of individual applications. Finally, we showed that *AutoControl* can enforce performance targets for different application-level metrics, including throughput and response time, under dynamically-varying resource demands.

CHAPTER 5

Automated Control of Shared Storage Resources

5.1 Introduction

The common mode of running applications in corporate environments is to consolidate them onto shared hardware in large data centers. This allows benefits such as improved utilization of the resources, higher performance, and centralized management. However, as more applications compete for shared resources, the system has to be flexible enough to enable each application to meet its performance requirements.

Applications running on the shared storage present very different storage loads and have different performance requirements: for example, Online Transaction Processing (OLTP) applications might present bursty loads and require bounded IO response time; business analytics may require high throughput; and back-up applications usually present intense, highly sequential workloads with high throughput requirements. When the requirements of all applications cannot be met, the choice of which application requirements to meet and which ones to abandon may depend upon the priority of the individual applications. For example, meeting the I/O response time requirement of an interactive system may take precedence over the throughput requirement of a backup system. A data center operator needs the flexibility to set the performance metrics and priority levels for the applications, and to adjust them as necessary.

The proposed solutions to this problem in the literature include using proportional share I/O schedulers (e.g., SFQ [55]) and admission control (I/O throttling) using feedback controllers (e.g., Triage [60]). Proportional share schedulers divide the throughput available from the storage device between the applications in proportion to the applications' shares (a.k.a. weights), which are set statically by an administrator. Such schedulers alone cannot provide application performance differentiation, for several reasons: 1) the application performance depends on the proportional share settings and the workload characteristics in a complex, non-linear, time-dependent manner, and it is difficult for an administrator to determine in advance the share to assign to each application, and how/when to change it; 2) applications have several kinds of performance targets, such as response time and bandwidth requirements, not just throughput; and 3) in overload situations, when the system is unable to meet all of the application QoS requirements, prioritization is necessary to enable important applications to meet their performance requirements.

In this chapter, we present an approach that combines an optimization-based feedback controller with an underlying IO scheduler. Our controller accepts performance metrics and targets from multiple applications, monitors the performance of each application, and periodically adjusts the IO resources given to the applications at the disk array to make sure that each application meets its performance goal. The performance metrics for the applications can be different: the controller normalizes the application metrics so that the performance received by different applications can be compared and traded off. Our controller continually models the performance of each application relative to the resources it receives, and uses this model to determine the appropriate resource allocation for the application. If the resources available are inadequate to provide all the applications with their desired performance, a Linear Programming optimizer is used to compute a resource allocation that will degrade each application's performance in inverse proportion to its priority. Initial evaluations using this controller with a large commercial disk array show very promising results.

5.2 Storage Controller Design

In this section, we first describe our system model. We then present our design of the storage controller and describe its components in detail.

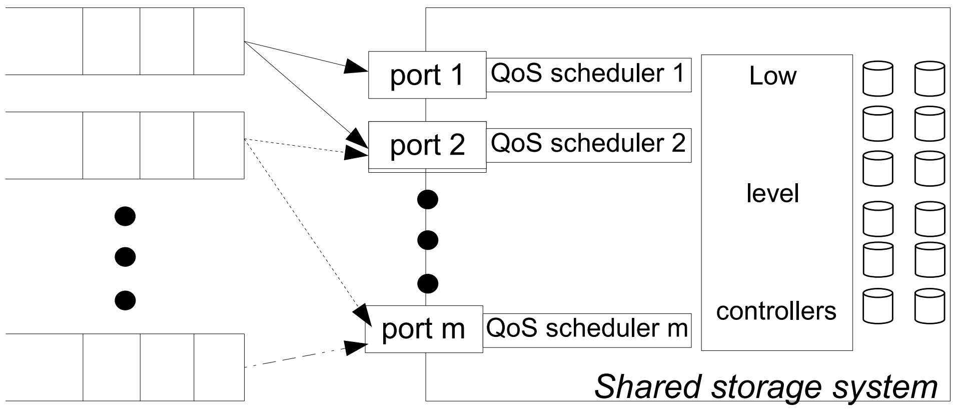

Figure 5.1: Storage system consists of a shared disk array with independent proportional share I/O scheduler running at each port.

5.2.1 System Modeling

Our system consists of a disk-array with a number of input ports where applications submit their I/O requests. The ports all share the same back-end resources and applications can use any combination of ports. Each port has an independent concurrency-limiting I/O scheduler, which controls the sharing among the I/O requests passing through its port. Once scheduled, an I/O request is released to the back-end of the disk array to access a shared array cache and disk devices. Each application using the system belongs to a service class used to indicate the desired level of service. Each service class has its own specified performance target (either I/O throughput or latency) and a priority level. In order to meet the QoS targets of the application classes, an external feedback controller periodically polls the disk array to determine the performance each class is receiving and then adjusts the parameters of all the schedulers running at each port of the disk array to meet the performance targets.

In our current system, the port IO schedulers have a single parameter: a per-application-class *concurrency bound.* The scheduler limits the number of IO requests outstanding at the disk array back-end from each application class to its concurrency bound. For example, if an application class has a concurrency bound of 2, and it has two I/O requests pending at the back-end, the scheduler will not send any more requests from that class to the back-end until at least one of the pending requests finishes. The total concurrency of the array (i.e., the total number of IOs permitted at the back-end from all ports) is limited, either by the

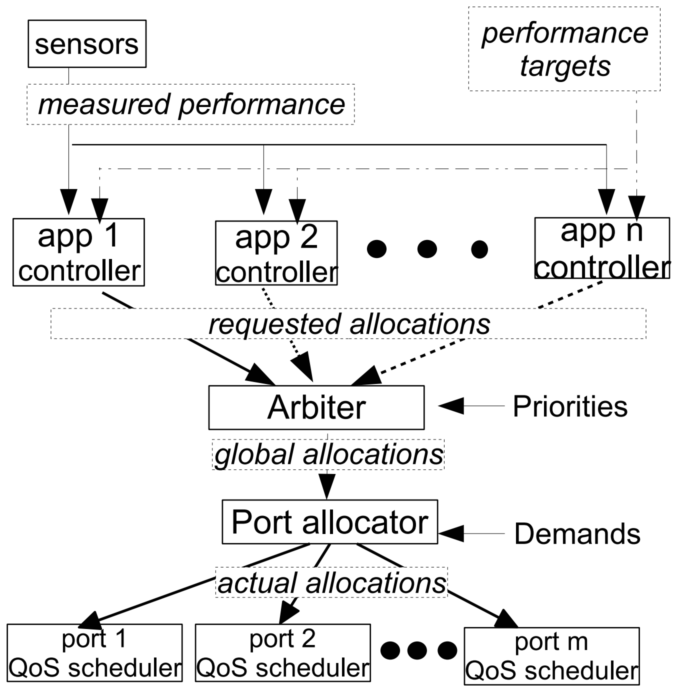

Figure 5.2: Architecture of the Storage QoS controller.

system, or by an administrative setting; we call this the *total concurrency bound.* We show that, by using the concurrency parameter, we can achieve per-application-class QoS targets across multiple ports even though each scheduler is independent.

We assume that an administrator specifies the QoS target for each application class. The specification includes a performance *metric*, a *target*, and a *priority.* The metric could be the desired throughput (IOs/sec), the bandwidth (bytes/sec), or the mean IO response time; other choices, such as the 90th percentile of the response time, are also possible. The target is the desired value of the metric specifying the desired performance. The priority provides an indication of how the application classes should be prioritized if the disk array cannot meet the targets of all the classes.

5.2.2 Storage QoS Controller

Our storage QoS controller consists of three layers, as shown in the Figure 5.2. The first layer is a set of *application controllers* that estimate the concurrency bound settings per application that will allow each application to reach its performance target. The second layer is an *arbiter*, which uses the application priorities with the concurrency requests and performance models generated by the application controllers to determine their global concurrency allocations. Finally, the *port allocator* determines the per-port concurrency settings for each application based on its global concurrency allocation and the recent distribution of its demands across the ports.

Application controller: Each application has a separate controller that computes the scheduler concurrency setting required to achieve its target. The application controller consists of two modules: a model estimator and a requirement estimator.

The model estimator module estimates a linear model for the dynamic relationship between the concurrency allocated to the application and its performance. Let $y_i(t)$ be the performance received by application i in control interval t, and $u_i(t)$ be the corresponding concurrency allocated to it. Then we use the approximation:

$$y_i(t) \approx y_i(t-1) + \beta_i(t)(u_i(t) - u_i(t-1))$$

The value of the slope $\beta_i(t)$ is re-estimated in every control interval using the past several measured values of application i's performance. These adjustments allow an application's model to incorporate implicitly the effects of the changing workload characteristics of all the applications (including itself). This linear estimation is designed to capture approximately the *local* behavior of the system, where the changes in the workload characteristics and the concurrencies allocated are small. These conditions apply because we re-estimate the model in every control interval (hence the workload characteristics do not change very much) and we constrain the controller to make only small changes to the concurrency allocations in each interval. We found empirically that the linear model performs reasonably well and provides an adequate approximation of the relationship between the concurrency allocations and the performance. The linearity can also be intuitively explained by the fact that if enough memory and disk bandwidth is available, performance is directly proportional to the concurrency.

The requirement estimator module uses the model to compute how much concurrency the application requires to meet its target. This estimate is sent to the arbiter as the application's requested allocation. However, we limit the requested change from the previous allocation (by 5% of the total concurrency bound in our current implementation) to ensure that the system remains in a local operating region where the estimated linear model still applies. Also, the data from which the model is estimated is often noisy, and the resulting models can occasionally be quite inaccurate. Limiting the change in concurrency within a control cycle also limits the harm caused by an inaccurate model. The cost of this limit is that convergence to a new operating point is slowed down when application characteristics change, but we found rate of convergence adequate in empirical tests.

Arbiter: The arbiter computes the applications' actual global concurrency settings based on their priorities. In each control cycle, the arbiter receives the concurrency requests and the models used to derive them from each of the application controllers. There are two cases, the *underload* case, where the total concurrency bound is large enough to meet the independent requests submitted by the application controllers, and the *overload* case, where the total concurrency bound is smaller than the sum of the requests. In the case of underload, the scheduler parameters are set based on the application controllers' requests, and any excess concurrency available is distributed in proportion to the application priorities. In the overload case, the arbiter uses a linear optimization to find concurrency settings that will degrade each application's performance (relative to its target) in inverse proportion to its priority, as far as possible. As in the application controllers, we limit the deviation from the previous allocations so that the estimated linear model is applicable.

More precisely, say that there are n applications, p_i is the priority of application i, c_i its current allocation, u_i the next (future) allocation, and f_i is the linear model estimating the performance of application i in terms of u_i. l_i is the limit on deviation, which we set to 0.05 for all applications. The concurrency allocations c_i and u_i are normalized to the range $[0, 1]$ by dividing the actual allocation by the total concurrency bound. The performance values $f_i(u_i)$ are normalized to be (performance/target) for throughput and bandwidth metrics and (target/performance) for latency, in order to make all normalized performance values better as they increase. In order to compute the future allocations u_i, the arbiter solves the following linear program:

$$\begin{aligned}
&\text{Find } u_1, \ldots, u_n, \epsilon \text{ to minimize } \epsilon \text{ subject to:} \\
&p_i(1 - f_i(u_i)) - p_j(1 - f_j(u_j)) < \epsilon \\
&\qquad\qquad\qquad\qquad \text{for } 1 \leq i \neq j \leq n \\
|u_i - c_i| \quad &\leq \quad l_i \qquad \text{for } 1 \leq i \leq n \\
u_1 + \cdots + u_n \quad &= \quad \min(1, c_1 + l_1 + \cdots + c_n + l_n).
\end{aligned}$$

Note that the quantity in the right-hand side of the last constraint is a constant for the linear program, and the constraint is therefore still linear.

In the LP above, $p_i(1 - f_i(u_i))$ is the fractional tracking error for application i, weighted by its priority. ϵ is the maximum difference between the priority-weighted fractional tracking errors for different applications, and the objective function tries to minimize this maximum difference. In the limit, $\epsilon = 0$, and the priority-weighted fractional tracking errors are equal; for example, in a scenario with two applications, if application 1 has the priority 1 and a performance value 10% below its target, and application 2 has the priority 2, then each has a priority-weighted tracking error of 0.1, and the performance value of application 2 should be 5% below its target.

Port allocator: The arbiter computes the aggregate concurrency setting for each application, but this concurrency has to be translated into per-port settings. Since application workloads may be dynamic and non-uniform across the ports, the port allocator uses the recently observed *demand* from each application at the ports to determine how much of the application's concurrency should be allocated to a port. We define an application's demand at a port as the mean number of IO requests outstanding from the application at the port during the previous control interval.

More precisely, let $d_{i,j}$ denote the the demand of application i through port j, and CG_i its aggregate concurrency as determined by the arbiter. Then the corresponding per-port normalized concurrencies are given by:

$$C_{i,j} = CG_i \left(\frac{d_{i,j}}{\sum_{k=1}^{n} d_{i,k}} \right)$$

where n is the number of ports. If $d_{i,j}$ is zero, then the corresponding concurrency is set to zero.

The normalized concurrencies are multiplied by the total concurrency bound and rounded up to determine the number of application IOs permitted to be scheduled simultaneously from that port. In addition, we set the concurrency setting to be at least one for all applications at all ports, in order to avoid blocking an application that begins sending IOs to a port during the control interval.

5.3 Evaluation Results

In this section, we present our initial results from a set of experiments we conducted to evaluate our storage controller. We designed our experiments to determine whether our controller can adjust the low-level scheduler parameters to achieve application targets. We also evaluated its ability to differentiate between multiple applications based on their priorities. Finally, we looked at the behavior of our controller when applications have different target metrics, for example a latency target and a throughput target.

We used two HP BL460c blade servers and a high-end XP-1024 disk array for our experiments. The blade servers are connected to separate ports of the XP-1024 disk array via two 4 Gbit/s QLogic Fibre channel adapters. Each of the blade servers had 8GB RAM, two 3GHz dual core Intel Xeon processors and used the Linux kernel version 2.6.18-8.el5 as their operating system. We allocated seven 4-disk RAID-1 logical disks for our experiments on the XP disk array.

Since the XP array did not have an appropriate port scheduler that can limit available concurrency to specific workloads, we implemented a scheduler in the Linux kernel and ran it at each of the hosts to emulate independent port schedulers. The scheduler module creates pseudo devices (entries in /dev), which are then backed up by the logical disks at the XP

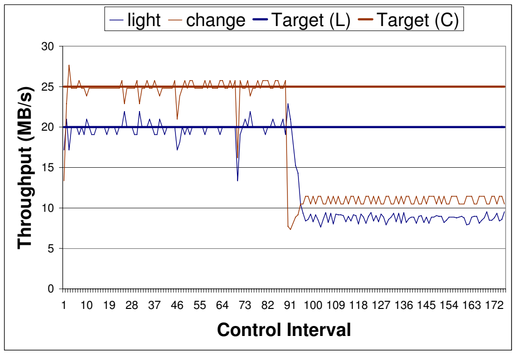

(a) Throughput

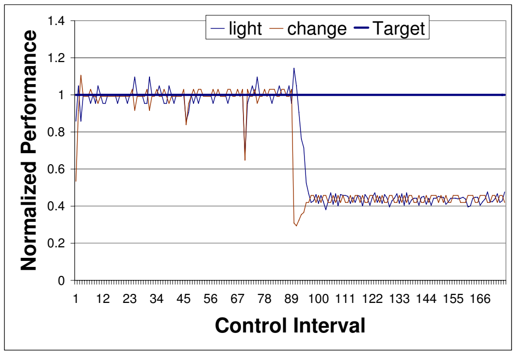

(b) Normalized Performance

Figure 5.3: Performance of a changing workload with throughput targets. The control interval is 2 seconds.

array. Each pseudo device implements a different service level and we can associate different targets for these through our controller. The scheduler module intercepts the requests made to the pseudo devices and passes them to the XP array so long as the number of outstanding requests are less than the concurrency associated with the service level. In addition, the scheduler module collects the performance statistics needed by the controller. The controller polls the scheduler module at each control interval (every 2 seconds in our experiments) and gathers the statistics to determine overall performance levels achieved by all the applications classes.

We used a variety of synthetic workloads in our evaluation. Our reference workload is called `light`, and it consists of 16KB fixed size accesses generated by 25 independent threads. These accesses were made to locations selected at random with uniform distribution. 90% of the accesses were reads and the 10% were writes. We also generated additional workloads based on `light` by varying the number of IO generating threads and the size of the IO requests in our evaluation.

Figure 5.3 presents the throughput of a `light` workload and a second, heavier workload with changing IO size, referred to as `change`. Initially, the `change` workload has 100 threads generating 16KB IOs. Midway through the experiment, the `change` workload starts sending small 4KB IOs instead. The targets for `light` and `change` are 20MB/s and 25MB/s

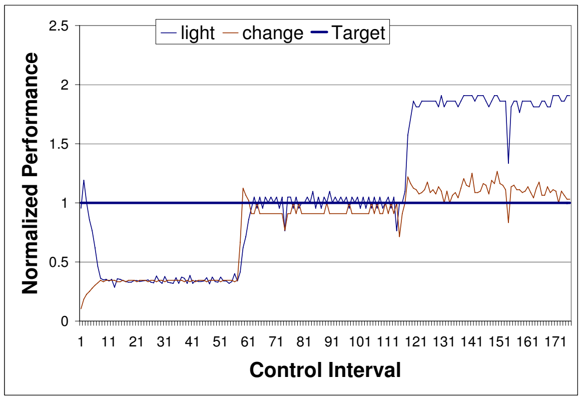

Figure 5.4: Workloads with different target metrics. The `light` workload has a throughput target of 20 MB/sec and the `heavy` workload has a latency target of 10ms.

respectively, and their priorities are equal. As the figure shows, both workloads initially meet their targets. However, when the request size of `change` drops, the it is unable to meet its target. Since the priorities of the two workloads are equal, the controller moves resources from `light` to `change`, so that the performance of both drops proportionately, which is the specified behavior. This is most clearly seen in Figure 5.3(b), which shows the throughputs of the two workloads normalized (divided) by their target values. The curves for the two workloads are superposed, as we expect for equal priorities, and the performance of each workload goes from 100% of the target value to around 45% of the target value in the second half of the experiment.

In the second experiment, we used two workloads with different target metrics: the `light` workload with a throughput target of 25 MB/s and a different variant of the `change` workload with a latency target of 10ms. In this experiment, the `change` workload varies the number of IO generations threads in three phases; it uses 100 threads in the first phase, 25 threads in the second phase, and 5 threads in the third phase. Figure 5.4 presents the normalized performance of both of these workloads. In the first phase of the experiment, neither of the two workloads are able to meet their targets due to high intensity (100 threads) of the `change` workload. In the second phase, `change` reduces its intensity to 25 threads and as a result, both workloads are able to meet their respective targets: `light`

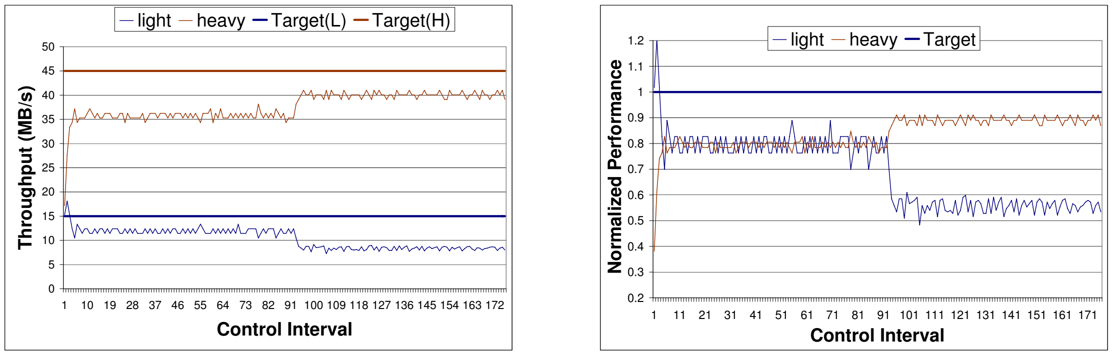

(a) Throughput (b) Normalized Performance

Figure 5.5: Effects of workload priorities.

achieves a throughput of about 25 MB/s and `change` experiences a reduction in its latency to about 10ms. Finally, in the last phase of the workload `change` reduces its intensity by using only five threads, and as a result, the `light` workload is able to further boost its throughput to about 38 MB/s without hurting the latency goals of the `change` workload. Note that, the `change` workload can not reduce its latency further as its requests are no longer queued (but instead dispatched directly); as a result the storage controller allocates the excess concurrency not used by the `change` workload to the `light` workload.

In the last experiment, we used two workloads `light` and `heavy`; the latter workload uses 100 threads to issue its requests. In this experiment, both `heavy` and `light` workloads start with equal priority in the first half of the experiment until the 90th control interval. Then, we adjusted the priority of the `heavy` workload to be four times that of the `light` workload. Figure 5.5 shows the effects of the priorities. It shows that the arbiter controller throttles the `light` workload so that the `heavy` workload is four times closer to its target compared to the `light` workload in the second phase of the experiment.

5.4 Storage Systems Control Related Work

Prior work on controlling storage resources include systems that provide performance guarantees in storage systems [36, 47, 55, 65]. However, one has to tune these tools to achieve application-level guarantees. Our work builds on top of our earlier work, where we developed an adaptive controller [60] to achieve performance differentiation, and efficient adaptive proportional share scheduler [48] for storage systems.

In prior work, feedback controllers have been proposed [36, 60] to implement application prioritization requirements by using client throttling. A centralized controller monitors the state of the storage device and the application clients, and then directs the clients to reduce or increase their IO request rate so that the requirements of the highest priority (or most demanding) client can be met. This approach can handle somewhat more complex prioritization requirements than a simple proportional share scheduler, but has the disadvantage that, by the time the clients implement the throttle commands, the state of the storage device may have changed; as a result, the controller may not be work-conserving, and the utilization of the storage device may be kept unnecessarily low.

In recent years, control theory has been applied to computer systems for resource management and performance control [52, 58]. Examples of its application include web server performance guarantees [22], dynamic adjustment of the cache size for multiple request classes [64], CPU and memory utilization control in web servers [43], adjustment of resource demands of virtual machines based on resource availability [103], and dynamic CPU allocations for multi-tier applications [63, 76]. In our prior work [75], we have developed a MIMO controller that can adjust the resource shares for multiple virtual machines to achieve application targets. In contrast, this work focuses on building a control system for a shared disk array with multiple ports. We also introduce the notion of resource control using dynamic concurrency bounds to provide performance differentiation across multiple ports.

5.5 Summary

In this chapter, we presented a storage controller that dynamically allocates storage resources to multiple competing applications accessing data on a multi-port shared disk array. The controller consists of three layers, a set of application controllers, an arbiter and a port allocator. The application controllers determine the required I/O resources to meet application performance goals, and the arbiter uses application priorities to arbitrate in the case of overload. The port allocator uses each application's demands through a particular port to determine the per-port concurrency. Our preliminary experiments show that our controller can achieve application targets by automatically adjusting the scheduler parameters. The controller can also enforce different application priorities and different targets for multiple applications.

CHAPTER 6

Automated Mechanisms for Saving Desktop Energy using Virtualization

6.1 Introduction

The energy consumed by the burgeoning computing infrastructure worldwide has recently drawn significant attention. While the focus of energy management has been on the data-center setting [37, 69, 73], attention has also been directed recently to the significant amounts of energy consumed by desktop computers in homes and enterprises [23, 71]. A recent study [74] estimates that PCs and their monitors consume about 100 TWh/year, constituting 3% of the annual electricity consumed in the U.S. Of this, 65 TWh/year is consumed by PCs in enterprises, which constitutes 5% of the commercial building electricity consumption.

The common approach to reducing PC energy wastage is to put a computer to sleep or turn it off when it is idle. However, the presence of the user makes this particularly challenging in a desktop computing environment. Users care about preserving long-running network connections (e.g., login sessions, IM presence, file sharing), background computation (e.g., syncing and automatic filing of new emails), and keeping their machine reachable even while it is idle. Putting a desktop PC to sleep is likely to cause disruption (e.g., broken connections), thereby having a negative impact on the user, who might then choose to disable the energy savings mechanism altogether.

To reduce user disruption while still allowing machines to sleep, the typical approach has been to have a *proxy* on the network for a machine that is asleep [74]. However, this approach suffers from an inherent tradeoff between functionality and complexity in terms of application-specific customization.

In this chapter, we present *LiteGreen*, a system to save desktop energy by employing a novel approach to avoiding user disruption as well as the complexity of application-specific customization. The basic idea is to virtualize the user's desktop computing environment as a virtual machine (VM) and then migrate it between the user's physical desktop machine and a VM server, depending on whether the desktop computing environment is being actively used or is idle. When the desktop becomes idle, say when the user steps away for several minutes (e.g., for a coffee break), the desktop VM is migrated away to the VM server and the physical desktop machine is put to standby sleep mode. When the desktop becomes active again (e.g., when the user returns), the desktop VM is migrated back to the physical desktop machine. Thus, even when it has been migrated to the VM server, the user's desktop environment remains alive (i.e., it is "always on"), so ongoing network connections and other activities (e.g., background downloads) are *not* disturbed, regardless of the application involved. A fundamental assumption is LiteGreen is that the current systems are not energy proportional.

The "always on" feature of LiteGreen allows energy savings whenever the opportunity arises, without having to worry about disrupting the user. Besides long idle periods (e.g., nights and weekends), energy can also be saved by putting the physical desktop computer to sleep even during short idle periods, such as when a user goes to a meeting or steps out for coffee. Indeed, our measurements indicate that the potential energy savings from exploiting short idle periods are significant (Section 6.3).

While virtualization is a useful primitive for continuously maintaining the desktop environment, the following two key challenges need to be addressed for virtualization to be useful for saving energy on desktop computers. First, how do we provide a normal (undisrupted) desktop experience to users, masking the effect of VMs and their migration? Second, how do we decide when and which VMs to migrate to/from the server in order to maximize energy savings while minimizing disruption to users?

To address the first challenge, LiteGreen uses the *live migration* feature supported by modern hypervisors [39] coupled with the idea of always presenting the desktop environment through a level of indirection (Section 6.4). Thus, whether the VM is at the server or desktop, users always access their desktop VM through a remote desktop (RD) session. So, in a typical scenario, when a user returns to their machine that has been put to sleep, the machine is woken up from sleep and the user is able to immediately access their desktop environment (whose state is fully up-to-date, because it has been "always on") through an RD connection to the desktop VM running on the VM server. Subsequently, the desktop VM is migrated back to the user's physical desktop machine without the user even noticing.

To address the second challenge, LiteGreen uses an energy-saving algorithm that runs on the server and carefully balances migrations based on two continuously-updated lists: 1) VMs in *mandatory to push* list need to be migrated to the desktop to minimize user disruption and 2) VMs in *eligible to pull* list may be migrated to server for energy savings, subject to server capacity constraints (Section 5.2). Based on an analysis of an aggregate of over 65,000 hours of data we have gathered from 120 desktop computers at Microsoft Research India (MSRI), we estimate that LiteGreen saves 72-86% of desktop energy, compared to 35% savings achieved by either users manually or automatically putting their machines to sleep through Windows power management.

We have prototyped LiteGreen on the Microsoft Hyper-V hypervisor (Section 6.7). We have a small-scale deployment running on the desktop machines of five users. Separately, we have conducted laboratory experiments using both the Hyper-V and Xen hypervisors to evaluate various aspects of LiteGreen. A simulator is also developed to analyze the gathered data and understand the finer aspects of our algorithms.

The main contributions of this work are the following:

1. A novel system that leverages virtualization to consolidate idle desktops on a VM server, thereby saving energy while avoiding user disruption.

2. Automated mechanisms to drive the migration of the desktop computing environment between the physical desktop machines and the VM server.

3. A prototype implementation and the evaluation of LiteGreen through a small-scale deployment.

4. Trace-driven analysis based on an aggregate of over 65,000 hours of desktop resource usage data gathered from 120 desktops, demonstrating total energy savings of 72-86% with short idle periods (< 3 hours) contributing 20% or more.

6.2 Background

In this section, we provide some background on the problem setting and and discuss related work.

6.2.1 PC Energy Consumption

Researchers have measured and characterized the energy consumed by desktop computers [23]. The typical desktop PC consumes 80-110 W when active and 60-80 W when idle, excluding the monitor, which adds another 35-80 W. The relatively small difference between active and idle modes is significant and arises because the processor itself only accounts for a small portion of the total energy. So saving energy using the multiple P ("processor") states, effected through dynamic voltage and frequency scaling (DVFS) [97], has limited effectiveness.

In view of the above, multiple S ("sleep") states have been defined as part of the ACPI standard [17]. In particular, the S3 state ("standby") suspends the machine's state to RAM, thereby cutting energy consumption to 2-3 W. S3 has the advantage of being much quicker to transition in and out of than S4 ("hibernate"), which involves suspending the machine's state to disk.

6.2.2 Proxy-Based Approach

As discussed above, the only way of cutting down the energy consumed by a PC is to put it to sleep. However, when a PC it put to sleep, it loses its network presence, resulting in ongoing connections breaking (e.g., remote login or file download sessions) and the machine even becoming inaccessible over the network. The resulting disruption has been recognized as a key reason why users are often reluctant to put their machines to sleep [23].

The general approach to allowing a PC to sleep while maintaining some network presence is to have a network proxy operate on its behalf while it is asleep [74]. The functionality of the proxy could span a wide range as follows.

- **WoL Proxy:** The simplest proxy allows the machine to be woken up using the *Wake-on-LAN* (WoL) mechanism [16] supported by the vast majority of Ethernet NICs in deployment. To be able to send the "magic" WoL packet, the proxy must be on the same subnet as the target machine and, moreover, needs to know the MAC address of the machine. Typically, machine wakeup is initiated manually.
- **Protocol Proxy:** A more sophisticated proxy performs automatic wakeup, triggered by a filtered subset of the incoming traffic [71]. The filters could be configured based on user input and also the list of network ports that the target machine was listening on before it went to sleep. Other traffic is either responded to by the proxy itself without waking up the target machine (e.g., ARP for the target machine) or ignored (e.g., ARP for other hosts).
- **Application Proxy:** An even more sophisticated proxy incorporates application-specific stubs that allow it to engage in network communication on behalf of applications running on the machine that is now asleep [71]. Such a proxy could even be integrated into a NIC augmented with processing and storage [23].

The greater functionality of a proxy comes at the cost of greater complexity, for instance, the need to create stubs for each application that the user wishes to keep alive. LiteGreen sidesteps this complexity by keeping the entire desktop computing environment alive, by consolidating it on the server along with other idle desktops.

6.2.3 Saving Energy through Consolidation

Consolidation to save energy has been employed in other computing settings—data centers and thin clients.

In the data center setting, server consolidation is used to approximate energy proportionality, wherein the overall energy consumption is roughly proportional to the workload. Since the individual computing nodes are far from being energy-proportional, the approach taken is to migrate computation, typically using virtualization, from several lightly-loaded servers onto fewer servers and then turn off the servers that are freed up [37, 86, 90]. Doing so saves not only the energy consumed directly by the servers but also the significant amount of energy consumed indirectly for cooling. For instance, there has been work on workload placement based on the spatial temperature profile within the data center [69] and coordinated power management in such settings [70].

Thin client based computing, an idea that is making a reappearance [41, 15] despite failures in the past, represents an extreme form of consolidation, with all of the computing resources being centralized. While the cost, management, and energy savings might make the model attractive in some environments, it may not be suitable in settings where power users want the flexibility of a PC or insulation from even transient dips in performance due to consolidation. Indeed, market projections suggest that PCs will continue to be the dominant desktop computing platform, with over 125 million units shipping each year from 2009 through 2013 [21], and with thin clients replacing only 15% of PCs by 2014 [19]. Thus, there will continue to be a sizeable and growing installed base of PCs for the foreseeable future, so addressing the problem of energy consumed by desktop PCs remains important.

While LiteGreen's use of consolidation is inspired by the above work, a key difference arises from the presence of users in a desktop computing environment. Unlike in a data center setting, where machines tend to run server workloads and hence substitutable to a large extent, a desktop machine is a user's *personal* computer. Users expect to have access to *their* computing environment. Furthermore, unlike in a thin client setting, users expect to have good interactive performance and the flexibility of attaching specialized hardware and peripherals (e.g., a high-end graphics card).

Central to the design of LiteGreen is preserving this PC model and minimizing user disruption by consolidating only idle desktops.

6.2.4 Virtualization in LiteGreen Prototype

For our LiteGreen prototype, we use the Microsoft Hyper-V hypervisor. While this is a server hypervisor, the five users in our deployment were able to use it without difficulty in their desktop computing environment. Since, Hyper-V currently does not support page

# PCs	# Aggregate duration (hours)	Peak users
130	65000	120

Table 6.1: Statistics of PC usage data at MSR India

sharing or memory ballooning, to evaluate memory ballooning, we conducted a separate set of experiments with the Xen hypervisor. Finally, since Hyper-V only supports live migration with shared storage, we set up a shared storage server connected to the same GigE switch as the desktop machines and the server (see Section 6.10 for a discussion on shared storage).

6.3 Motivation Based on Measurement

To provide concrete motivation for our work beyond the prior work discussed above, we conducted a measurement study on the usage of PCs. Our study was set in the MSRI lab during the summer of 2009, at which time the lab's population peaked at around 130 users. Of these, 120 users at the peak volunteered to run our measurement tool, which gathered information on the PC resource usage (in terms of the CPU, network, disk, and memory) and also monitored user interaction UI). In view of the sensitivity involved in monitoring keyboard activity on the volunteers' machines, we only monitored mouse activity to detect UI.

We have collected over 65000 hours worth of data from these users. We placed the data gathered from each machine into 1-minute buckets, each of which was then annotated with the level of resource usage and whether there was UI activity. We classify a machine as being *idle* (as opposed to being *active*) during a 1-minute bucket using one of the two policies discussed later in Section 6.5.2: the *default* policy, which only looks for the absence of UI activity in the last 10 minutes, and a more *conservative* policy, which additionally checks whether the CPU usage was below 10%.

Based on this data, we seek to answer two questions.

Q1. How (under)utilized are desktop PCs?

To help answer this question, Figure 6.1a plots the distribution of CPU usage and UI activity, binned into 1-minute buckets and aggregated across all of the PCs in our study. To

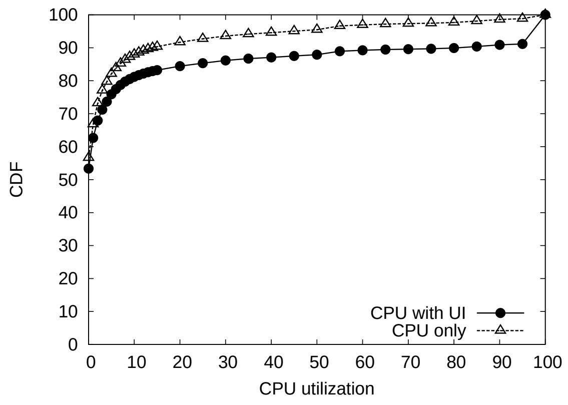

(a) Distribution of CPU utilization

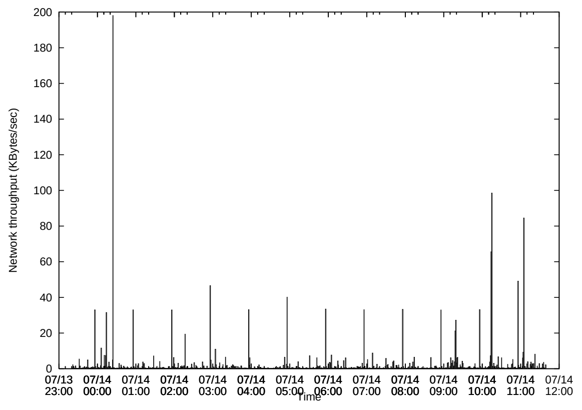

(b) Network activity during the night on one idle desktop machine

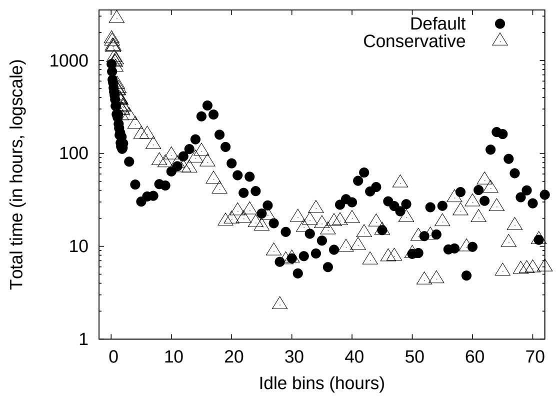

(c) Distribution of idle periods

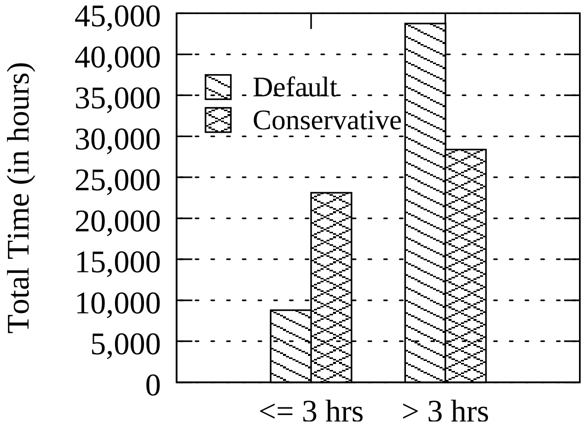

(d) Comparison of aggregate duration of short and long idle periods

Figure 6.1: Analysis of PC usage data at MSR India

allow plotting both CPU usage and UI activity in the same graph, we adopt the convention of treating the presence of UI activity in a bucket as 100% CPU usage. The “CPU only” curve in the figure shows that CPU usage is low, remaining under 10% for about 90% of the time. The “CPU with UI” curve shows that UI activity is present, on average, only in 10% of the 1-minute buckets, or about 2.4 hours in a day. However, since even an active user might have 1-minute buckets with no UI activity (e.g., they might just be reading from the screen), the total UI activity is very likely larger than 10%.[1] For multi-core CPUs, we could use the total amount of CPU utilization as a guiding metric.

[1]It is possible that we may have missed periods when there was keyboard activity but no mouse activity. However, we ran a test with a small set of 3 volunteers, for whom we monitored keyboard activity as well mouse activity, and found it rare to have instances, where there was keyboard activity but no mouse activity in the following 10 minutes.

While both CPU usage and UI activity are low, it still does not mean that the PC can be simply put to sleep. The reason is that there is network activity even when the machine is idle, as depicted in Figure 6.1b. Hence, as observed in prior work [23, 71], it is important to preserve the network presence of a machine, even while it is idle, to avoid user disruption.

Q2. How are the idle periods distributed?

Given that there is much idleness in PCs, the next question is how the idle periods are distributed. We define an idle period as a contiguous sequence of 1-minute buckets, each of which is classified as being idle. The conventional wisdom is that idle periods are long, e.g., overnight periods and weekends. Figures 6.1c shows the distribution of idle periods based on the default (UI only) and conservative (UI and CPU usage) definitions of idleness noted above. Each data point shows the aggregate idle time (shown on the y axis on a log scale) spent in idle periods of the corresponding length (shown on the x axis). The x axis extends to 72 hours, or 3 days, which encompasses idle periods stretching over an entire weekend.

The default curve shows distinctive peaks at around 15 hours (overnight periods) and 63 hours (weekends). It also shows a peak for short idle periods, under about 3 hours in length. In the conservative curve, the peak at the short idle periods dominates by far. The overnight and weekend peaks are no longer distinctive since, based on the conservative definition of idleness, these long periods tend to be interrupted, and hence broken up, by intervening bursts of background CPU activity.

Figure 6.1d shows that with the default definition of idleness, idle periods shorter than 3 hours add up to about 20% of the total duration of idle periods longer than 3 hours. With the conservative policy, the short idle periods add up to over 80% of the total duration of the long idle periods. Thus, the short idle periods, which correspond to lunch breaks, meetings, etc., during a work day, represent a significant opportunity for energy savings over and above the savings from the long idle periods considered in prior work.

In summary, we to make two primary observations from our analysis. First, desktop PCs are often idle, and there is significant opportunity to exploit short idle periods. Second, it is important to maintain network presence even during the idle periods to avoid user disruption when the user comes back later.

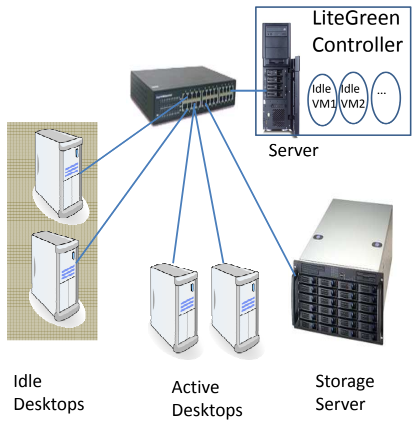

Figure 6.2: **LiteGreen architecture**: Desktops are in active (switched on) or idle (sleep) state. Server hosts idle desktops running in VMs

6.4 System Architecture

Figure 6.2 shows the high-level architecture of LiteGreen. The desktop computing infrastructure is augmented with a VM server and a shared storage node. In general, there could be more than one VM server and/or shared storage node. All of these elements are connected via a low-latency, high-speed LAN.

Each desktop machine as well as the server run a hypervisor. The hypervisor on the desktop machine hosts a VM in which the client OS runs (Figure 6.3a). This VM is migrated away to the server when the user is not active and the desktop is put to sleep (Figure 6.3b). When the user returns, the desktop is woken up and the VM is “live migrated” back to the desktop(Figure 6.3c). To insulate the user from such migrations, the desktop hypervisor also runs a remote desktop (RD) client [8], which is used by the user to connect to, and remain connected to, their VM, regardless of where it is running. The mechanism is similar to Internet suspend and resume [61] (ISR), but we keep the machine alive when it is migrated to the server. The crucial difference is that in ISR, the VM is suspended and written to a distributed file system, while we have the VM running in a remote server.

The user’s desktop VM uses, in lieu of a local disk, the shared storage node, which is also shared with the server. This aspect of the architecture arises from the limitations of live migration in hypervisors currently in production and can be done away with once live migration with local VHDs is supported (Section 6.10).

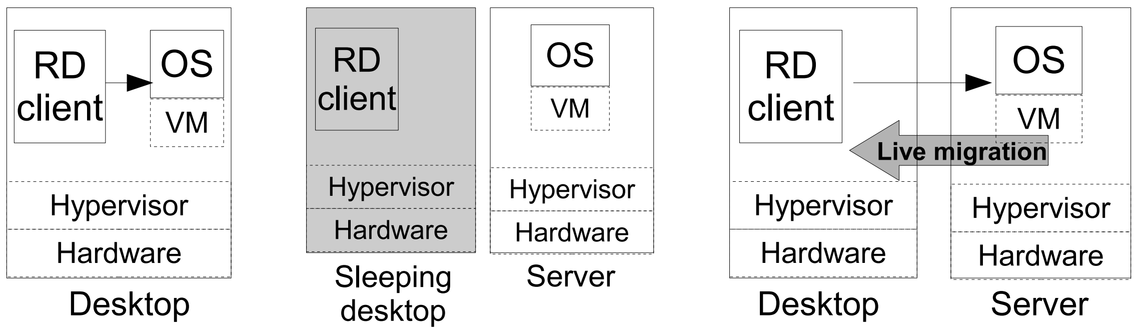

(a) **Virtualized desktop**: OS in current desktops is run in a VM

(b) **Idle VM on the server**: After the VM is migrated, desktop is put to sleep

(c) **Migrating VM**: While the VM is being migrated, RD client allows access to graphical desktop

Figure 6.3: Desktop states

The hypervisor on the server hosts the guest VMs that have been migrated to it from (idle) desktop machines. The server also includes a *controller*, which is the brain of LiteGreen. The controller receives periodic updates from *stubs* on the desktop hypervisors on the level of user and computing activity on the desktops. The controller also tracks resource usage on the server. Using all of this information, the controller orchestrates the migration of VMs to the server and back to the desktop machines, and manages the allocation of resources on the server.

6.5 Design

Having provided an overview of the architecture, we now detail the design of LiteGreen. The design of LiteGreen has to deal with two somewhat conflicting goals: maximizing energy savings from putting machines to sleep while minimizing disruption to users. When faced with a choice, LiteGreen errs on the side of being conservative, i.e., avoiding user disruption even if it means reduced energy savings.

The operation of LiteGreen can be described in terms of a control loop effected by the controller based on local information at the server as well as information reported by the desktop stubs. We discuss the individual elements before putting together the whole control loop.

6.5.1 Which VMs to Migrate?

The controller maintains two lists of VMs:

- *Eligible for Pull:* list of (idle) VMs that currently reside on the desktop machines but could be migrated (i.e., "pulled") to the server, thereby saving energy without user disruption.

- *Mandatory to Push:* list of (now active) VMs that had previously been migrated to the server but must now be migrated (i.e., "pushed") back to the desktop machines at the earliest to minimize user disruption.

In general, the determination of whether a VM is active or idle is made based on both UI activity initiated by the user and computing activity, as discussed next.

6.5.2 Determining If Idle or Active

The presence of any UI activity initiated by the user, through the mouse or the keyboard (e.g., mouse movement, mouse clicks, key presses), in the recent past (*actvityWindow*, set to 10 minutes by default) is interpreted as an indicator that the machine is active. Even though the load imposed on the machine might be rather minimal, we make this conservative choice to reflect our emphasis on minimizing the impact on the interactive performance perceived by the user.

In the *default policy*, the presence of UI activity is taken as the *only* indicator of whether the machine is active. So, the absence of recent UI activity is taken as the machine is idle.

A more *conservative policy*, however, also considers the actual computational load on the machine. Specifically, if the CPU usage is above a threshold, the machine is deemed to be active. So, for the machine to be deemed idle, both the absence of recent UI activity and CPU usage being below the threshold are necessary conditions. To avoid too much bouncing between the active and idle states, we introduce hysteresis in the process by (a) measuring the CPU usage as the average over an interval (e.g., 1 minute) rather than instantaneously, and (b) having a higher threshold, c_{push}, for the push list (i.e., idle$\rightarrow$active transition of a VM currently on the server) than the threshold, c_{pull}, for the pull list (i.e., for a VM currently on a desktop machine).

6.5.3 Server Capacity Constraint

A second factor that the controller considers while making migration decisions is the availability of resources on the server. If the server's resources are saturated or close to it, the controller migrates some VMs back to the desktop machines to relieve the pressure. Thus, an idle VM is merely *eligible* for being consolidated on the server and, in fact, might not be if the server does not have the capacity. On the other hand, an active VM must be migrated back to the desktop machine even if the server has the capacity. This design reflects the choice to err on the side of being conservative, as noted above.

There are two server resource constraints that we focus on. The first is *memory availability*. Given a total server memory, M, and the allocation, m, made to each VM, the number of VMs that can be hosted on the server is bounded by $n_{RAM} = \frac{M}{m}$. Note that m is the memory allocated to a VM after ballooning and would typically be some minimal value such as 384 MB that allows an idle VM to still function (Section 6.8.4).

The second resource constraint arises from *CPU usage*. Basically, the aggregate CPU usage of all the VMs on the server should be below a threshold. As with the conservative client-side policy discussed in Section 6.5.2, we introduce hysteresis by (a) measuring the CPU usage as the average over a time interval (e.g., 1 minute), and (b) having a higher threshold, s_{push}, for pushing out VMs, than the threshold, s_{pull}, for pulling in VMs. The server tries to pull in VMs (assuming the pull list is non-empty) so long as the aggregate CPU usage is under s_{pull}. Then, if the CPU usage rises above s_{push}, the server pushes back VMs. Thus, there is a bound, n_{CPU}, on the number of VMs that can be accommodated such that $\sum_{i=1}^{i=n_{CPU}} x_i \leq s_{push}$, where x_i is the CPU usage of the i^{th} VM. Adding system overhead to get a more accurate assessment of amount of CPU and memory required is left as future work.

The total number of VMs that can be consolidated on the server is bounded by $min(n_{RAM}, n_{CPU})$. While one could extend this mechanism to other resources such as network and disk, our evaluation in Section 6.9 indicates that enforcing CPU constraints also ends up limiting the usage of other resources.

6.5.4 Bin Packing for Consolidation

The problem of consolidating VMs within the constraints of the server's resources can be viewed as a bin-packing problem [46]. For instance, one VM could have high CPU usage but still be deemed idle when the default policy, which only considers UI activity, is being used to make the idle vs. active determination (Section 6.5.2). There might be the opportunity to push out this VM and instead pull in *multiple* other VMs from the pull list. As noted in Section 6.2.1, the energy consumed by a PC increases only minimally with increasing CPU load. So, consolidating the multiple new VMs in place of the one that is evicted would likely help save energy.

Accordingly, if the controller finds that the server is saturated (i.e., its CPU usage is greater than s_{pull}), it sorts the consolidated VMs based on their CPU usage and, likewise, sorts the VMs on the pull list based on their CPU usage. If the VM with the highest CPU usage in the former list (say VM^{push}) has been consuming more CPU than two or more VMs (say $VM_1^{pull} \cdots VM_k^{pull}$) with the lowest CPU usage from the pull list put together (i.e., $CPU^{push} \geq \sum_{i=1}^{i=k} CPU_i^{pull}, k \geq 2$), then the controller does a swap. A swap involves pushing VM^{push} back to its desktop machine, which is woken up from sleep, and pulling in $VM_1^{pull} \cdots VM_k^{pull}$ for consolidation on the server, after which their respective desktop machines are put to sleep.

6.5.5 Measuring & Normalizing CPU Usage

Given the heterogeneity of desktop and server physical machines, one question is how CPU usage is measured and how it is normalized across the machines. All measurement of CPU usage in LiteGreen, both on the server and on the desktop machines, is made at the hypervisor level, where the controller and stubs run, rather than within the guest VMs. Besides leaving the VMs untouched and also accounting for CPU usage by the hypervisor itself, measurement at the hypervisor level has the advantage of being unaffected by the configuration of the virtual processors. The hypervisor also provides uniform interface to interact with multiple operating systems.

Another issue is normalizing measurements made on the desktop machines with respect to those made on the server. For instance, when a decision to pull a VM is made based on its CPU usage while running on the desktop machine, the question is what its CPU usage would be once it has been migrated to the server. In our current design, we only normalize at the level of cores, treating cores as equivalent regardless of the physical machine. So, for example, a CPU usage of $x\%$ on a 2-core desktop machine would translate to a CPU usage of $\frac{x}{4}\%$ on an 8-core server machine. One could consider refining this design by using the CPU benchmark numbers for each processor to perform normalization.

6.5.6 Putting All Together: LiteGreen Control Loop

To summarize, LiteGreen's control loop operates as follows. Based on information gathered from the stubs, the controller determines which VMs, if any, have become idle, and adds them to the pull list. Furthermore, based both on information gathered from the stubs and from local monitoring on the server, the controller determines which VMs, if any, have become active again and adds these to the push list. If the push list is non-empty, the newly active VMs are migrated back to the desktop right away. If the pull list is non-empty and the server has the capacity, additional idle VMs are migrated to the server. If at any point, the server runs out of capacity, the controller looks for opportunities to push out the most expensive VMs in terms of CPU, memory usage and pull in the least expensive VMs from the pull list. Pseudocode for the control loop employed by the LiteGreen controller is provided in section 6.6.

6.6 Pseudocode of the LiteGreen Controller

```
$isVMidle(VM_i)$
begin
    if ($\exists$ UI activity anytime in activityWindow) then
        return false
    end
    if (conservative policy) then
        if (CPU usage of $VM_i > c_{pull}$ anytime in activityWindow) then
            return false
        end
    end
    return true
end

$isVMactive(VM_i)$
begin
    if ($\exists$ UI activity anytime in activityWindow) then
        return true
    end
    if (conservative policy) then
        if (CPU usage of $VM_i > c_{push}$ anytime in activityWindow) then
            return true
        end
    end
    return false
end

$PushBackVM(VM_i)$
begin
    Wake up desktop machine $i$
    Migrate $VM_i$ back to its desktop
    $pushlist \leftarrow pushlist - \{VM_i\}$
    $VMsOnServer \leftarrow VMsOnServer - \{VM_i\}$
    $VMsOnDesktop \leftarrow VMsOnDesktop \cup \{VM_i\}$
end

$PullInVMToServer(VM_i)$
begin
    Migrate $VM_i$ to server
    Put desktop machine $i$ to sleep
    $pulllist \leftarrow pulllist - \{VM_i\}$
    $VMsOnServer \leftarrow VMsOnServer \cup \{VM_i\}$
    $VMsOnDesktop \leftarrow VMsOnDesktop - \{VM_i\}$
end
```

Pseudo Code: Supporting subroutines

```
$VMsOnDesktop \leftarrow \{VM_1, \cdots, VM_n\}$
$VMsOnServer \leftarrow \emptyset$
$pulllist \leftarrow \emptyset$ ; $pushlist \leftarrow \emptyset$
foreach ($VM_i \in VMsOnDesktop$) do
    if ($isVMidle(VM_i)$) then
        $pulllist \leftarrow pulllist \cup \{VM_i\}$
    end
end
foreach ($VM_i \in VMsOnServer$) do
    if ($isVMactive(VM_i)$) then
        $pushlist \leftarrow pushlist \cup \{VM_i\}$
    end
end
foreach ($VM_i^{push} \in pushlist$) do
    $PushBackVMToDesktop(VM_i^{push})$
end
for ($VM_i^{pull} \in sortCPU(pulllist)$) do
    if ($isThereRoomFor(VM_i^{pull})$) then
        $PullInVMToServer(VM_i^{pull})$
    else
        break
    end
end
while (server CPU usage $> s_{push}$) do
    $VM^{push} \leftarrow \max_{VM_i \in VMsOnServer}(CPU)$
    $PushBackVM(VM^{push})$
end
while (server CPU usage $> s_{pull}$) do
    $VM^{push} \leftarrow \max_{VM_i \in VMsOnServer}(CPU)$
    $swapset \leftarrow \emptyset$ ; $cpu_{swap} \leftarrow 0$ ;
    $count_{swap} \leftarrow 0$
    for ($VM_i^{pull} \in sortCPU(pulllist)$) do
        $cpu_{swap}$ += $cpu_{VM_i^{pull}}$
        if ($cpu_{swap} \leq cpu_{VM^{push}}$) then
            $swapset \leftarrow swapset \cup \{VM_i^{pull}\}$
            $count_{swap}$++
        else
            break
        end
    end
    if ($\text{count}_{pull} \geq 2$) then
        $PushBackVM(VM^{push})$
        foreach ($VM_i^{pull} \in swapset$) do
            $PullInVMToServer(VM_i^{pull})$
        end
    else
        break
    end
end
```

Pseudo Code: Main function

6.7 Implementation and Deployment

We have built a prototype of LiteGreen based on the Hyper-V hypervisor, which is available as part of the Microsoft Hyper-V Server 2008 R2 [4]. The Hyper-V server can host Windows, Linux, and other guest OSes and also supports live migration.

Our implementation comprises the controller, which runs on the server, and the stubs, which run on the individual desktop machines. The controller and stubs are written in C# and add up to 1600 and 600 lines of code, respectively. The stubs use WMI (Windows Management Instrumentation)[13] and Powershell to perform the monitoring and migration. The controller also includes a GUI, which shows the state of all of the VMs in the system.

In our implementation, we ran into issues arising from the limitations of Hyper-V and had to work around them. Here we discuss a couple of these.

Lack of support for sleep: Since Hyper-V is intended for use on servers, it does not support sleep once the hypervisor service has been started. Also, once started, the hypervisor service cannot be turned off without a reboot. We worked around this as follows: when the desktop VM has been migrated away to the server and the desktop machine is to be put to sleep, we set a registry key to disable the hypervisor and then reboot the machine. When the machine boots up again, the hypervisor is no longer running, so the desktop machine can be put to sleep. Later, when the user returns and the machine is woken up, the hypervisor service is restarted, without requiring a reboot. Note that since a reboot is needed only when the machine is put to sleep but *not* when it is woken up, the user does not perceive any delay or disruption due to the reboot.

Surge in CPU usage right after live migration: We have found that for a period of 2-3 minutes after the completion of live migration, there is a surge in the CPU usage of the VM, with the VM saturating its virtual processor. This surge might be due to the final copying phase of live migration, though no official documentation is available in this regard. Nevertheless, the surge could potentially confuse the controller. In particular, if the conservative policy is being used to determine whether a VM is active or idle (Section 6.5.2) and if the VM has just been pulled into the server, the surge in CPU usage could trigger the controller to incorrectly conclude that the VM is active again and push it back immediately. We work around this in our implementation by adding a few minutes' of hysteresis in the controller's control loop, thereby allowing time for the surge to subside.

6.7.1 Deployment

We have deployed LiteGreen to 5 users at MSR India. Each user has LiteGreen installed on a second desktop machine, which is in addition to their existing desktop machine that is left untouched.

Different users use their LiteGreen desktop machine in different ways. Some use it only for specific tasks, such as browsing or checking email, so that the LiteGreen desktop only sees a subset of their activity. Others use it for all of their computing activity, including connecting to their existing desktop machine through their LiteGreen desktop. Our findings are reported in Section 6.8.3. While our deployment is very small in size and moreover, has not entirely replaced the users' existing desktop machines, we believe it is a valuable first step that we plan to build on in future.

6.8 Evaluation Results

We begin by presenting experimental results based on our prototype. These results are drawn both from controlled experiments in the lab and from our deployment. The results are, however, limited by the small scale of our testbed and deployment, so in Section 6.9 we present a larger scale trace-driven evaluation using the traces gathered from the 120 machines at our lab.

6.8.1 Testbed

Our testbed mirrors the architecture depicted in Figure 6.2. It comprises 5 desktop machines, a server, and a storage node, all connected to a GigE switch. The hardware and software details are listed in Table 6.2.

We first used the testbed for controlled experiments in the lab (Section 6.8.2). We then used the same setup but with the desktop machines installed in the offices of the

Component	Make/Model	Hardware	Software
Desktops (5)	HP WS xw4600	Intel E8200 Core 2 Duo @2.66GHz	Hyper-V + Win7 guest
Server	HP Proliant ML350	Intel Xeon E5440 DualProc 4Core 2.83GHz	Hyper-V
Storage	Dell Optiplex 755	Intel E6850 Core 2 Duo 3.00 GHz, 32GB	Win 2008 + iSCSI
Switch	DLink DGS-1016D	NA	NA

Table 6.2: Testbed details

participating users, for our deployment (Section 6.8.3).

6.8.2 Results from Laboratory Experiments

We start by walking through a migration scenario similar to that shown in the LiteGreen video clip [3], before presenting detailed measurements.

6.8.2.1 Migration Timeline

The scenario, shown in Figure 6.4a, starts with the user stepping away from his/her machine (Event A), causing the machine to become idle. After *actvityWindow* amount of time elapses, the user's VM is marked as idle and the server initiates the VM pull (Event B). After the VM migration is complete (Event C), the physical desktop machine goes to sleep (Event D). Figure 6.4b shows the timeline for waking up. When the user returns to his/her desktop, the physical machine wakes up (Event A) and immediately establishes a remote desktop (RD) session to the user's VM (Event B). At this point, the user can start working even though his/her VM is still on the server. A VM push is initiated (Event C) and the VM is migrated back to the physical desktop machine (Event D), in the background using live migration feature.

Figures 6.4a and 6.4b also shows the power consumed by the desktop machine and the server over time, measured using Wattsup power meters [12]. While the timeline shows the measurements from one run, we also made more detailed measurements of the individual components and operations, which we present next.

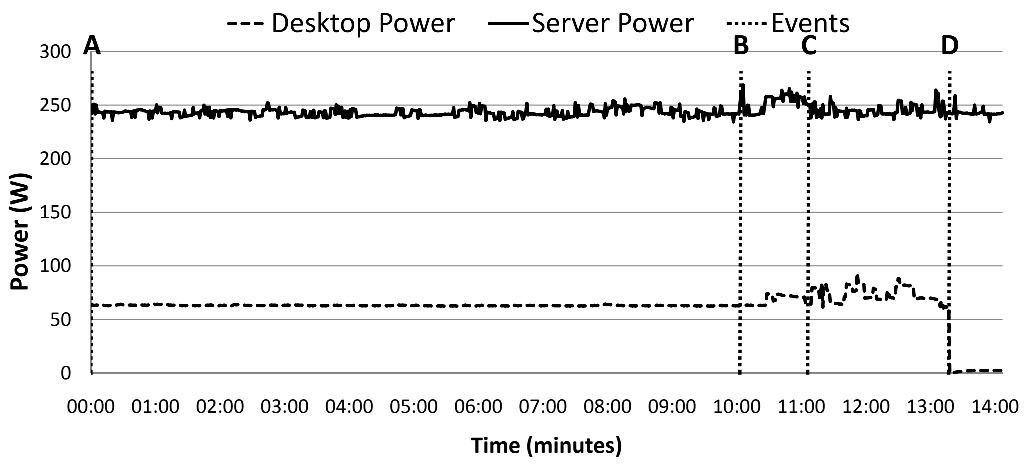

(a) Sleep timeline

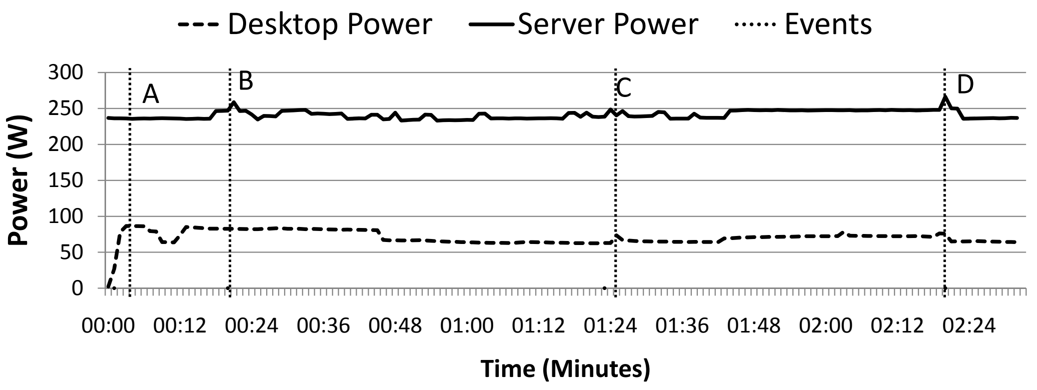

(b) Wakeup timeline

Figure 6.4: Migration timelines

6.8.2.2 Timing of individual operations

We made measurements of the time taken for the individual steps involved in migration. In Table 6.3, we report the results derived from 10 repetitions of each step.

6.8.2.3 Power Measurements

Table 6.4 shows the power consumption of a desktop machine, the server, and the switch in different modes, measured using a Wattsup power meter.

The main observation is that power consumption of both the desktop machines and the servers is largely unaffected by the amount of CPU load. It is only when the machine is put to sleep that the power drops significantly. The amount of power consumed during heavy

Step	Sub-step	Time (sec) [mean (sd)]
Going to Sleep		840.5 (27)
	Pull Initiation	638.8 (20)
	Migration	68.5 (5)
	Sleep	133.2 (5)
Resuming from sleep		164.6 (16)
	Wakeup	5.5 ()
	RD connection	14 ()
	Push Initiation	85.1 (17)
	Migration	60 (6)

Table 6.3: Timing of individual steps in migration

Component	Mode	Power (W)
Desktop	idle	60-65W
Desktop	100% CPU	95W
Desktop	sleep	2.3-2.5W
Server	idle	230-240W
Server	100% CPU	270W
Switch	idle	8.7 - 8.8W
Switch	during migration	8.7-8.8W

Table 6.4: Power measurements

load and low load in desktops or servers does not vary much because current systems are not energy proportional systems. We also see that the power consumption of the network switch is low and is unaffected by any active data transfers.

6.8.2.4 Discussion of the Results

We make several observations based on the timeline shown in Figure 6.4a, Figure 6.4b and Tables 6.3 and 6.4. First, the time to put the machine to sleep is 133 seconds, much of it due to the reboot necessitated by the lack of support for sleep in Hyper-V (Section 6.7). With a *client* hypervisor that includes support for sleep, we expect the time to go to sleep to shrink to just about 10 seconds.

Second, the time to migrate the VM — either push or pull — is essentially the memory size of the VM divided by the network throughput. In our setup, that translates to 2GB divided by 0.5Gbps (the effective throughput of active migration on the GigE network), yielding 32 seconds. Including the migration initiation overhead, the total migration time is about 60seconds, which matches with the numbers shown in the timeline and in Table 6.3.

Third, the time from when the user returns till when they are able to start working is longer than we would like — about 19.5 seconds. Of this, resuming the desktop machine from sleep only constitutes 5.5 seconds. About 4 more seconds are taken by the user to key in their login credentials. The remaining 10 seconds are taken to launch the remote desktop application and make a connection to the user's VM, which resides on the server. This longer than expected duration is because Hyper-V freezes for several seconds after resuming from sleep. We have reason to believe that this happens because our unconventional use of Hyper-V, specifically putting it to sleep when it is not designed to support sleep, triggers some untested code paths. We expect that this issue would be resolved with a desktop hypervisor.

Finally, the power consumption curves in Figures 6.4a and 6.4b show the marked difference in the impact of migration on the power consumed by the desktop machine and the server. When a pull happens, the power consumed by the desktop machine goes down from about 60W in idle mode to 2.5W in sleep mode (with a transient surge to 75W during the migration process). On the other hand, the power consumption of the server barely changes. This difference underlies the significant net energy gain to be had from moving idle desktops to the server.

6.8.3 Results from Deployment

As noted in Section 6.7.1, we have had a deployment of LiteGreen on 5 users' desktops running for 8 days, from Sep 24 through Oct 2, 2009, a period that included a 3-day weekend. While it is hard to draw general conclusions given the small scale and duration of the deployment thus far, it is nevertheless interesting to consider some of the initial results.

For our deployment, we used the default policy from Section 6.5.2 to determine whether a VM was idle or active. During the deployment period, the desktop machines were able to sleep for about 81.1% of the time. Even the machine of the most active user, who used

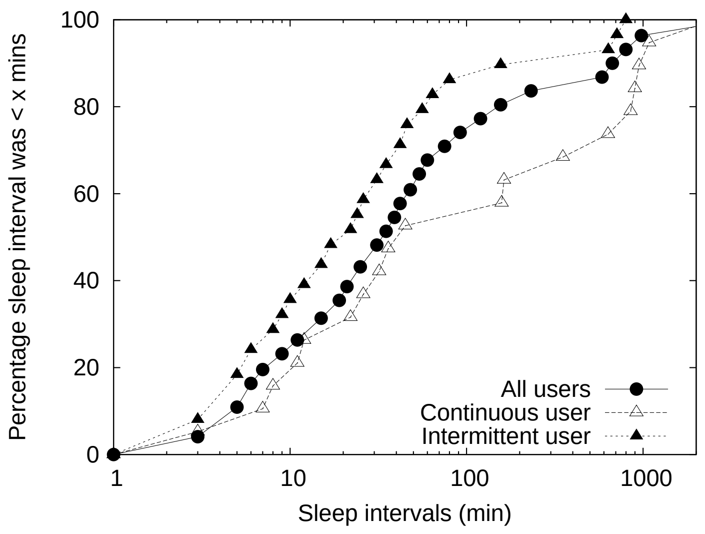

Figure 6.5: Distribution of desktop sleep durations

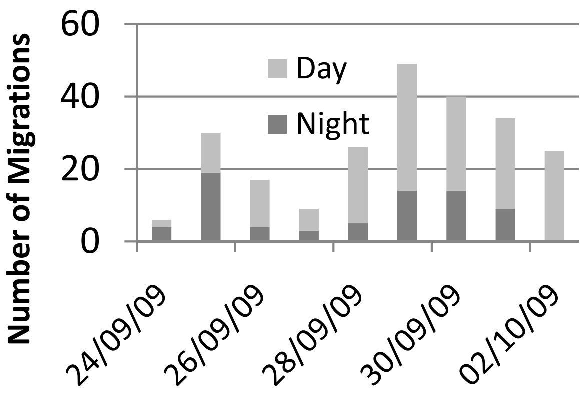

Figure 6.6: Number of migrations

their LiteGreen desktop for all of their computing activity, slept for 79.4% of the time.

Figure 6.5 shows the distribution of the sleep durations. The sleep times tended to be quite short, with a median of 34 mins across the 5 users. The median sleep duration for the most active user was 45 mins whereas that for a much less active user was 21 mins. Since the active user was using their LiteGreen desktop for all of their computing activities, there are fewer short period of inactivity. On the other hand, since the less active user was using their LiteGreen desktop only for browsing (and using their regular desktop for the rest of their activities), there are many more short sleep intervals between browsing sessions. While using two desktop machines like this is not the norm, the less active user could be considered akin to a user whose only computing activity is occasional browsing.

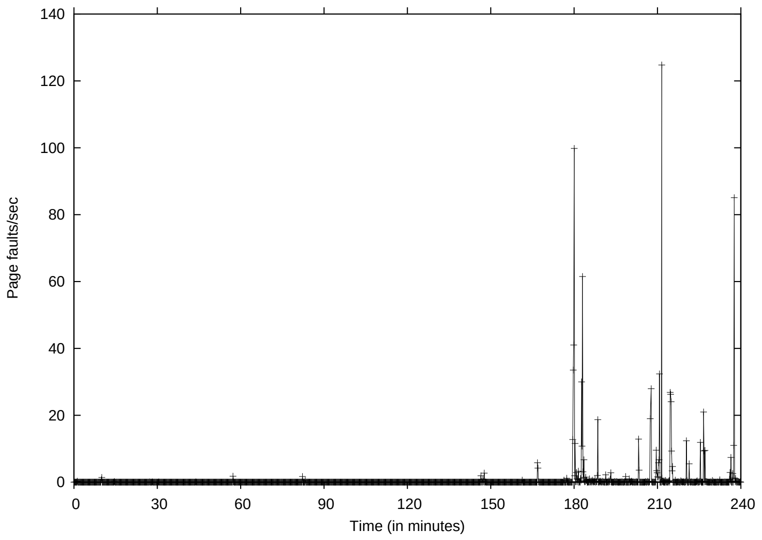

(a) Memory ballooning experiment: every 30 minutes memory of a desktop VM is reduced by 128M. Initial memory size is 1024M

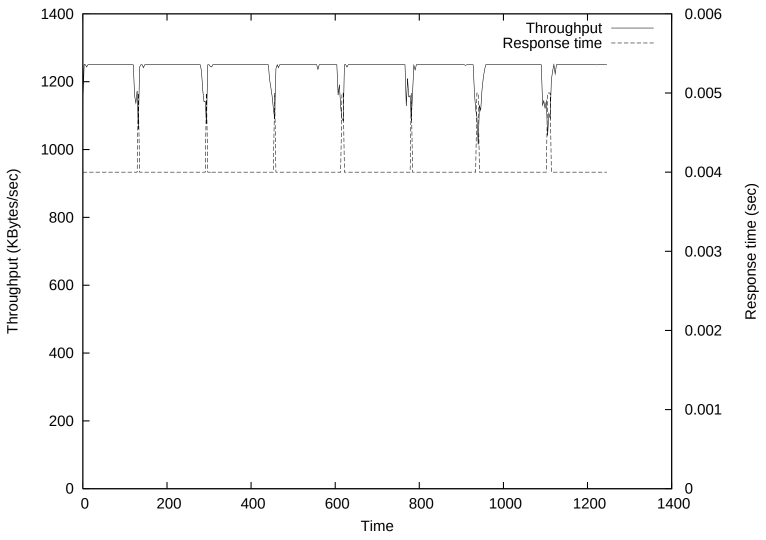

(b) Performance of a VM in consolidation

Figure 6.7: Xen experiments

Finally, Figure 6.6 shows the number of migrations during each day, separately for the daytime (8 am–8 pm) and the nighttime (8 pm–8 am). There were a total of 236 migrations during the deployment period. The number of migrations is higher during the day and higher in the weekdays compared to the weekends. This is consistent with the LiteGreen approach of exploiting short idle intervals.

6.8.4 Experiments with Xen

6.8.4.1 Prototype with Xen

One question we would like to evaluate is the effectiveness of memory ballooning in relieving pressure on server's memory resources due to consolidation. However, Hyper-V does not currently support memory ballooning, so we conducted experiments using the Xen hypervisor, which supports memory ballooning for the Linux guest OS using a balloon driver (we are not aware of a balloon driver for Windows on Xen).

We used the Xen hypervisor (v3.1 built with 2.6.22.5-31 SMP kernel) with the Linux guest OS (OpenSuSE 10.3) on a separate testbed comprising two HP C-class blades, each equipped with two dual-core 2.2 GHz 64-bit processors with 4GB memory, two Gigabit Ethernet cards, and two 146 GB disks. One blade was used as the desktop machine and the other as the server.

6.8.4.2 Effect of memory ballooning

We used the memory ballooning feature, which uses a balloon driver installed in the guest operating system. Each VM can be assigned initial memory and maximum memory by specifying the *mem* and *maxmem* options. By over-committing memory to multiple VM using *maxmem*, we can reduce or increase the amount of memory for a guest OS. By using migration and ballooning, we evaluated the consolidated scenario of LiteGreen.

The desktop Linux VM was initially configured with 1024 MB of RAM. It ran an idle workload comprising the Gnome desktop environment, two separate Firefox browser windows, with a Gmail account and the CNN main page open (each of these windows auto-refreshed periodically without any user's involvement), and the user's home directly mounted through SMB (which also generated background network traffic). The desktop VM was migrated to the server. Then, memory ballooning was used to shrink the VM's memory all the way down to 128 MB, in steps of 128 MB every 30 minutes.

Figure 6.7a shows the impact of memory ballooning on the page fault rate. The page fault rate remains low even when the VM's memory is shrunk down to 384 MB. However, shrinking it down to 256 MB causes the page fault rate to spike, presumably because the working set no longer fits within memory.

It is interesting, though, that beyond the initial spike, the page fault rate remains low during the rest of the 30-minute period even with the memory set to 256 MB.

We conclude that in our setup with the idle workload that we used, memory ballooning could be used to shrink the memory of an idle VM by almost a factor of 3 (1024 MB down to 384 MB), without causing thrashing. Further savings in memory could be achieved through memory sharing. While we were not able to evaluate this in our testbed since neither Hyper-V nor Xen supports it, the findings from prior work [51] are encouraging, as discussed in Section 6.10.

6.8.4.3 Consolidation of multiple VMs

To evaluate the consolidation of VMs, we again used two blades. A desktop Linux VM is started on one of the blades, migrated and ballooned. A workload representing idle desktop workload is run in the VM. This workload is generated using a micro benchmark that follows an idle desktop trace from our data collection. The micro benchmark runs a set of operations based on amount of resource to be consumed. For example, to consume 50% CPU, it would run 5000 operations and so on.

After 200 seconds, a second desktop running another idle workload is migrated and ballooned into the server. We continue to migrate the idle desktops until no memory is left.

Figure 6.7b shows the performance of the first desktop VM. You can see that there are a few blips in performance whenever a new desktop is migrated.

6.9 Simulation

To evaluate our algorithms further, we have built a discrete event simulator written in Python using the SimPy package. The simulator runs through the desktop traces, and simulates the default and conservative policies based on various parameters including c_{pull}, c_{push}, s_{pull}, s_{push} and $ServerCapacity$. In the rest of the section, we will report on energy savings achieved by LiteGreen and utilization of various resources (CPU, network, disk) at the server as a result of consolidation of the idle desktop VMs.

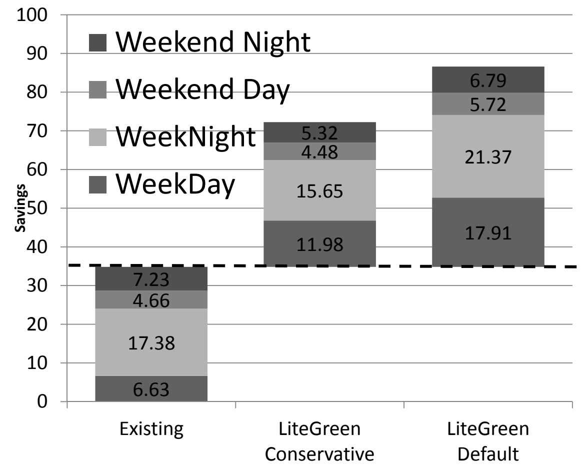

(a) Energy savings

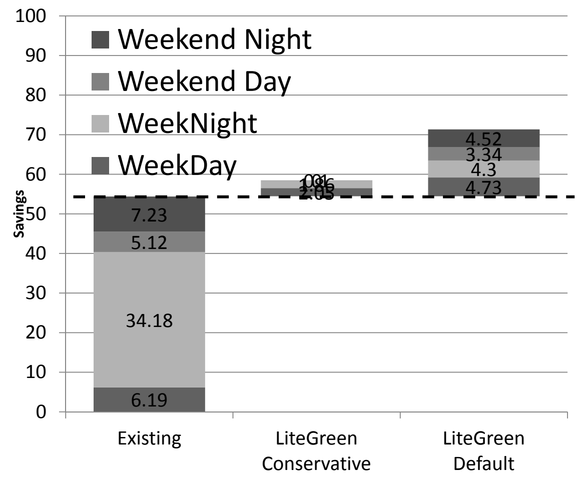

(b) Energy savings for user1

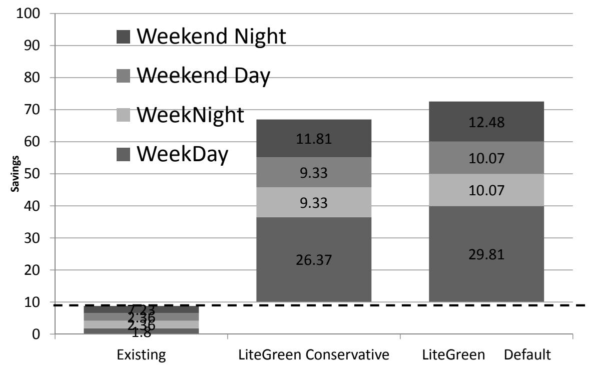

(c) Energy savings for user2

Figure 6.8: Energy savings from existing power management and LiteGreen's default and conservative policies

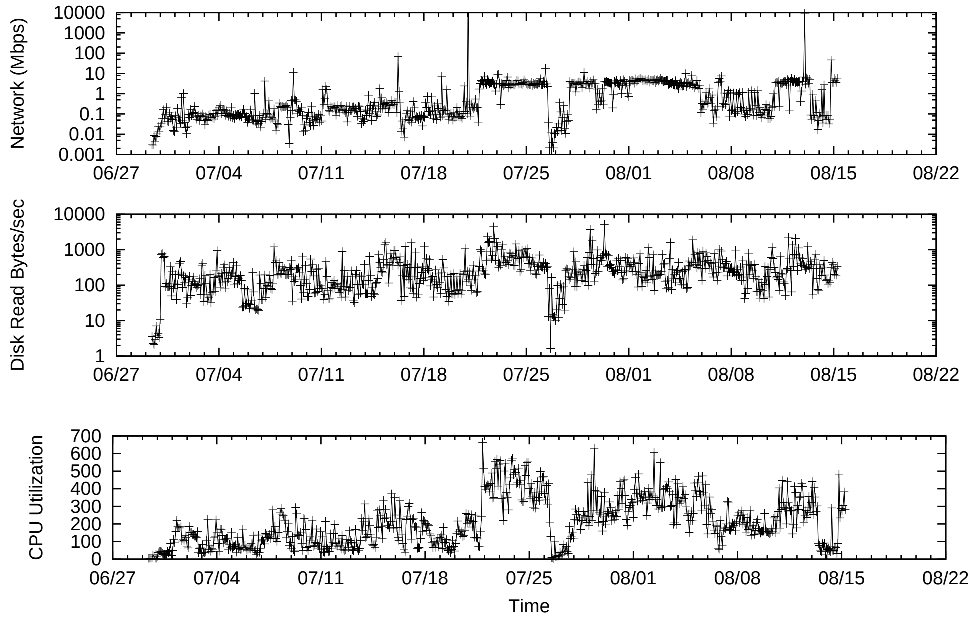

(a) Default policy

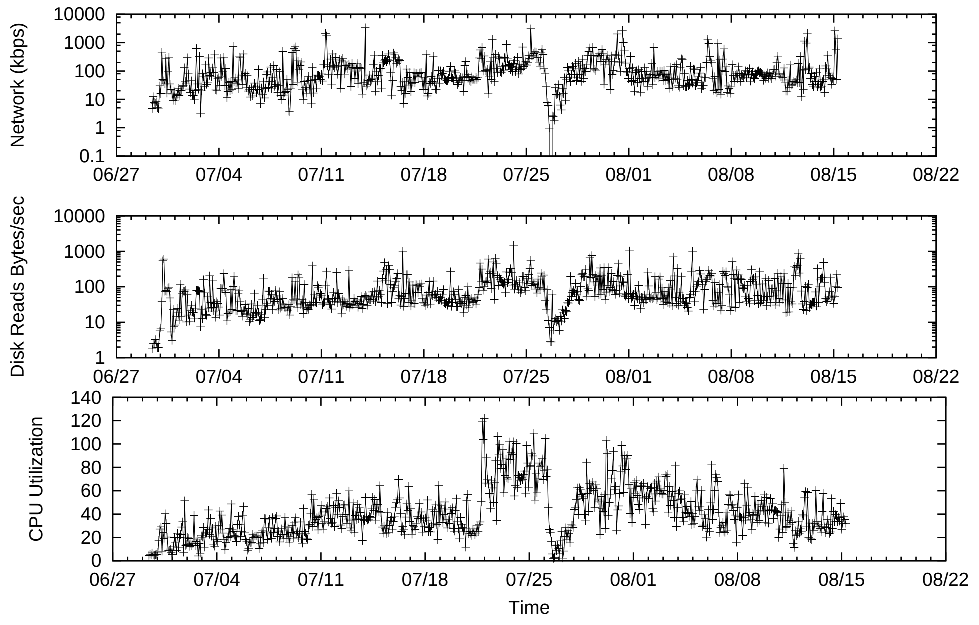

(b) Conservative policy

Figure 6.9: Resource utilization during idle desktop consolidation

6.9.1 LiteGreen Energy Savings

Figure 6.8a shows the energy savings for all the users with existing mechanisms and LiteGreen, default and conservative. For both the policies, we use $c_{pull} = 10$ (less than 10%

desktop usage classified as idle), $c_{push} = 20$, $s_{pull} = 600$, $s_{push} = 700$ and $ServerCapacity = 800$ intended to represent a Server with 8 CPU cores.

As mentioned earlier, our desktop trace gathering tool records a number of parameters, including CPU, memory, UI activity, disk, network, etc. every minute after its installation. In order to estimate energy savings using existing mechanisms (either automatic windows power management or manual desktop sleep by the user), we attribute any unrecorded interval or "gaps" in our desktop trace to energy savings via existing mechanisms. Using this technique, we estimate that existing mechanisms would have saved 35.2% of desktop energy.

We then simulate the migrations of desktop VMs to/from the server depending on the desktop trace events and the above mentioned thresholds for the conservative and default policy. Using the conservative policy, we find that LiteGreen saves 37.3% of desktop energy. This is in addition to the existing savings, for a total savings of 72%. If we use the more aggressive default policy, where the desktop VM is migrated to the server unless there is UI activity, we find that LiteGreen saves 51.3% on top of the existing 35.2% of savings for a total savings of 86%. In the savings masurement, we assume that the desktop power consumption is the same irrespective of the load on the machine. Power measurements done by using tools like WattsUpMeter [12] can be used to more accurately measure the savings for certain load.

The savings of the different approaches are also classified by day (8AM-8PM) and night (8PM-8AM) and also whether it was a weekday or a weekend. We note that substantial portion of LiteGreen savings comes from weekdays, thereby highlighting the importance of exploiting short idle intervals in desktop energy savings.

6.9.2 Resource Utilization During Consolidation

While the default policy provides higher savings than the conservative policy, it is clear that the default policy would stress the resources on the server more, due to hosting of a higher number of desktop VMs, than the conservative policy. We examine this issue next.

Figures 6.9a and 6.9b show the resource utilization due to idle desktop consolidation at the server for the default and conservative policies, respectively. The resources shown are

CPU usage, Bytes read/second from the disk, and network usage in Mbps.

First consider CPU. Notice that the CPU usage at the server in the default policy spikes up to between $s_{pull} = 600$ an $s_{push} = 700$ but, as intended, never goes above s_{push}. In contrast, since the conservative policy pushes the VM back to the desktop as soon as $c_{push} = 20$ is exceeded, the CPU usage at the server hardly exceeds a utilization value of 100. Next consider Disk Reads. It varies between 10B-10KB/s for the default policy (average of 205 B/s) while it varies between 10B-1KB/s for the conservative policy (average of 41 B/s). While these numbers can be quite easily managed by the server, note that these are disk reads of idle, and not active, desktop VMs. Finally, let us consider network activity of the consolidated idle desktop VMs. For the default policy, the network traffic mostly varies between 0.01 to 10Mbps, but with occasional spikes all the way up to 10Gbps. In the case of conservative policy, the network traffic does not exceed 10Mbps and rarely goes above 1Mbps. While these network traffic numbers are manageable by a server, scaling the server for consolidation of active desktop VMs, as in the thin client model, will likely be expensive.

6.9.3 Energy Savings for Selected Users

Figure 6.10a and 6.10b depict the CPU utilization for two specific users. It appears user1 has bursts of significant activity separated by periods of no activity, likely because he/she manually switches off his/her machine when not in use as can be seen by the large gaps in Figure 6.10a. For this particular case, LiteGreen is unable to significantly improve the savings of existing mechanisms (including savings due to manual power management). This is reflected in the energy savings for user1 in Figure 6.8b. In contrast, we see that user2's desktop has activity almost continuously, with only short gaps of inactivity. The small CPU utilization spikes appears to have prevented Windows power management from putting the desktop to sleep, thereby wasting a lot of energy. However, LiteGreen is able to exploit this situation effectively, and saves a significant amount of energy as shown in Figure 6.8c.

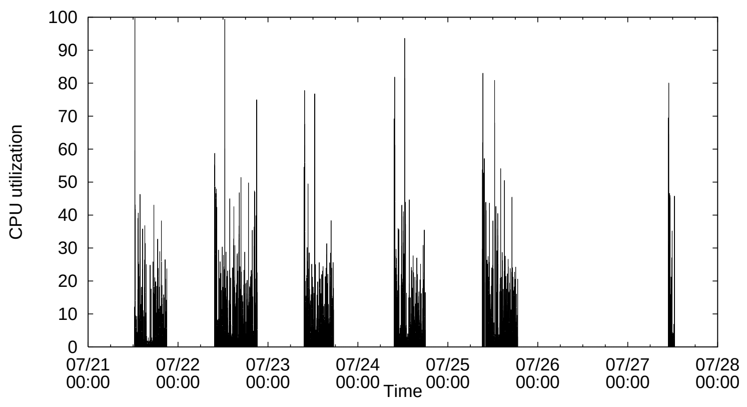

(a) CPU utilization for user1

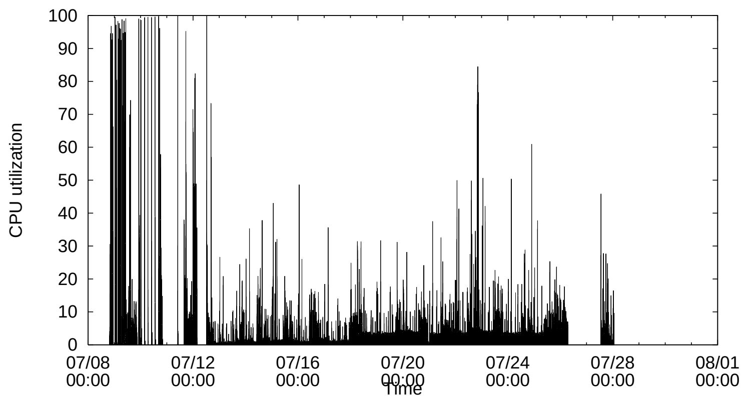

(b) CPU utilization for user2

Figure 6.10: CPU utilization of selected users

6.10 Discussion

The design of LiteGreen anticipates advances in virtualization technology that have been reported in the research literature and can reasonably be expected to become mainstream in the not-too-distant future. A complete discussion of various issues is presented in 8.

6.11 Summary

Recent work has recognized that desktop computers in enterprise environments consume a lot of energy in aggregate while still remaining idle much of the time. The question is how to save energy by letting these machines sleep while avoiding user disruption. LiteGreen uses virtualization to resolve this problem, by migrating idle desktops to a server where they can remain "always on" without incurring the energy cost of a desktop machine. The seamlessness offered by LiteGreen allows us to aggressively exploit short idle periods as well as long periods. Data-driven analysis of more than 65000 hours of desktop usage traces from 120 users shows that LiteGreen can help desktops sleep for 72-86% of the time and also scales well. The experience from our small-scale deployment of LiteGreen has also been encouraging.

As the next step, we plan to expand our deployment. In future work, we plan to study local disk migration, memory optimizations and extending it to multiple VM servers.

CHAPTER 7

Performance Evaluation of Server Consolidation in Xen and OpenVZ

7.1 Introduction

There has been a rapid growth in servers within data centers driven by growth of enterprises since the late nineties. The servers are commonly used for running business-critical applications such as enterprise resource planning, database, customer relationship management, and e-commerce applications. Because these servers and applications involve high labor cost in maintenance, upgrades, and operation, there is a significant interest in reducing the number of servers necessary for the applications. This strategy is supported by the fact that many servers in enterprise data centers are under-utilized most of the time, with a typical average utilization below 30%. On the other hand, some servers in a data center may also become overloaded under peak demands, resulting in lower application throughput and longer latency.

Server consolidation has become a common practice in enterprise data centers because of the need to cut cost and increase return on IT investment. Many enterprise applications that traditionally ran on dedicated servers are consolidated onto a smaller and shared pool of servers. Although server consolidation offers great potential to increase resource utilization and improve application performance, it may also introduce new complexity in managing the consolidated servers. This has given rise to a re-surging interest in virtualization technology. There are two main types of virtualization technologies today — *hypervisor-based technology*

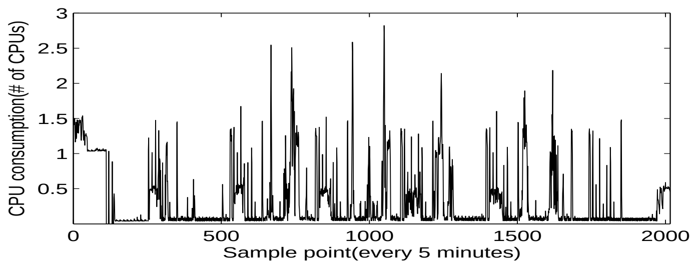

(a) CPU consumption of node 1

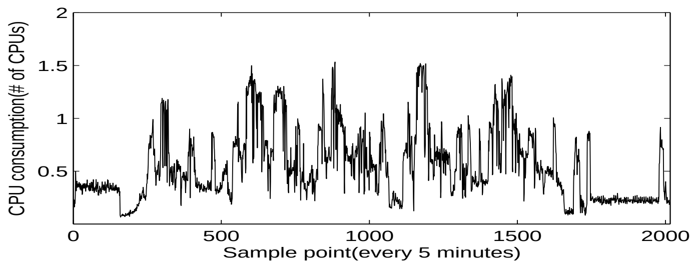

(b) CPU consumption of node 2

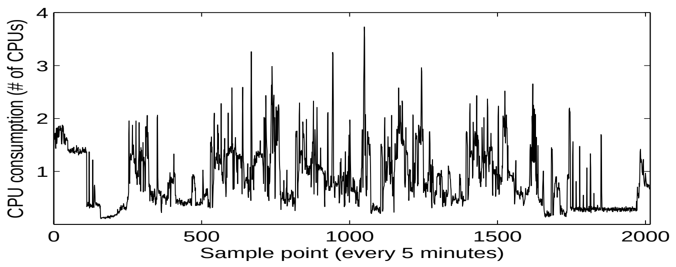

(c) Sum of CPU consumptions from both nodes

Figure 7.1: An example of data center server consumption

including VMware [83], Microsoft Virtual Server [5], and Xen [30]; and *operating system (OS) level virtualization* including OpenVZ [6], Linux VServer [2], and Solaris Zones [78]. These technologies allow a single physical server to be partitioned into multiple isolated virtual containers for running multiple applications at the same time. This enables easier centralized server administration and higher operational efficiency.

However, capacity management for the virtual containers is not a trivial task for system administrators. One reason is that enterprise applications often have resource demands that vary over time and may shift from one tier to another in a multi-tiered system. Figures 7.1a and 7.1b show the CPU consumptions of two servers in an enterprise data center for a week. Both have a high peak-to-mean ratio in their resource usage, and their peaks are not synchronized. This means if the two servers were to be consolidated into two virtual containers on a shared server, the resources may be dynamically allocated to the two containers such that both of the hosted applications could meet their quality-of-service (QoS) goals while utilizing server resources more efficiently. An adaptive CPU resource controller was described in [76] to achieve this goal. Similar algorithms were developed for dynamic memory management in VMware ESX server [93].

There is another important issue that is worth considering in terms of capacity management. Figure 1.3c shows the total CPU consumption from the two nodes. As we can see, the peak consumption is at about 3.8 CPUs. However, it does not necessarily imply that a total of 3.8 CPUs are sufficient to run the two virtual containers after consolidation due to potential virtualization overhead. Such overhead may vary from one virtualization technology to another. In general, hypervisor-based virtualization incurs higher performance overhead than OS-level virtualization does, with the benefit of providing better isolation between the containers. To the best of our knowledge, there is little published work quantifying how big this difference is between various virtualization technologies, especially for multi-tiered applications. In this paper, we focus on two representative virtualization technologies, Xen from hypervisor-based virtualization, and OpenVZ from OS-level virtualization. Both are open-source, widely available, and based on the Linux operating system. We use RUBiS [25] as an example of a multi-tiered application and evaluate its performance in the context of server consolidation using these two virtualization technologies.

In particular, we present the results of our experiments that answer the following questions, and compare the answers to each question between OpenVZ and Xen.

- How is application-level performance, including throughput and response time, impacted compared to its performance on a base Linux system?

- As workload increases, how does application-level performance scale up and what is the impact on server resource consumption?

- How is application-level performance affected when multiple tiers of each application are placed on virtualized servers in different ways?

- As the number of multi-tiered applications increases, how do application-level perfor-

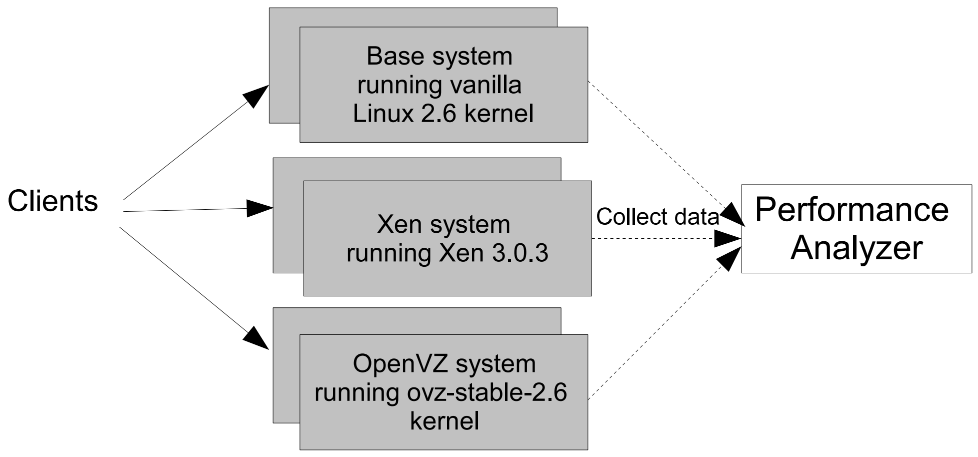
Base system running vanilla Linux 2.6 kernel
Clients
Xen system running Xen 3.0.3
Collect data
Performance Analyzer
OpenVZ system running ovz-stable-2.6 kernel

(a) Testbed setup

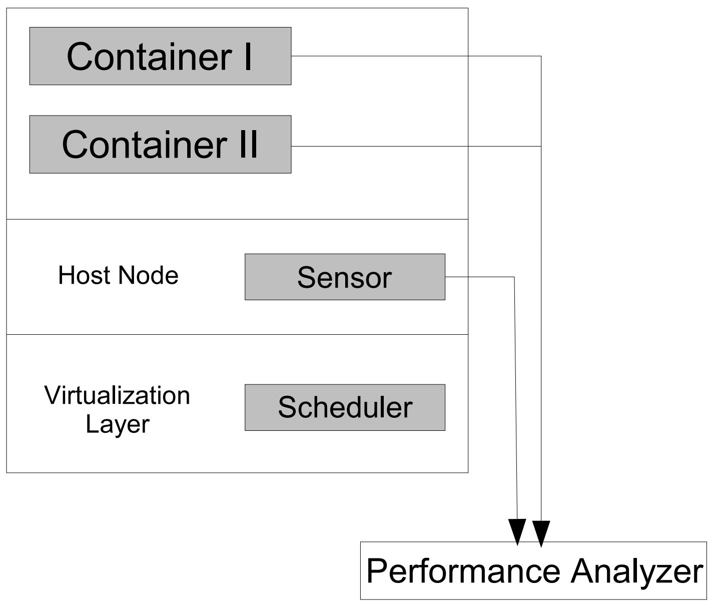

(b) A virtualized server

Figure 7.2: System architecture

mance and resource consumption scale?

- In each scenario, what are the values of some critical underlying system metrics and what do they tell us about plausible causes of the observed virtualization overhead?

7.2 Testbed Architecture

Figure 7.2a shows the architecture of our testbed. We run experiments in three systems with identical setup. We compare the performance of Xen- and OpenVZ-based systems with that of a vanilla Linux system (referred to as *base system* here after). In a virtualized configuration, each physical node may host one or more virtual containers supported by Xen or OpenVZ as shown in Figure 7.2b. Because we are interested in multi-tiered applications, two separate nodes may be used for the Web and the database tiers. Each node is equipped with a sensor collecting various performance metrics including CPU consumption, memory consumption and other performance events collected by Oprofile [7]. This data is collected on a separate machine and analyzed later.

We use HP Proliant DL385 G1 for all our servers and client machines. Every server has two 2.6 GHz processors, each with 1MB of L2 cache, 8 GB of RAM, and two Gigabit network interfaces.

7.2.1 System Configurations

We conduct our experiments on three different systems as explained below. All systems are carefully set up to be as similar as possible with the same amount of resources (memory and CPU) allocated to a particular virtual container.

7.2.1.1 Base system

We use a plain vanilla 2.6 Linux kernel that comes with the Fedora Core 5 standard distribution as our base system. Standard packages available from Fedora repository are used to set up various applications.

7.2.1.2 Xen system

Xen is a *paravirtualization* [98] technology that allows multiple guest operating systems to be run in virtual containers (called *domains*). The Xen hypervisor provides a thin software virtualization layer between the guest OS and the underlying hardware. Each guest OS is a modified version of the base Linux (XenLinux) because the hardware abstraction presented by the hypervisor is similar but not identical to the raw hardware. The hypervisor contains a CPU scheduler that implements various scheduling policies including proportional fair-share, along with other modules such as the memory management unit.

We use the Xen 3.0.3 unstable branch [14] for our experiments as it provides a credit-based CPU scheduler (in short, credit scheduler), which, in our experiments, provides better performance than the earlier SEDF scheduler. The credit scheduler allows each domain to be assigned a *cap* and a *weight*. A non-zero cap implements a non-work-conserving policy for the CPU by specifying the maximum share of CPU time a domain can consume, even if there exist idle CPU cycles. When the cap is zero, the scheduler switches to a work-conserving mode, where weights for multiple domains determine their relative shares of CPU time when the CPU is under contention. At the same time, a domain can use extra CPU time beyond its share if other domains do not need it. In all our experiments, we use the *non-capped* mode of the credit scheduler, and the system is compiled using the uni-processor architecture. In this case, Dom0 and all the guest domains share the full capacity of a single processor.

7.2.1.3 OpenVZ system

OpenVZ [6] is a Linux-based OS-level server virtualization technology. It allows creation of secure, isolated virtual environments (VEs) on a single node enabling server consolidation. Each VE performs and behaves exactly like a stand-alone server. They can be rebooted independently and a different distribution with separate root directory can be set up. One distinction between OpenVZ and Xen is that the former uses a single kernel shared by all VEs. Therefore, it does not provide the same level of fault isolation as in the case of Xen.

In our experiments, we use the uni-processor version of OpenVZ stable 2.6 kernel that provides a FSS scheduler, which also allows the CPU share of each VE to be either capped or not capped. Similar to the Xen system, the non-capped option is used in the OpenVZ system.

In the remainder of this paper, we use the term *virtual container* to refer to either a domain in Xen or a VE in OpenVZ.

7.2.2 Instrumentation

To measure the CPU consumption accurately, we wrote scripts that use existing tools to gather data. In the base system, the output from command `top -b` is gathered and then analyzed later. Similarly, `xentop -b` is used in the Xen case, which provides information on the CPU consumptions of individual domains. For OpenVZ, there is no existing tool to directly measure the CPU consumption by a particular container. We use the data provided from `/proc/vz/vestat` to measure the amount of CPU time spent by a particular VE.

7.2.2.1 Oprofile

Oprofile [7] is a tool for measuring certain hardware events using hardware performance counters. For example, one can measure the number of cache misses that happen in a particular application. The profiles generated by Oprofile are very detailed and can provide a wealth of information. Menon *et al.* [67] have modified Oprofile to support Xen. The resulting tool, *Xenoprof*, allows one to profile multiple domains in a Xen system. For each set of experiments, we analyze the data generated by Oprofile and provide our insights on the performance overheads.

We concentrate on two aspects when analyzing the data generated by Oprofile:

- Comparing hardware performance counters for various configurations;
- Understanding differences in overheads experienced within specific kernels. We want to identify particular kernel sub-systems where most of the overhead occurs and quantify it.

We monitor three hardware counters for our analysis:

- `CPU_CLK_UNHALT`: The number of cycles outside of halt state. It provides a rough estimate of the CPU time used by a particular binary or a symbol.
- `RETIRED_INSTRUCTIONS`: The number of instructions that are retired. It is a rough estimate of the number of instructions executed by a binary or a symbol.
- `L2_CACHE_MISS`: The number of L2 cache misses. It measures the number of times the memory references in an instruction miss the L2 cache and access main memory.

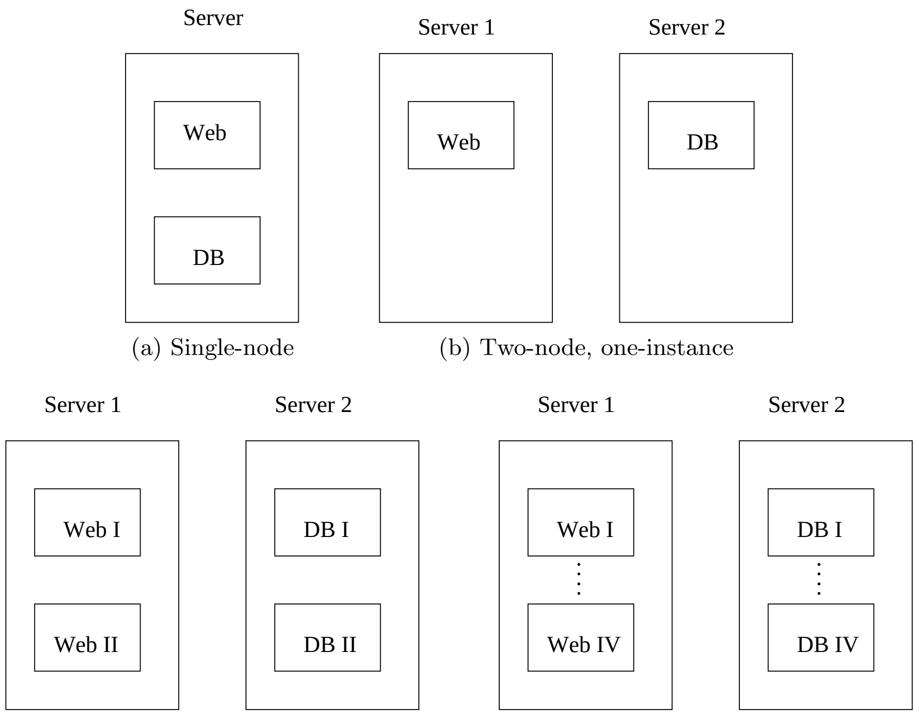

(a) Single-node (b) Two-node, one-instance

(c) Two-node, two-instance (d) Two-node, four-instance

Figure 7.3: Various configurations for consolidation

We thoroughly analyze differences in these counter values in various configurations, and infer sources of overhead in respective virtualization technologies.

7.3 Design of Experiments

The experiments are designed with the goal of quantitatively evaluating the impact of virtualization on server consolidation. Specifically, we are not interested in performing micro benchmarks that compare the performance of system calls, page miss penalties, etc. Instead, we focus more on how application-level performance, including throughput and response time, are affected when using different virtualization technologies as well as different configurations for consolidation.

Today's enterprise applications typically employ a multi-tiered architecture, where the Web and the application tiers serve static files and implement business logic, and the database (DB) tier executes data queries and interacts with the storage devices. During server consolidation, the various tiers of an application that are traditionally hosted on dedicated servers are moved onto shared servers. Moreover, when virtualization is involved, each of these tiers is hosted in a virtual container, which can have performance implications for the application.

We have chosen RUBiS [25], an online auction site benchmark, as an example of a multi-tiered application. We use a version of the application that has a two-tier structure: the Web tier contains an Apache Web server with PHP, and the DB tier uses a MySQL database server. RUBiS clients connect to the Web tier and perform various operations simulating auctions. Each client starts a session in which the client browses through items, looks at prices, and buys or sells items. In each session, the client waits for a request to complete before sending out the next request. If the request fails due to timed-outs, the session is aborted and a new session is started. This gives rise to a closed-loop behavior where the clients wait for the server when it is overloaded. Although RUBiS provides different workload mixes, we use the *browsing mix* in our experiments, which introduces higher load on the Web tier than on the DB tier.

We consider running RUBiS on consolidated servers. In addition to the comparison between OpenVZ and Xen, we also need to understand how application performance is impacted by different placement of application tiers on the consolidated servers. We evaluate the following two configurations for consolidation.

- **Single-node:** Both the Web and the DB tiers of a single RUBiS application are hosted on a single physical node (Figure 7.3a).
- **Two-node:** The Web and the DB tiers of a single RUBiS application are distributed on two separate nodes (Figure 7.3b).

There are additional reasons why one configuration may be chosen over the other in a practical scenario. For example, the single-node configuration may be chosen since it reduces network traffic by hosting multiple tiers of the same application on a single server, whereas the two-node option may be preferable in a case where it can reduce software licensing cost. In this work, we only focus on application performance differences in the two configurations and how performance scales as the workload increases.

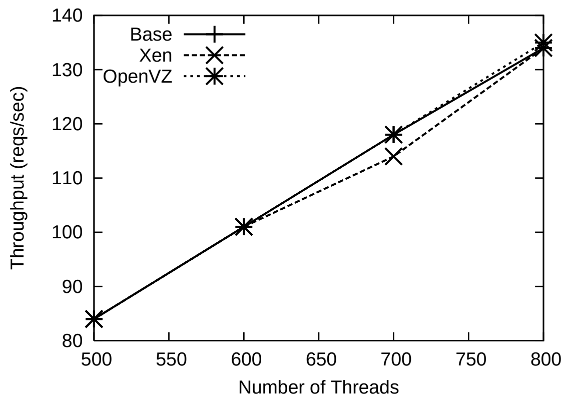

(a) Throughput

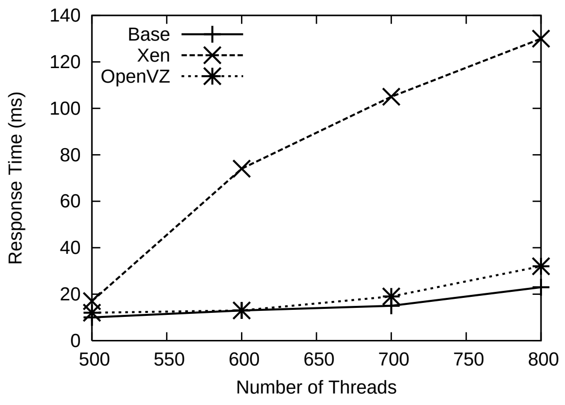

(b) Average response time

Figure 7.4: Single-node - application performance

In addition, we are also interested in scalability of the virtualized systems when the number of applications hosted increases in the two-node case. Each node may host multiples of the Web or the DB tier as shown in Figures 7.3c and 7.3d. In our experiments, we increase the number of RUBiS instances from one to two and then to four, and compare OpenVZ with Xen in application-level performance and system resource consumption. For each scenario, we provide a detailed analysis of the corresponding Oprofile statistics and point to plausible causes for the observed virtualization overheads.

7.4 Evaluation Results

This section reports the results of our experimental evaluation using the RUBiS benchmark. In particular, we compare two different configuration options, *single-node* vs. *two-node*, for placing the two tiers of a single RUBiS application on physical servers. All experiments are done on the base, OpenVZ, and Xen systems, and a three-way comparison of the results is presented.

7.4.1 Single-node

In this configuration, both the Web and the DB tiers are hosted on a single node, as shown in Figure 7.3a. In both the Xen and the OpenVZ systems, the two tiers run in two separate virtual containers. To evaluate the performance of each system, we scale up the workload by increasing the number of concurrent threads in the RUBiS client from 500 to 800. Each workload is continuously run for 15 minutes, and both application-level and system-level metrics are collected.

7.4.1.1 Performance evaluation

Figures 7.4a and 7.4b show the throughput and average response time as a function of workload for the base, Xen, and OpenVZ systems. In all three cases the throughput increases linearly as the the number of threads increases, and there is little difference between the three systems. However, we do see a marked difference in the response time between the Xen system and the other two systems, indicating higher performance overhead in Xen compared to OpenVZ. As the workload increases from 500 to 800 threads, the response time goes up only slightly in the base and OpenVZ cases, whereas in the Xen system, it grows from 18 ms up to 130 ms, an increase of over 600%. For 800 threads, the response time for Xen is almost 4 times that for OpenVZ. Therefore, in the single-node case, the observed performance overhead is minimum in OpenVZ but quite significant in Xen. Moreover, the overhead in Xen grows quickly as the workload increases. As a result, the Xen system is less scalable with the workload than OpenVZ or a non-virtualized system.

Figure 7.5a shows the average CPU consumptions of the Web and the DB tiers as a function of workload in the three systems. For both tiers in all the three cases, the CPU consumption goes up linearly with the number of threads in the workload. The database consumption remains very low at about 1-4% of total CPU capacity, due to the Web-intensive nature of the browsing mix workload. A bigger difference can be seen in the Web tier consumption from the three systems. For each workload, the Web tier consumption in Xen is roughly twice the consumption experienced by the base system, while the OpenVZ consumption stays very close to the base case. As the workload increases, the slope of increase is higher in the case of Xen compared to the other two systems. This indicates higher CPU overhead in Xen than in OpenVZ, and should be related to the higher response times we observe from the application.

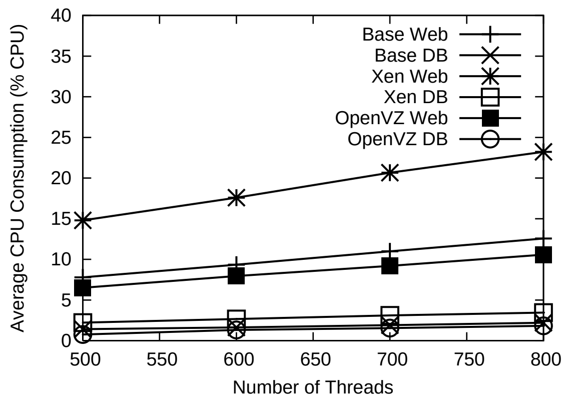

(a) Single-node - average CPU consumptions

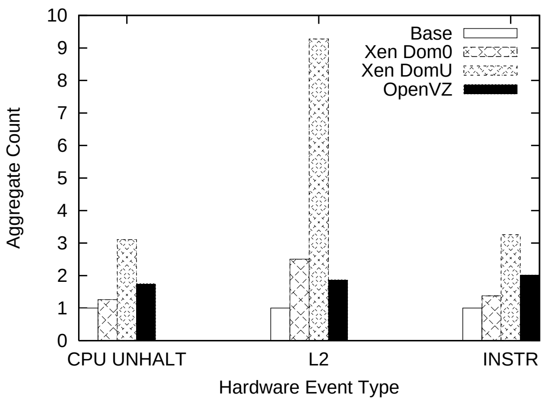

(b) Single-node - Oprofile analysis

Figure 7.5: Single-node analysis results

7.4.1.2 Oprofile Analysis

Figures 7.5b shows the aggregate values of the selected hardware counters for the three systems when running 800 threads. For OpenVZ, each of the counter values is for the whole system including the shared kernel and all the virtual containers. For Xen, Oprofile provides us with a counter value for each of the domains, including Dom0. The DomU value in the figure is the sum of the values from the Web and DB domains. All counter values are normalized with respect to the base case. While all the counter values for OpenVZ are less than twice the corresponding values for the base case, the total number of L2 cache misses in Xen (Dom0 + DomU) is more than eleven times the base number. We therefore speculate that L2 cache misses are the main cause of the observed response time differences between Xen and OpenVZ. This is consistent with the higher CPU overhead in Xen from Figure 7.5a, because more L2 cache misses causes more memory access overhead and puts higher pressure on the processor.

Table 7.1 shows the percentage of L2 cache misses for OpenVZ and the base system for high overhead kernel functions. The function `do_anonymous_page` is used to allocate pages for a particular application by the kernel. The functions `__copy_to_user_ll` and `__copy_from_user_ll` copy data back and forth from the user-mode to kernel-mode pages. The data indicates that cache misses in OpenVZ result mainly from page re-mapping due to switching between virtual containers. The increase in the number of L2 cache misses

Symbol Name	OpenVZ	Base
`do_anonymous_page`	31.84	25.24
`__copy_to_user_ll`	11.77	9.67
`__copy_from_user_ll`	7.23	0.73

Table 7.1: Base vs OpenVZ - % of L2 cache misses

Symbol name	L2 cache misses (%)
`hypervisor_callback`	32.00
`evtchn_do_upcall`	44.54
`__copy_to_user_ll`	3.57
`__do_IRQ`	2.45

Table 7.2: Xen Web tier - % of L2 cache misses

causes the instructions to stall and reduces the total number of instructions executed.

Because Xen uses a modified kernel, it is not possible to directly compare calls within it with the numbers obtained from the base system and OpenVZ. Table 7.2 shows the highest cache miss functions identified using Oprofile for the Web domain in the Xen system.

The function `hypervisor_callback` is called when an event occurs that needs hypervisor attention. These events include various activities including cache misses, page faults, and interrupt handling that usually happen in privileged mode in a normal kernel. After some preliminary processing of stack frames, the function `evtchn_do_upcall` is called to process the event and to set up the domain to continue normally. These functions are the main source of overhead in Xen and reflect the cost of hypervisor-based virtualization.

Looking at the number of retired instructions for the Xen kernel (Table 7.3) for different functions, we see that in addition to overheads in hypervisor callback and upcall event handling, 10% of the instructions are executed to handle interrupts, which also is a major source of overhead. The higher percentage is due to increase in the interrupts caused by switching between the two domains.

We also looked at the hardware counters for a particular binary (like `httpd`, `mysqld`).

Symbol name	Number of ret instr(%)
`hypervisor_callback`	39.61
`evtchn_do_upcall`	7.53
`__do_IRQ`	10.9l

Table 7.3: Xen kernel - % of retired instructions

Binary	OpenVZ	Base
`libphp5.so`	0.85	0.63
`vmlinux`	3.13	2.85
`httpd`	4.56	2.40
`mysqld`	4.88	2.30

Table 7.4: Base vs. OpenVZ - % cache misses/instruction for binaries

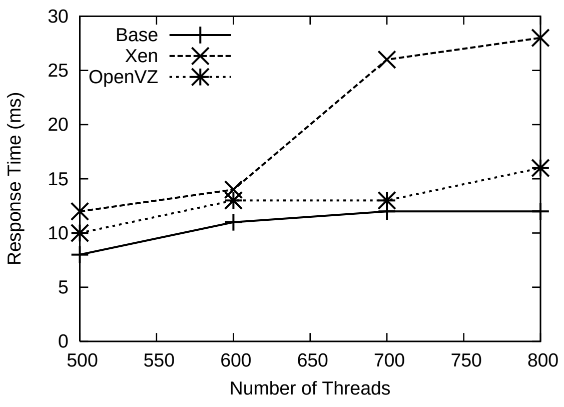

(a) Two-node - average response time

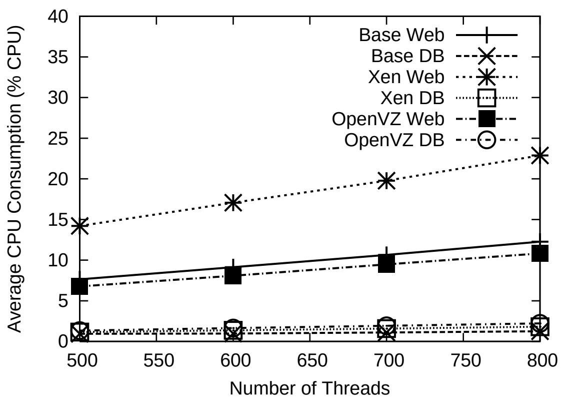

(b) Two-node - average CPU consumption

Figure 7.6: Two-node analysis results

As we compare OpenVZ to the base system, we do not see a clear difference between the two in either the percentage of cache misses or the percentage of instructions executed for each binary. However, there is larger difference in the percentage of cache misses per instruction. Table 7.4 shows this ratio for particular binaries that were running in OpenVZ and the base system. The dynamic library `libphp5.so` is responsible for executing the PHP scripts on the apache side. We can see that the percentage of cache misses per instruction is higher in OpenVZ for all four binaries. This indicates some degree of overhead in OpenVZ, which contributes to small increase in response times (Figure 7.4b) and slightly higher CPU consumption (Figure 7.5a) compared to the base case. Unfortunately, we cannot directly compare the numbers obtained from particular domains in Xen to the numbers in the Table 7.4 as they do not include the associated work done in Dom0.

7.4.2 Two-node

In this configuration, we run the Web and the DB tiers of a single RUBiS application on two different nodes, as shown in Figure 7.3b. The objective of the experiment is to compare

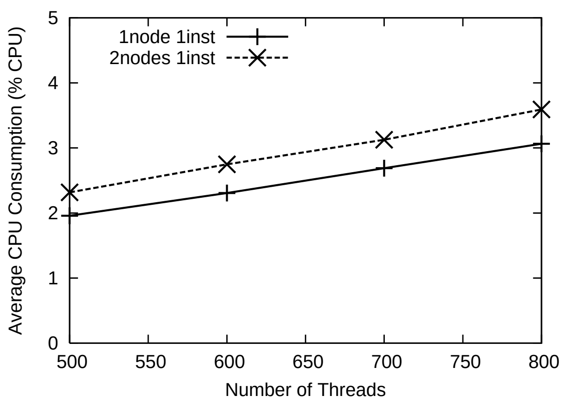

Figure 7.7: Single-node vs. two-node - Xen Dom0 CPU consumption

this way of hosting a multi-tiered application to the single-node case. Note that in the case of Xen and OpenVZ, there is only one container hosting each of the application components (Web tier or DB tier).

7.4.2.1 Performance Evaluation

Figure 7.6a shows the average response time as a function of workload for the three systems. The throughput graph is not shown because it is similar to the single-node case, where the throughput goes up linearly with the workload and there is little difference between the virtualized systems and the base system. We see a small overhead in OpenVZ compared to the base case with the maximum difference in the mean response time below 5 ms. In contrast, as the workload increases from 500 to 800 threads, the response time from the Xen system goes from 13 ms to 28 ms with an increase of 115%. However, this increase in response time is significantly lower than that experienced by using Xen in the single-node case (28 ms vs. 130 ms for single-node with 800 threads).

Figures 7.6b shows the average CPU consumption as a function of workload for both the Web and the DB tiers. The trend here is similar to the single-node case, where the DB tier consumption remains low and the Web tier consumption goes up linearly as the the number of threads increases. The slope of increase in the Web tier consumption is higher for Xen compared to OpenVZ and the base system. More specifically, 100 more concurrent threads consume roughly 3% more CPU capacity for Xen and only 1% more for the other

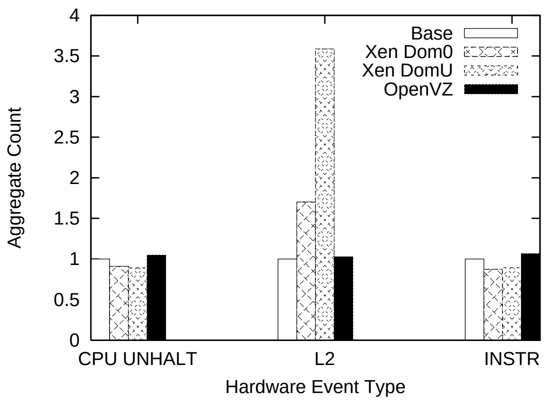

(a) Web tier

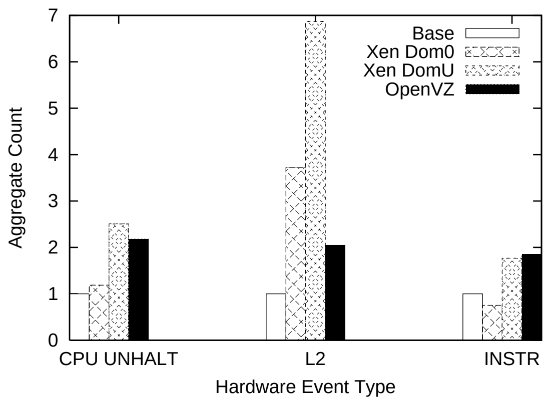

(b) DB tier

Figure 7.8: Two-node - Oprofile analysis

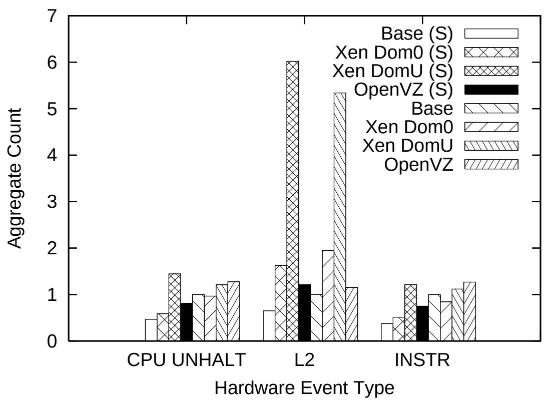

Figure 7.9: Single-node vs. two-node - Oprofile analysis

two systems.

Figure 7.7 shows the Dom0 CPU consumptions for both the single-node and two-node configurations for Xen. In the two-node case, we show the sum of the Dom0 consumptions from both nodes. In both cases, the Dom0 CPU consumption remains low (below 4% for all the workloads tested), and it goes up linearly as the workload increases. If the fixed CPU overhead of running Dom0 were high, we would have expected the combined consumption in the two-node case to be roughly twice that from the single-node case, since the former has two Dom0's. But the figure suggests it is not the case. The difference between the two cases is within 0.5% of total CPU capacity for all the worklaods. This implies that Dom0 CPU consumption is mostly workload dependent, and there is very little fixed cost.

Symbol Name	Single	Two
do_anonymous_page	25.25	24.33
__copy_to_user_ll	9.68	12.53
__copy_from_user_ll	0.73	1.11

Table 7.5: Single-node vs. two-node - base system % of L2 cache misses

Symbol Name	Single	Two
do_anonymous_page	31.84	33.10
__copy_to_user_ll	11.77	15.03
__copy_from_user_ll	7.23	7.18

Table 7.6: Single-node vs. two-node - OpenVZ % of L2 cache misses

7.4.2.2 Oprofile Analysis

We now analyze the sources of overhead in the two-node case using Oprofile. Figures 7.8a and 7.8b show the values of the hardware counters for the two nodes hosting the Web tier and the DB tier, respectively, for a workload of 800 threads. For both tiers, we see that the total number of L2 cache misses in Xen (Dom0 + DomU) is between five to ten times those from the base case, and the OpenVZ number is only twice that of the base case.

Figure 7.9 provides a comparison of these values between the single-node and two-node cases. Each counter value shown for the two-node case is the sum of the two values from the two nodes. All values are normalized with respect to the base system in the two-node setup. We observe that relative L2 cache misses are higher for the single-node case as compared to the two-node case for both OpenVZ and Xen. For example, for the total number of L2 cache misses, the ratio between the Xen number (Dom0 + Domu) and the base number is 11 in the single-node case vs. 7.5 in the two-node case. This is expected due to extra overhead caused by running two virtual containers on the same node.

Table 7.5 shows the number of L2 cache misses in the base kernel for both the single-node and two-node configurations. For the two-node case, we add the aggregate counters

Symbol Name	Single	Two
hypervisor_callback	32.00	43.00
evtchn_do_upcall	44.53	36.31
__do_IRQ	2.50	2.73

Table 7.7: Single-node vs. two-node - Xen Web tier % of L2 cache misses

Symbol Name	Single	Two
`hypervisor_callback`	6.10	4.15
`evtchn_do_upcall`	44.21	42.42
`__do_IRQ`	1.73	1.21

Table 7.8: Single-node vs. two-node - Xen Web tier % of L2 cache misses/instruction

for each kernel function in both nodes and normalize them with respect to the total number of cache misses from the two nodes. The same comparison is shown in Table 7.6 for the OpenVZ system. The percentage of L2 cache misses for different kernel functions stay almost the same between the single-node and two-node cases (within 4% of each other), except for the `__copy_to_user_ll` function where we see the two-node value being 28% higher. Comparing Table 7.6 to Table 7.5, we see that all the values are higher in OpenVZ than in the base case indicating higher page re-mapping overhead in the OpenVZ system.

Table 7.7 shows a similar comparison for Xen-specific kernel calls in the Xen system Web tier. If we add the first two rows, we see that the total number of cache misses for the functions `hypervisor_call_back` and `evtchn_do_upcall` is very similar in the single-node and two-node cases. The values for the `_do_IRQ` call are similar too. However, the difference is larger in the number of cache misses per instruction, which is shown in Table 7.8. We see the sum of the first two rows being 10% higher in the single-node case, and the percentage of L2 cache misses/instruction for interrupt handling being 43% higher. The reason is that more instructions are executed in the two-node case because of less stalling due to cache misses.

7.5 Scalability Evaluation

In this section, we investigate the scale of consolidation that can be achieved by different virtualization technologies. We increase the number of RUBiS instances from one to two then to four in the two-node configuration, and compare the scalability of Xen and OpenVZ with respect to application performance and resource consumption.

7.5.1 Response Time

We omit figures for application throughput. Even as the number of RUBiS instances is increased to four, we still observe linear increase in the throughput as a function of workload, and approximately the same throughput from both the OpenVZ and the Xen systems.

Figure 7.10a shows the average response time as a function of workload when running two instances of RUBiS on two nodes. For either Xen or OpenVZ, there are two curves corresponding to the two instances I and II. The response time remains relatively constant for OpenVZ but goes up about 500% (15 ms to roughly 90 ms) as the workload increases from 500 to 800 threads.

Figure 7.10b shows the same metric for the case of running four instances of RUBiS, and we see an even greater increase in the average response time in the Xen case. As the workload increases from 500 to 800 threads, the average response time experienced by each application instance goes from below 20 ms up to between 140 and 200 ms, an increase of more than 600%, yet the average response time in the OpenVZ case stays near or below 30 ms in all cases.

In Figure 7.11a, we compare the four consolidation configurations for a workload of 800 threads per application, and show the mean response time averaged across all the application instances in each configuration. In the Xen system, the average response time per application in the two-node case grows from 28 ms for one instance to 158 ms for four instances, an over 400% increase. In contrast, this increase is only about 100% in the OpenVZ case. This indicates much better scalability of OpenVZ with respect to application-level performance.

What is also interesting is that the single-node configuration (one-node one-inst in Figure 7.11a) results in worse application performance and worse scalability than the two-node case using Xen. For example, if a maximum average response time of 160 ms is desired, we can use the two-node option to host four instances of RUBiS with 800 threads each, but would require four separate nodes for the same number of instances and comparable performance if the single-node option is used.

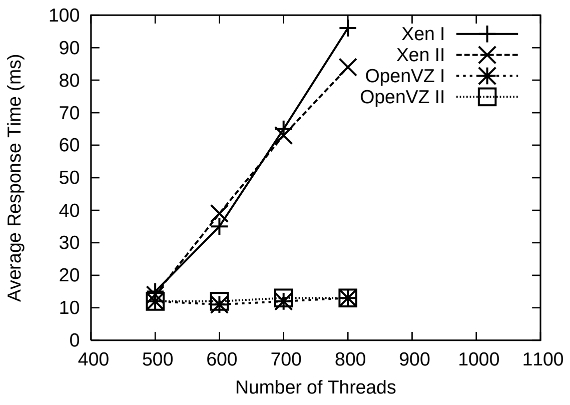

(a) Two instances

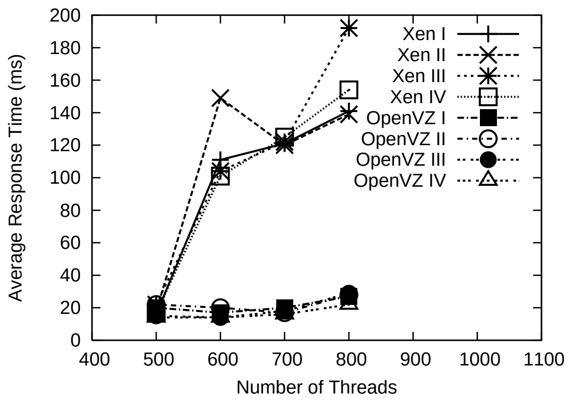

(b) Four instances

Figure 7.10: two-node multiple instances - average response time

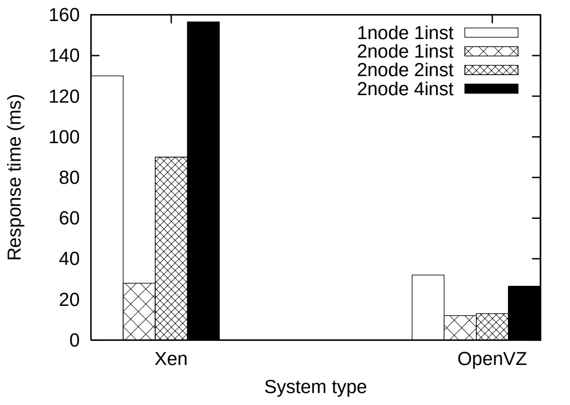

(a) Average response time

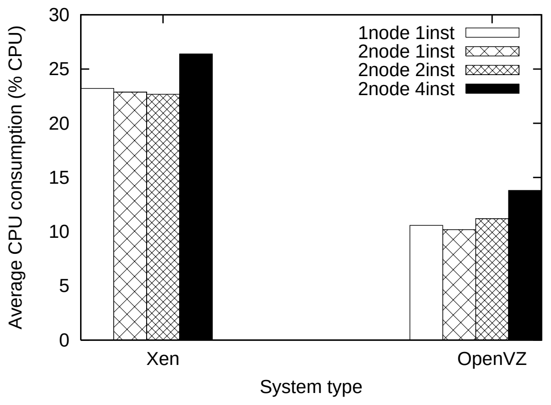

(b) Web tier CPU consumptions

Figure 7.11: Comparison of all configurations (800 threads)

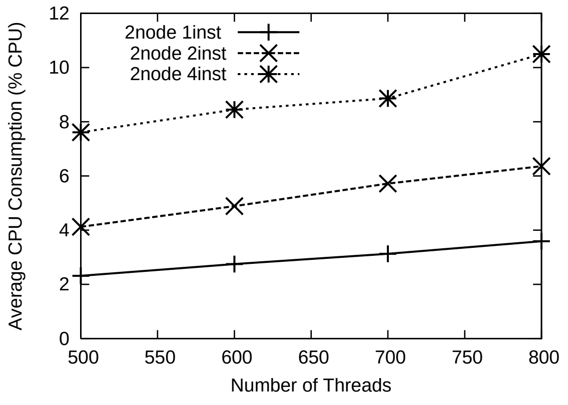

Figure 7.12: two-node multiple instances - Xen Dom0 CPU consumption

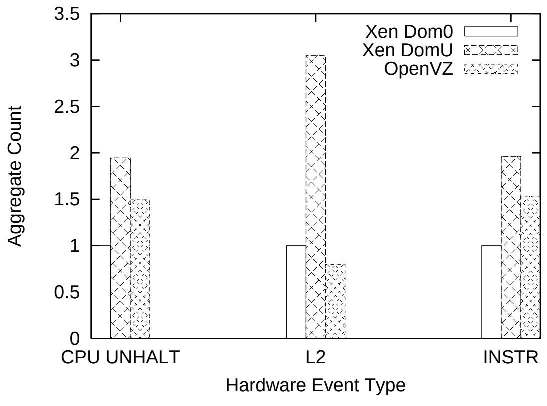

(a) Web tier

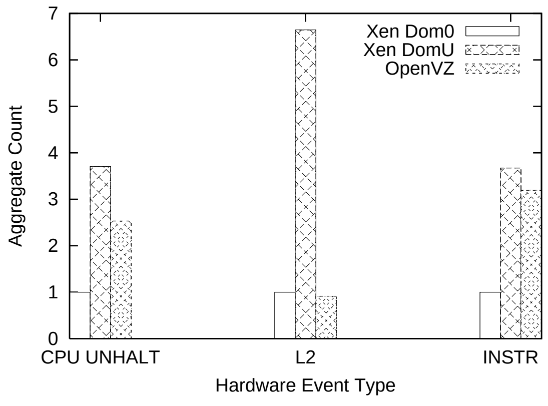

(b) DB tier

Figure 7.13: two-node two instances - Oprofile analysis for Xen and OpenVZ

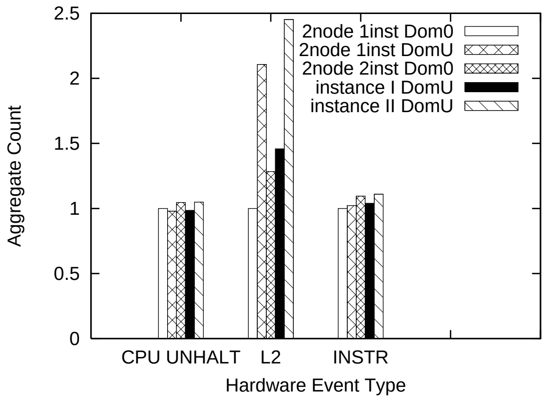

(a) Web tier

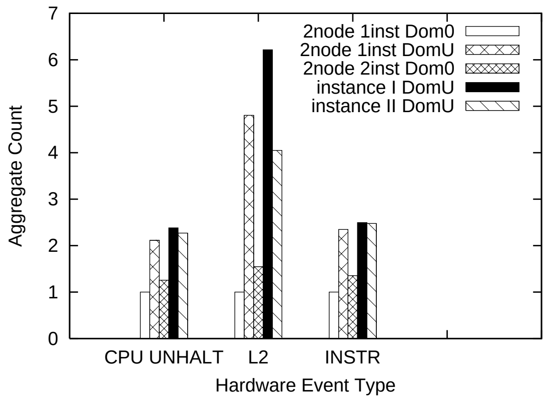

(b) DB tier

Figure 7.14: Single instance vs. two instances - Oprofile analysis for Xen

7.5.2 CPU Consumption

In Figure 7.11b, we compare the four consolidation configurations in terms of the average Web tier CPU consumption seen by all the application instances with a workload of 800 threads each. We can see that the average consumption per application instance for Xen is roughly twice that for OpenVZ. Moreover, with four instances of RUBiS, the Xen system is already becoming overloaded (with the sum of all four instances exceeding 100%), whereas the OpenVZ system has the total consumption below 60% and should be able to fit at least two more instances of the RUBiS application.

Figure 7.12 shows the Xen Dom0 CPU consumption as a function of workload in the

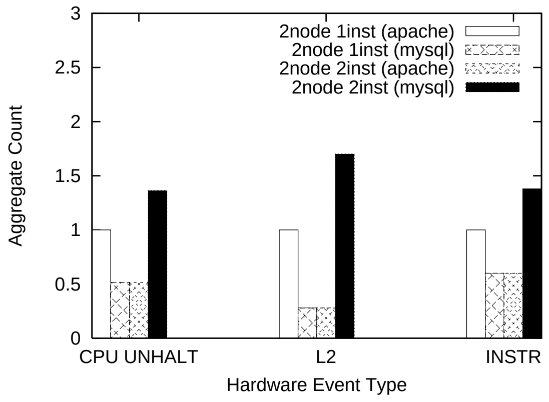

Figure 7.15: Single instance vs. and two instances - Oprofile analysis for OpenVZ

two-node case. The different lines in the graph correspond to different number of RUBiS instances hosted. For each scenario, the Dom0 consumption goes up approximately linearly as the workload increases from 500 to 800 threads. This is expected because Dom0 handles I/O operations on behalf of the domains causing its consumption to scale linearly with the workload. There is a slight increase in the slope as the number of RUBiS instances grows. Moreover, as the number of instances goes from one to four, the Dom0 consumption increases by a factor of 3 instead of 4, showing certain degree of multiplexing in Dom0.

To investigate how much more overhead is generated in the Xen system, we ran the four instances on two CPUs running the SMP kernel. We observed that the average CPU consumption by the Web domains is 25% and the average Dom0 consumption is 14%. The latter is higher than that obtained using the UP kernel.

7.5.3 Oprofile Analysis

We also perform overhead analysis using Oprofile for the case of two instances, and compare it to the results from the one instance case. Figures 7.13a and 7.13b show the hardware counter values from the two nodes hosting the Web and the DB tiers for both Xen and OpenVZ. All values are normalized with respect to the Xen Dom0 values. As seen before, the L2 cache misses are considerably higher in Xen user domains on both nodes and are the main source of overhead.

We now compare the counter values with those from the two-node one-instance case.

Binary	One-inst	Two-inst I	Two-inst II
`libphp5.so`	0.80	0.73	2.10
`vmlinux`	5.20	7.35	7.53
`httpd`	3.01	3.13	4.80

Table 7.9: Web tier % L2 cache misses/instruction for binaries in Xen

Figures 7.14a and 7.14b show the comparison of counter values from both nodes in the Xen system. We can see that the number of L2 cache misses for both tiers is 25% higher with two instances. It is also interesting to note that the number of instructions and percentage of execution time do not differ by much. We infer that the overhead is mainly due to the cache misses caused by memory remapping etc.

Figure 7.15 shows the corresponding data for OpenVZ. We observe similar patterns but the increase in the L2 cache misses is not as high as in Xen. Note that the L2 cache misses from both containers are included in the two instance case.

Turning our attention to the cause of this overhead, let us look into the hardware counters for particular binaries in Xen. Table 7.9 shows the percentage of cache misses per instruction for the Web tier with one and two instances of RUBiS. The percentage of cache misses per instruction experienced in the kernel (`vmlinux`) is 30% lower with single instance (5.20%) than with two instances (7.44% on average).

Table 7.10 shows the comparison of the percentage of L2 cache misses for different kernel functions in Xen. We see that there is not much difference in the percentage of L2 cache misses for any function. However, the percentage of L2 cache misses per instruction is different. We can conclude that the main reason of overhead comes from the higher L2 cache misses caused by page re-mapping, but the percentage of cache misses remains the same.

We see similar patterns in the OpenVZ case shown in Table 7.11. Note that we cannot differentiate between the different containers in OpenVZ. It is interesting to note that the addition of another instance does not increase the overhead in OpenVZ that much.

Symbol name	One-inst	Two-inst I	Two-inst II
`hypervisor_callback`	43.00	37.09	38.91
`evtchn_do_upcall`	36.31	42.09	34.32
`__copy_to_user_ll`	2.84	3.11	2.61
`__do_IRQ`	2.73	2.33	2.62

Table 7.10: Web tier % of L2 cache misses in Xen kernel

Binary	One-inst	Two-inst I + II
`libphp5.so`	0.60	0.78
`vmlinux`	2.40	2.86
`httpd`	2.94	4.73
Symbol name	One-inst	Two-inst I + II
`do_anonymous_page`	33.10	33.31
`__copy_to_user_ll`	10.59	11.78
`__copy_from_user_ll`	7.18	7.73

Table 7.11: Web tier % L2 cache misses/instruction for binaries and symbols in OpenVZ

7.6 Summary

We summarize our key findings and provide answers to the questions we raised in the introduction in terms of how Xen and OpenVZ perform when used for consolidating multi-tiered applications, and how performance is impacted by different configurations for consolidation.

- For all the configurations and workloads we have tested, Xen incurs higher virtualization overhead than OpenVZ does, resulting in larger difference in application performance when compared to the base Linux case.
- Performance degradation in Xen increases as application workloads increase. The average response time can go up by over 600% in the single-node case, and between 115% and 600% in the two-node case depending on the number of applications.
- For all the cases tested, the virtualization overhead observed in OpenVZ is limited, and can be neglected in many scenarios.

- For all configurations, the Web tier CPU consumption for Xen is roughly twice that of the base system or OpenVZ. CPU consumption of all systems and all containers goes up linearly as the workload increases. The slope of increase in the case of Xen is higher than in OpenVZ and the base cases.

- The main cause of performance overhead in Xen is the number of L2 cache misses.

- In the Xen system, relative L2 cache misses are higher in the single-node case compared to the sum of cache misses in the two-node case. Between the base and OpenVZ systems, the difference is minor.

- In the Xen system, the percentage of L2 cache misses for a particular function in the kernel is similar in the single-node and two-node cases. But the percentage of misses per instruction is higher in the single-node case.

- The percentage increase in the number of L2 cache misses for single and multiple instances of RUBiS is higher in Xen than in OpenVZ. In other words, as the number of applications increases, OpenVZ scales with less overhead.

- In the Xen system in a two-node setup, the percentage increase in response time from single application instance to multiple instances is significant (over 400% for 800 threads per application) while in OpenVZ this increase is much smaller (100%). With our system setup in the two-node case, the Xen system becomes overloaded when hosting four instances of RUBiS, while the OpenVZ system should be able to host at least six without being overloaded.

- Hosting multiple tiers of a single application on the same node is not an efficient solution compared to the case of hosting them on different nodes as far as response time and CPU consumption are concerned.

In summary, there are many complex issues involved in consolidating servers running enterprise applications using virtual containers. In this paper, we evaluated different ways of consolidating multi-tiered systems using Xen and OpenVZ as virtualization technologies and provided quantitative analysis to understand the differences in performance overheads.

More work can be done in extending this evaluation for various other complex enterprise applications, including applications with higher memory requirements or database-intensive applications. We hope that systems researchers can use these findings to develop optimizations in virtualization technologies in the future to make them more suited for server consolidation.

CHAPTER 8

Conclusions and Future Work

Virtualized data centers have seen explosive growth in recent years, but managing them is still a hard problem. The main objective of this thesis is to automate the management of a virtualized data center to achieve SLOs.

To that end, we have designed and implemented a set of tools that allow dynamic allocation of resources to meet application SLOs.

We presented *AutoControl*, a feedback control system to dynamically allocate resources to applications running on shared virtualized infrastructure. It consists of an online model estimator that captures the dynamic relationship between application-level performance and resource allocations and a MIMO resource controller that determines appropriate allocations of multiple resources to achieve application-level SLOs.

We evaluated *AutoControl* using two testbeds consisting of varying numbers of Xen virtual machines and various single- and multi-tier applications and benchmarks. Our experimental results confirmed that *AutoControl* can detect dynamically-changing CPU and disk bottlenecks across multiple nodes and can adjust resource allocations accordingly to achieve end-to-end application-level SLOs. In addition, *AutoControl* can cope with dynamically-shifting resource bottlenecks and provide service differentiation according to the priorities of individual applications. Finally, we showed that *AutoControl* can enforce performance targets for different application-level metrics, including throughput and response time, under dynamically-varying resource demands.

We have also built *LiteGreen*, an automated tool for saving desktop energy through server consolidation. LiteGreen uses virtualization to resolve the problem of wasting energy, by migrating idle desktops to a server where they can remain “always on” without incurring the energy cost of a desktop machine. The seamlessness offered by LiteGreen allows us to aggressively exploit short idle periods as well as long periods. Data-driven analysis of more than 65000 hours of desktop usage traces from 120 users shows that LiteGreen can help desktops sleep for 72-86% of the time and also scales well. The experience from our small-scale deployment of LiteGreen has also been encouraging.

8.1 Limitations and Discussion

8.1.1 AutoControl

8.1.1.1 Limitations of control theory

Control theory provides a rich body of theory for building sound feedback systems. However, applying control theory to computing systems is neither easy nor perfect.

1. **Inherent non-linearity**: Computer systems are inherently non-linear, making modeling difficult. Unlike the classical linear control theory that is more intuitive and accessible to people outside the field of control, nonlinear control theory and adaptive control theory are much harder to understand and to apply in practice. Adaptive control also imposes limitation on how fast workloads or system behavior can change.

2. **Lack of first-principle models**: Computer systems lack first-principle models, making it necessary to build black box models. However, this approach requires controlled experiments. Existing data collected from production systems are hard to use for modeling purposes because it often lacks sufficient excitation to identify all relevant correlations. It is difficult to design a set of controlled experiments to build a model offline. An adaptive model may solve the problem, but will be more difficult to reason about.

3. **Tracking vs. Optimization**: Most classical control problems are formulated as tracking problems, i.e., the controller maintains the outputs at certain reference values.

However, this may not be appropriate for all design problems in systems. For example, a meaningful design objective for a Web server may be to minimize the mean or percentage response time instead of keeping it at a certain value. For such problems, design methodologies that provide stability guarantees are not generally available.

4. **Dealing with discrete inputs**: Classical control theory only deals with continuous inputs. Many computing systems have input variables that only take on discrete values that have boundaries. For the systems where input values are discrete and numerical (e.g., number of servers allocated or P-states in a processor with dynamic voltage scaling enabled), it is possible to design controllers assuming continuous input variables. This approach may suffer from instability or inefficiency due to quantization errors. For systems with input values that are logical (e.g., Linux kernel version), discrete-event control theory [35] can be explored.

8.1.1.2 Actuator & sensor behavior

The behavior of sensors and actuators affects our control. In existing systems, most sensors return accurate information, but many actuators are poorly designed. We observed various inaccuracies with Xen's earlier SEDF scheduler and credit scheduler that are identified by other researchers [49] as well. These inaccuracies cause VMs to gain more or less CPU than set by the controller. Empirical evidence shows that our controller is robust to CPU scheduler's inaccuracies.

8.1.1.3 Open Loop vs. Closed Loop Workloads

We have used closed loop workloads in our evaluation of AutoControl, but the AutoControl framework can work with open loop workloads as well without any modifications. We treat the workload as a disturbance in the system that is external to the system, as a result it does not matter how the workload behaves. As long as we can measure application performance, the controller can use the adaptive online model to allocate the resources.

8.1.2 LiteGreen

The design of LiteGreen anticipates advances in virtualization technology that have been reported in the literature and can reasonably be expected to become mainstream in the not-too-distant future.

8.1.2.1 Memory ballooning and sharing challenges

Consolidation of multiple VMs on the same physical server can put pressure on the the server's memory resources. *Page sharing* is a technique to decrease the memory footprint of VMs by sharing pages that are in common across multiple VMs [93]. Recent work [51] has advanced the state-of-the-art to also include sub-page level sharing, yielding memory savings of up to 90% with homogeneous VMs and up to 65% otherwise.

Even with page sharing, memory can become a bottleneck depending on the number of VMs that are consolidated on the server. *Memory ballooning* is a technique to dynamically shrink or grow the memory available to a VM with minimal overhead relative to statically provisioning the VM with the desired amount of memory [93]. Advances in memory ballooning will help in LiteGreen consolidation.

8.1.2.2 Shared storage in live migration

Live migration assumes that the disk is shared between the source and destination machines, say, in the form of network attached storage (NAS) on the LAN. This avoids the considerable cost of migrating disk content. However, recent work has demonstrated the migration of VMs with local virtual hard disks (VHDs) by using techniques such as pre-copying and mirroring of disk content [32] to keep the downtime to under 3 seconds in a LAN setting.

8.1.2.3 Desktop hypervisors

While much attention has been focused on server hypervisors, there has recently been significant interest in client hypervisors, introducing challenges such as compatibility with a diversity of devices and ensuring good graphics performance. In early 2009, both Citrix and VMWare announced plans to build type-1 client hypervisors in collaboration with Intel [18, 20].

While our prototype is constrained by the virtualization technology available to us today, we believe that LiteGreen makes a contribution that is orthogonal to the advances noted above.

8.1.3 Energy Proportional Systems

A fundamental assumption in LiteGreen is that the current desktop systems are not energy proportional, as a result wasting great amount of energy, even when the system is largely idle. There have been research advances in building energy proportional systems [79, 80], and achieving energy proportionality with existing systems [89]. But, there is still a long way to go before energy proportionality can be achieved. When energy proportional systems are available, there is no need for LiteGreen.

8.1.4 Idleness Indicactors

In this thesis, we have used UI activity and CPU resource utiliaztion as an indicator for measuring the idleness. However, these are only proxies for real user interactivity. Other measures like network, disk activity, video display activity can be used to more accurately determine the idleness. Other sensing based on location can be used to determine user's interactivity. Applying LiteGreen to use other indicators is left to future work.

8.2 Future Work

8.2.1 Network and Memory control

Our initial efforts in adding network resource control have failed, because of inaccuracies in network actuators. Since Xen's native network control is not fully implemented, we tried to use Linux's existing traffic controller (`tc`) to allocate network resources to VMs. We found that the network bandwidth setting in (`tc`) is not enforced correctly when heavy network workloads are run. We plan to fix these problems and add network control as well. The MIMO resource controller, we developed in this thesis is directly applicable to any number of resources.

The memory ballooning supported in VMware [93] provides a way of controlling the memory required by a VM. However, the ballooning algorithm does not know about application goals or multiple tiers, and only uses the memory pressure as seen by the operating system. We have done preliminary work [54] in controlling CPU and memory together and plan to integrate it with *AutoControl*.

8.2.2 Handling a Combination of Multiple Targets

AutoControl is shown to be able to handle different metrics, including throughput and response time as performance metrics. *How do we handle applications that require specifying a combination of metrics for performance?* For example, a web application might want to specify certain maximum response time and minimum throughput goal. We have developed a preliminary utility-based framework, where we introduce the concept of utility that is a representative "value" of an application. For example, a utility function like $U(y) = max[\alpha(1 - e^{y-y_{ref}}, 0)]$ represents higher utility for an application as it reaches its target metric y_{ref}. Continuing this, we can create a utility function using two or more metrics that are of interest to the application. An example utility function using both response time and throughput is: $U(thr, rt) = g(rt - rt_{ref} + f(thr_{ref} - thr))$, where $g(x) = (1 + erf(\alpha * x))/2 \quad f(x) = \beta * g(x)$.

A 3-D visualization of the function is shown in Figure 8.1.

8.2.3 Extending AutoControl to other applications

AutoControl is designed with allocating resources to single and multi-tier applications. However, the modeling framework can be extended to other applications where individual components can be modeled. This requires more support from the applicaiton, as *AutoControl* requires knobs to adjust resources for each of the components.

In this thesis, we have also assumed that we can identify the dependencies that can be modeled explicitly. We assumed that in a 3-tier application, the dependency chain goes from web server to application server to database server. However, this may not always

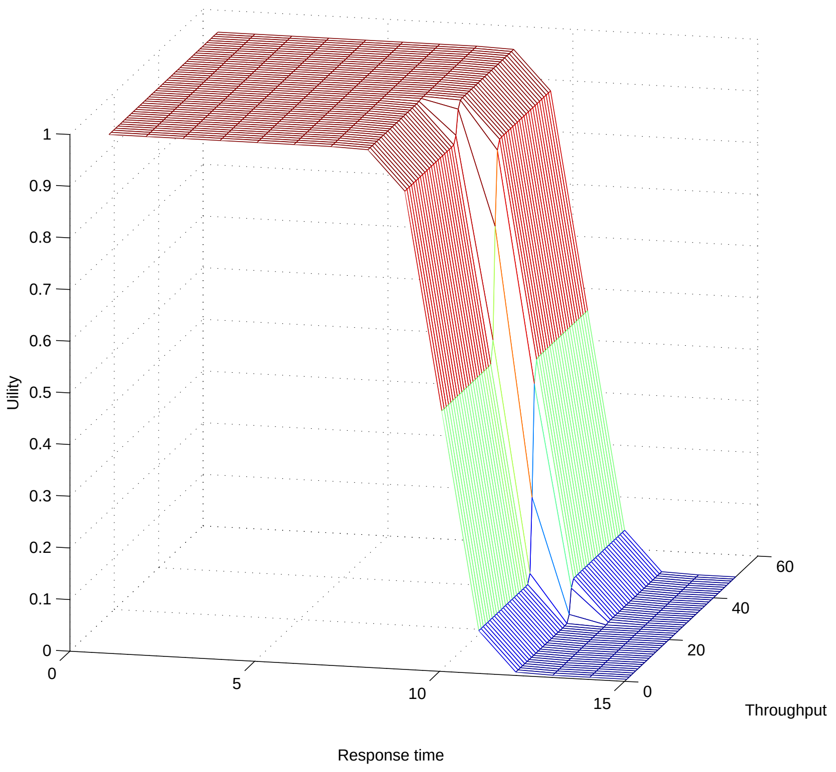

Figure 8.1: Combined metrics, $thr_{ref} = 25$, $rt_{ref} = 10$, $\alpha = 1$, $\beta = 1$, $thr = 0 - 50$, $rt = 0 - 15$

be apparent for components in an application. A domain expert is needed to identify such dependencies in such cases. However, our model is generic enough to capture dependencies once they are identified.

8.3 Summary

We have built a set of tools that provide automated mechanisms to manage virtualized data centers. The tools consist of *AutoControl* and *LiteGreen*. *AutoControl* is a multi-resource controller that can dynamically adjust virtualized resources so that application SLOs can be met. *LiteGreen* is a controller that manages the consolidation of idle desktop consolidation to save energy.

BIBLIOGRAPHY

BIBLIOGRAPHY

[1] Amazon EC2: http://www.amazon.com/gp/browse.html ?node=201590011. http://www.amazon.com/gp/browse.html?node=201590011.

[2] Linux VServer, http://linux-vserver.org/. http://linux-vserver.org/.

[3] LiteGreen demo video. http://research.microsoft.com/en-us/projects/litegreen/default.aspx.

[4] Microsoft Hyper-V. http://www.microsoft.com/windowsserver2008/en/us/hyperv-main.aspx.

[5] Microsoft Virtual Server, http://www.microsoft. com/windowsserversystem/virtualserver/. http://www.microsoft.com/windowsserversystem/virtualserver/.

[6] OpenVZ: http://en.wikipedia.org/wiki/OpenVZ. http://en.wikipedia.org/wiki/OpenVZ.

[7] Oprofile: A system profiler for Linux, http://oprofile.sourceforge.net/. http://oprofile.sourceforge.net/.

[8] Remote Desktop Protocol. http://msdn.microsoft.com/en-us/library/aa383015(VS.85).aspx.

[9] Virtual Box. http://www.virtualbox.org/.

[10] Virtuozzo. http://www.parallels.com/products/virtuozzo/.

[11] VMWare ESX Server. http://www.vmware.com/products/esx/.

[12] Wattsup Meter. http://www.wattsupmeters.com.

[13] Windows Management Instrumentation. http://msdn.microsoft.com/en-us/library/aa394582(VS.85).aspx.

[14] XenSource, http://www.xensource.com/. http://www.xensource.com/.

[15] White Paper: Benefits and Savings of Using Thin Clients, 2X Software Ltd., 2005. http://www.2x.com/whitepapers/WPthinclient.pdf.

[16] White Paper: Wake on LAN Technology, June 2006. http://www.liebsoft.com/pdfs/Wake_On_LAN.pdf.

[17] Advanced Configuration and Power Interface (ACPI) Specification, June 2009. http://www.acpi.info/DOWNLOADS/ACPIspec40.pdf.

[18] Citrix XenClient Announcement, Jan. 2009. `http://www.citrix.com/site/resources/dynamic/partnerDocs/CitrixXenClient_SolutionBrief_Sept09.pdf`.

[19] Emerging Technology Analysis: Hosted Virtual Desktops, Gartner, Feb. 2009. `http://www.gartner.com/DisplayDocument?id=887912`.

[20] VMWare Client Virtualization Platform (CVP) Announcement, Feb. 2009. `http://www.vmware.com/company/news/releases/cvp-intel-vmworld.html`.

[21] Worldwide PC 20092013 Forecast, IDC, Mar. 2009. `http://idc.com/getdoc.jsp?containerId=217360`.

[22] Abdelzaher, T., Shin, K., and Bhatti, N. Performance guarantees for Web server end-systems: A control-theoretical approach. *IEEE Transactions on Parallel and Distributed Systems 13*, 1 (2002).

[23] Agarwal, Y., Hodges, S., Chandra, R., Scott, J., Bahl, P., and Gupta, R. Somniloquy: Augmenting Network Interfaces to Reduce PC Energy Usage. In *NSDI* (Apr. 2009).

[24] Agency, U. E. P. Report to Congress on Server and Data Center Energy Efficiency Public Law 109-431, Aug. 2007. `\url{http://www.energystar.gov/ia/partners/prod_development/downloads/EPA_Datacenter_Report_Congress_Final1.pdf}`.

[25] Amza, C., Chanda, A., Cox, A., Elnikety, S., Gil, R., Rajamani, K., Cecchet, E., and Marguerite, J. Specification and implementation of dynamic Web site benchmarks. In *Proceedings of the 5th IEEE Annual Workshop on Workload Characterization* (Oct. 2002).

[26] Andrzejak, A., Arlitt, M., and Rolia, J. Bounding the resource savings of utility computing models. Tech. Rep. HPL-2002-339, HP Labs, Dec. 2002. `http://www.hpl.hp.com/techreports/2002/HPL-2002-339.html;http://www.hpl.hp.com/techreports/2002/HPL-2002-339.pdf`.

[27] Aron, M., Druschel, P., and Zwaenepoel, W. Cluster reserves: A mechanism for resource management in cluster-based network servers. In *Proceedings of ACM SIGMETRICS* (2000), pp. 90–101.

[28] Astrom, K., and Wittenmark, B. *Adaptive Control*. Addition-Wesley, 1995.

[29] Banga, G., Druschel, P., and Mogul, J. Resource containers: A new facility for resource management in server systems. In *Proceedings of the 3rd Symposium on Operating Systems Design and Implementation (OSDI)* (1999), pp. 45–58.

[30] Barham, P., Dragovic, B., Fraser, K., Hand, S., Harris, T., Ho, A., Neugebauer, R., Pratt, I., and Warfield, A. Xen and the art of virtualization. In *Proceedings of the 19th symposium on Operating systems principles (SOSP)* (New York, Oct. 19–22 2003), vol. 37, 5 of *Operating Systems Review*, ACM Press, pp. 164–177.

[31] Bellard, F. QEMU, a fast and portable dynamic translator. In *USENIX Annual Technical Conference, FREENIX Track* (2005), USENIX, pp. 41–46. `http://www.usenix.org/events/usenix05/tech/freenix/bellard.html`.

[32] Bradford, R., Kotsovinos, E., Feldmann, A., and Schioeberg, H. Live Wide-Area Migration of Virtual Machines Including Local Persistent State. In *ACM VEE* (June 2007).

[33] Bugnion, E., Devine, S., and Rosenblum, M. Disco: Running Commodity Operating Systems on Scalable Multiprocessors. In *SOSP* (Oct. 1997).

[34] Cain, H., Rajwar, R., Marden, M., and Lipasti, M. H. An architectural evaluation of Java TPC-W. In *Proceedings of the 7th International Symposium on High Performance Computer Architecture (HPCA)* (2001).

[35] Cassandras, C. G., and Lafortune, S. *Introduction to Discrete Event Systems.* Springer-Verlag New York, Inc., 2006.

[36] Chambliss, D., Alvarez, G., Pandey, P., Jadav, D., Xu, J., Menon, R., and Lee, T. Performance virtualization for large-scale storage systems. In *Proceedings of the 22nd Symposium on Reliable Distributed Systems (SRDS)* (Oct. 2003).

[37] Chase, J., Anderson, D., Thakar, P., Vahdat, A., and Doyle, R. Managing energy and server resources in hosting centers. In *SOSP* (October 2001).

[38] Clark, B., Deshane, T., Dow, E., Evanchik, S., Finlayson, M., Herne, J., and Matthews, J. Xen and the art of repeated research. In *USENIX Annual Technical Conference, FREENIX Track* (2004), pp. 135–144.

[39] Clark, C., Fraser, K., Hand, S., Hansen, J. G., Jul, E., Limpach, C., Pratt, I., and Warfield, A. Live migration of virtual machines. In *Proceedings of the 2nd Symposium on Networked Systems Design and Implementation (NSDI)* (2005), USENIX.

[40] Creasy, R. J. The origin of the VM/370 time-sharing system. *IBM Journal of Research and Development 25*, 5 (1981), 483–490.

[41] David, B. White Paper: Thin Client Benefits, Newburn Consulting, Mar. 2002. `http://www.thinclient.net/technology/Thin_Client_Benefits_Paper.pdf`.

[42] DeCandia, G., Hastorun, D., Jampani, M., Kakulapati, G., Lakshman, A., Pilchin, A., Sivasubramanian, S., Vosshall, P., and Vogels, W. Dynamo: amazon's highly available key-value store. In *SOSP* (2007), T. C. Bressoud and M. F. Kaashoek, Eds., ACM, pp. 205–220. `http://doi.acm.org/10.1145/1294261.1294281`.

[43] Diao, Y., Gandhi, N., Hellerstein, J., Parekh, S., and Tilbury, D. MIMO control of an Apache Web server: Modeling and controller design. In *Proceedings of American Control Conference (ACC)* (2002).

[44] Elnikety, S., Nahum, E., Tracey, J., and Zwaenepoel, W. A method for transparent admission control and request scheduling in e-commerce web sites. In *Proceedings of the Int. Conf. on WWW* (2004).

[45] Galley, S. W. Pdp-10 virtual machines. In *Proceedings of the workshop on virtual computer systems* (New York, NY, USA, 1973), ACM, pp. 30–34.

[46] Garey, M. R., and Johnson, D. S. *Computers and intractability; a guide to the theory of NP-completeness.* W.H. Freeman, 1979.

[47] Goyal, P., Modha, D., and Tewari, R. CacheCOW: Providing QoS for storage system caches. In *Proceedings of ACM SIGMETRICS* (2003), pp. 306–307.

[48] Gulati, A., Merchant, A., Uysal, M., and Varman, P. Efficient and adaptive proportional share I/O scheduling. Tech. Rep. HPL-2007-186, HP Labs, Nov. 2007.

[49] Gupta, D., Cherkasova, L., Gardner, R., and Vahdat, A. Enforcing performance isolation across virtual machines in Xen. In *Proceedings of International Middleware Conference* (2006), vol. 4290, pp. 342–362.

[50] Gupta, D., Gardner, R., and Cherkasova, L. XenMon: QoS monitoring and performance profiling tool. In *HP Labs Technical Report HPL-2005-187* (October 2005).

[51] Gupta, D., Lee, S., Vrable, M., Savage, S., Snoeren, A. C., Varghese, G., Voelker, G. M., and Vahdat, A. Difference Engine: Harnessing Memory Redundancy in Virtual Machines. In *OSDI* (Dec. 2008).

[52] Hellerstein, J. L. Designing in control engineering of computing systems. In *Proceedings of American Control Conference (ACC)* (2004).

[53] Hellerstein, J. L., Diao, Y., Parekh, S., and Tilbury, D. M. *Feedback Control of Computing Systems.* Wiley Interscience, 2004.

[54] Heo, J., Zhu, X., Padala, P., and Wang, Z. Memory overbooking and dynamic control of Xen virtual machines in consolidated environments. In *Proceedings of IFIP/IEEE Symposium on Integrated Management (IM'09) mini-conference* (June 2009).

[55] Jin, W., Chase, J., and Kaur, J. Interposed proportional sharing for a storage service utility. In *Proceedings of ACM SIGMETRICS* (2004).

[56] Jones, M. B., Rosu, D., and Rosu, M.-C. CPU reservations and time constraints: Efficient, predictable scheduling of independent activities. In *Proceedings of the 16th Symposium on Operating System Principles (SOSP)* (October 1997).

[57] Kamra, A., Misra, V., and Nahum, E. Yaksha: A self-tuning controller for managing the performance of 3-tiered Web sites. In *Proceedings of International Workshop on Quality of Service (IWQoS)* (June 2004).

[58] Karamanolis, C., Karlsson, M., and Zhu, X. Designing controllable computer systems. In *Proceedings of HotOS* (June 2005).

[59] Karlsson, M., Karamanolis, C., and Zhu, X. Triage: Performance isolation and differentiation for storage systems. In *Proceedings of the 12th IEEE International Workshop on Quality of Service (IWQoS)* (2004).

[60] Karlsson, M., Karamanolis, C., and Zhu, X. Triage: Performance differentiation for storage systems using adaptive control. *IEEE Transactions on Storage 1*, 4 (Nov. 2005), 457–480.

[61] Kozuch, M., and Satyanarayanan, M. Internet suspend/resume. In *WMCSA* (2002), IEEE Computer Society, p. 40. `http://csdl.computer.org/comp/proceedings/wmcsa/2002/1647/00/16470040abs.htm`.

[62] Lawton, K. Running multiple operating systems concurrently on an IA32 PC using virtualization techniques. `http://www.plex86.org/research/paper.txt`.

[63] Liu, X., Zhu, X., Padala, P., Wang, Z., and Singhal, S. Optimal multivariate control for differentiated services on a shared hosting platform. In *Proceedings of IEEE Conference on Decision and Control (CDC)* (2007).

[64] Lu, Y., Abdelzaher, T., and Saxena, A. Design, implementation, and evaluation of differentiated caching serives. *IEEE Transactions on Parallel and Distributed Systems 15*, 5 (May 2004).

[65] Lumb, C., Merchant, A., and Alvarez, G. Façade: Virtual storage devices with performance guarantees. In *Proceedings of File and Storage Technologies (FAST)* (2003), USENIX.

[66] Menon, A., Cox, A., and Zwaenepoel, W. Optimizing network virtualization in Xen. In *Proceedings of the 2006 USENIX Annual Technical Conference* (June 2006), pp. 15–28.

[67] Menon, A., Santos, J. R., Turner, Y., Janakiraman, G. J., and Zwaenepoel, W. Diagnosing performance overheads in the Xen virtual machine environment. In *Proceedings of International Conference on Virtual Execution Environments (VEE)* (June 2005), pp. 13–23.

[68] Meyer, R. A., and Seawright, L. H. A virtual machine time-sharing system. *IBM Systems Journal 9*, 3 (1970), 199–218.

[69] Moore, J., Chase, J., Ranganathan, P., and Sharma, R. Making Scheduling Cool: Temperature-aware Workload Placement in Data Centers. In *Usenix ATC* (June 2005).

[70] Nathuji, R., and Schwan, K. VirtualPower: Coordinated Power Management in Virtualized Enterprise Systems. In *SOSP* (Oct. 2007).

[71] Nedevschi, S., Chandrashekar, J., Liu, J., Nordman, B., Ratnasamy, S., and Taft, N. Skilled in the Art of Being Idle: Reducing Energy Waste in Networked Systems. In *NSDI* (Apr. 2009).

[72] Nieh, J., and Lam, M. The design, implementation, and evaluation of smart: A scheduler for multimedia applications. In *Proceedings of the 16th Symposium on Operating System Principles (SOSP)* (October 1997).

[73] Nordman, B. Networks, Energy, and Energy Efficiency. In *Cisco Green Research Symposium* (2008).

[74] Nordman, B., and Christensen, K. Greener PCs for the Enterprise. In *IEEE IT Professional* (2009), vol. 11, pp. 28–37.

[75] Padala, P., Hou, K., Zhu, X., Uysal, M., Wang, Z., Singhal, S., Merchant, A., and Shin, K. G. Automated control of multiple virtualized resources. In *ACM Proc. of the EuroSys* (Mar. 2009).

[76] Padala, P., Zhu, X., Uysal, M., Wang, Z., Singhal, S., Merchant, A., Salem, K., and Shin, K. G. Adaptive control of virutalized resources in utility computing environments. In *Proceedings of EuroSys* (2007).

[77] Popek, G. J., and Goldberg, R. P. Formal requirements for virtualizable third generation architectures. *Commun. ACM 17*, 7 (1974), 412–421.

[78] Price, D., and Tucker, A. Solaris Zones: Operating system support for consolidating commercial workloads. In *Proceedings of the 18th Large Installation System Administration Conference (LISA)* (Nov. 2004), USENIX, pp. 241–254.

[79] Ranganathan, P. A recipe for efficiency? some principles of power- aware computing. Tech. Rep. HPL-2009-294, Hewlett Packard Laboratories, Sep 2009. `http://www.hpl.hp.com/techreports/2009/HPL-2009-294.html`.

[80] Ranganathan, P., Rivoire, S., and Moore, J. D. Models and metrics for energy-efficient computing. *Advances in Computers 75* (2009), 159–233. `http://dx.doi.org/10.1016/S0065-2458(08)00803-6`.

[81] Reumann, J., Mehra, A., Shin, K., and Kandlur, D. Virtual services: A new abstraction for server consolidation. In *Proceedings of the 2000 USENIX Annual Technical Conference (USENIX-00)* (June 2000), pp. 117–130.

[82] Rolia, J., Cherkasova, L., Arlit, M., and Andrzejak, A. A capacity management service for resource pools. In *Proceedings of International Workshop on Software and Performance* (July 2005).

[83] Rosenblum, M. VMware's Virtual Platform: A virtual machine monitor for commodity PCs. In *Hot Chips 11* (1999).

[84] Shen, K., Tang, H., Yang, T., and Chu, L. Integrated resource management for cluster-based internet services. *ACM SIGOPS Operating Systems Review 36*, SI (2002), 225 – 238.

[85] Soltesz, S., Potzl, H., Fiuczynski, M., Bavier, A., and Paterson, L. Container-based operating system virtualization: A scalable, high-performance alternative to hypervisors. In *Proceedings of EuroSys 2007 (to appear), http://www.cs.princeton.edu/ mef/research/vserver/ paper.pdf* (2007). `http://www.cs.princeton.edu/~mef/research/vserver/paper.pdf`.

[86] Srikantaiah, S., Kansal, A., and Zhao, F. Energy Aware Consolidation for Cloud Computing. In *HotPower* (Dec. 2008).

[87] Steere, D., Goel, A., Gruenberg, J., McNamee, D., Pu, C., and Walpole, J. A feedback-driven proportion allocator for real-rate scheduling. In *Proceedings of the 3rd Symposium on Operating Systems Design and Implementation (OSDI)* (February 1999).

[88] Tang, W., Fu, Y., Cherkasova, L., and Vahdat, A. Long-term streaming media server workload analysis and modeling. Tech. Rep. HPL-2003-23, HP Labs, Feb. 07 2003.

[89] Tolia, N., Wang, Z., Marwah, M., Bash, C., Ranganathan, P., and Zhu, X. Delivering energy proportionality with non energy-proportional systems - optimizing the ensemble. In *HotPower* (2008), F. Zhao, Ed., USENIX Association. `http://www.usenix.org/events/hotpower08/tech/full_papers/tolia/tolia.pdf`.

[90] Tolia, N., Wang, Z., Marwah, M., Bash, C., Ranganathan, P., and Zhu, X. Delivering Energy Proportionality with Non Energy Proportional Systems Optimizations at the Ensemble Layer. In *HotPower* (Dec. 2008).

[91] VMware. "Understanding Full Virtualization, Paravirtualization, and Hardware Assist. `\url{http://www.vmware.com/files/pdf/VMware_paravirtualization.pdf}`.

[92] VMware. VMware Distributed Resource Scheduler (DRS). `http://www.vmware.com/products/drs/`.

[93] Waldspurger, C. Memory resource management in VMware ESX server. In *Proc. of Symposium on Operating Systems Design and Implementation (OSDI)* (Dec. 2002).

[94] Waldspurger, C. A., and Weihl, W. Lottery scheduling: Flexible proprotional-share aresource management. In *Proceedings of the 1st Symposium on Operating Systems Design and Implementation (OSDI)* (Nov. 1994).

[95] Wang, X., and Chen, M. Cluster-level feedback power control for performance optimization. In *HPCA* (2008), IEEE Computer Society, pp. 101–110. `http://dx.doi.org/10.1109/HPCA.2008.4658631`.

[96] Wang, Z., Zhu, X., and Singhal, S. Utilization and slo-based control for dynamic sizing of resource partitions. Tech. Rep. HPL-2005-126R1, Hewlett Packard Laboratories, Feb 2005. `http://www.hpl.hp.com/techreports/2003/HPL-2003-53.html;http://www.hpl.hp.com/techreports/2003/HPL-2003-53.pdf`.

[97] Weiser, M., Welch, B., Demers, A., and Shenker, S. Scheduling for Reduced CPU Energy. In *OSDI* (Nov. 1994).

[98] Whitaker, A., Shaw, M., and Gribble, S. Scale and performance in the Denali isolation kernel. In *Proceedings of the 5th Symposium on Operating Systems Design and Implementation (OSDI)* (December 2002).

[99] White, B., Lepreau, J., Stoller, L., Ricci, R., Guruprasad, S., Newbold, M., Hibler, M., Barb, C., and Joglekar, A. An integrated experimental environment for distributed systems and networks. In *Proceedings of the 5th Symposium on Operating Systems Design and Implementation (OSDI)* (Dec. 2002), USENIX.

[100] Wikipedia. Virtualization. `http://en.wikipedia.org/wiki/Virtualization`.

[101] Wood, T., Shenoy, P. J., Venkataramani, A., and Yousif, M. S. Black-box and gray-box strategies for virtual machine migration. In *NSDI* (2007), USENIX. `http://www.usenix.org/events/nsdi07/tech/wood.html`.

[102] Wood, T., Shenoy, P. J., Venkataramani, A., and Yousif, M. S. Black-box and Gray-box Strategies for Virtual Machine Migration. In *NSDI* (Apr. 2007).

[103] Zhang, Y., Bestavros, A., Guirguis, M., Matta, I., and West, R. Friendly virtual machines: Leveraging a feedback-control model for application adaptation. In *Proceedings of the Virtual Execution Environments (VEE)* (2005).